iCSD 2024

International Conference on
Spreading Depolarizations

COSBID and beyond...

13-17 November 2024
Papillon Ayscha, Antalya, Türkiye

Müge Yemişçi, MD, PhD

Hacettepe University

Hülya Karataş, MD, PhD

Hacettepe University

Cenk Ayata, MD, PhD

Harvard Medical School

NEUROVASCULAR RESEARCH UNIT

ORGANIZING COMMITTEE

Eszter Farkas, PhD

Jed Hartings, PhD

Jens Dreier, MD PhD

Johannes Woitzik, MD PhD

Bill Shuttleworth, PhD

Martin Fabricius, MD

Martin Lauritzen, MD

Britta Lindquist, MD PhD

Sharon Jewell, MD PhD

K.C. Brennan, MD

SCIENTIFIC PROGRAMME

13 NOVEMBER 2024, WEDNESDAY

20:00-22:00 Late Session

20:00-20:15 Welcome and Orientation
Hülya Karataş, Müge Yemişçi Özkan

20:15-22:00 Introduction to Spreading Depolarizations: Consensus and Controversies
with Audience Participation
Jed Hartings

14 NOVEMBER 2024, THURSDAY

08:30-09:30 Keynote
Moderator: **Muge Yemisci**

Re-Evaluation of the Role of CSD in Migraine Headache
Hayrunnisa Bolay

09:30-09:40 Coffee Break

09:40-12:05 Oral Presentations
Chairs: David Chung, Lydia Hawley

Initial Results of The Indict Feasibility Trial of Spreading Depolarization Monitoring to Guide Management of Severe Traumatic Brain Injury
Jed Hartings

Continuous Monitoring of Cerebrovascular Autoregulation Using Functional Ultrasound İmaging in The Piglet Brain
Alan Urban

Spatial Dynamics of Human Spreading Depolarizations: Preliminary Results Applying a Newly Developed Two-Dimensional Strip
Liangchen Guo

Cortical Spreading Depolarization During Surgical Management of Cerebral Arteriovenous Malformations and Arteriovenous Fistulas
Patrick Dömer

10:45-11:00 Coffee Break

Spreading Depolarization Continuum in The Aged Non-Human Primate After Focal Ischemic Stroke
Sergei Kirov

High-Frequency Oscillations During Cortical Spreading Depolarization
Azat Nasretdinov

Noninvasive Optical Detection of Spreading Depolarization in Rat
Elyssa Alber

The Introduction of a Novel Visualization Method of Cerebral Blood Flow Changes in Mice With an Rgb Camera: The Effects of Bosentan on Spreading Depolarizations Induced by Experimental Air-Emboli Model Via External Carotid Artery Cannulation
Ergin Dileköz

12:05-13:00 Lunch Break

13:00-14:35 Oral Presentations
Chairs: **Jens Dreier, Melike Sever Bahçekapılı**

Mems-Based Su-8 Neural Probes for Enhanced Neuromonitoring
Hasan Uluşan

Noninvasive, Automated Detection of Spreading Depolarizations Using Scalp Electroencephalography: A Multicenter Validation in Patients With and Without Skull Defect
Alireza Chamanzar

Standardising Direct Cortical Response Monitoring of Spreading Depolarisations: A Matlab-Based Approach For Automating Optimal Stimulation Channel Selection
Khevna Vasani

Noninvasive vs. Invasive Detection of Cortical Spreading Depolarization Via Dc-Shift Comparison
Stephen Jones

Step Response of Metallic Electrodes
Kevan Hashemi

Monitoring High-Resolution Electrophysiological Activity of Brain Slices With A Multi-Functional High-Density Microelectrode Array
Hasan Ulusan

14:35-16:30 Posters with Coffee+Snacks

Detection of Spreading Depolarization-Associated Blood-Brain Barrier Disruption Using Dynamic Contrast-Enhanced MRI
Magnus Kreiberg

Impairment Of Na+-K+-Atpase in The Human Cortex Under Halogenated Ether Anesthetics is Associated with Disrupted Ion Homeostasis
Mathilde Maechler

Electrophysiological Characterization of The Pericyte-Endothelial Cell Syncytium in Human Brain Slices From Patients with Pharmacoresistant Mesial Temporal Lobe Epilepsy
Mirja grote Lambers

Case Report: A Patient With Hemiplegic Migraine And Unilateral Transient Cerebral Hyperperfusion
Yasemin Gürsoy Özdemir

Protocol Overview: Inhibiting The Nmdar/Trpm4 Interaction as a Neuroprotective Strategy in a Gyrencephalic Brain Model of Ischemic Stroke Through Modulation of Spreading Depolarization
Juan Manuel Lopez Navarro

A Mems-Based Thin Film Microelectrode Array For Monitoring of Traumatic Brain Injury
Hasan Uluşan

Alzheimer-Stroke Continuum: The Role Of Spreading Depolarization
Anna Törteli

Cognitive Impairment and Platelet Dynamics in Mild Traumatic Brain Injury: Insights from a North Indian Cohort
Arulselvi Subramaniam

16:30-17:30 Keynote
Moderator: **Hayrunnisa Bolay**

Capillaries as Multi-Modal Sensors of Brain Activity
Mark T. Nelson

20:00-21:00 Late Night Roundtables

SD and Migraine
KC Brennan, Müge Yemişçi Özkan, Elif Akaydın

Is SD Good or Bad?
Hayrunnisa Bolay, Kadir Oğuzhan Soylu

15 NOVEMBER 2024, FRIDAY

08:30-10:05 Oral Presentations
Chairs : **Bill Shuttleworth, Else Tolner**

The Impact of Cortical Spreading Depolarization on The Autonomous Nervous System in Critically Brain Injured Patients
Gwendan PERCEVAULT

Impact of Sd Initiation Site on Outcome of Transient Focal Ischemia
Michael Bennett

Repetitive Cortical Spreading Depolarizations Exacerbate Tissue Damage and Neurological Deficits Following Traumatic Brain Injury
Faith Best

Every Cloud Has a Silver Lining: Spreading Depolarization Induction of Neuroprotective Pathways Through Gene Expression Changes
Michela DellOrco

Correlation of BDNF Levels with Concussion Symptoms and Neurobehavior Deficits Associated with a Mild Traumatic Brain Injury
Venencia Albert

Migrainous Infarction: Myth or Reality? A Systematic Review
Emilie Schou

10:05-10:15 Coffee Break

10:15-11:50 Oral presentations
Chairs: **KC Brennan, Annika Köhne**

A Novel Model of In Vitro Cortical Spreading Depolarization
Yasemin Gürsoy-Özdemir

Olfactory Bulb Induction of Cortical Spreading Depolarization
Muhammed Miran Oncel

Effect of Long-Term Optogenetic Stimulation on Electrophysiological Spreading Depolarization Parameters in Mice
Annika Köhne

Loss of Arousal Following Induction of Cortical Spreading Depolarisation in Awake Mice
Kağan Ağan

Spontaneous Spreading Depolarizations in Atp1a2 And Atp1a3 Mutant Mice
Else Tolner

Acute Levcromakalim Injection Induces Migraine-Like Phenotype Without Cortical Spreading Depolarization in Male Wistar Rats
Elif Akaydın

Palytoxin Evokes Reversible Spreading Depolarization in The Locust CNS
R. David Andrew

11:50-12:50 Lunch Break

TBA The Antalya Museum (Antalya Archeological Museum) and Antalya Tour

20:00-21:00 Late Night Roundtable
Clinical SD Recordings
Martin Fabricius, Beyza Türken

16 NOVEMBER 2024, SATURDAY

08:30-09:30 Keynote
Moderator: **Hülya Karatas**

Spreading Depolarization in the Waking Brain: Insights from Animal Models
Lyudmila Vinogradova

09:30-09:40 Coffee Break

09:40-11:50 Oral Presentations
Chairs: **Yasemin Gürsoy Özdemir, Johannes Woitzik**

The Slope of The Spreading Depolarization Related Blood Flow Transients is a Potential Biomarker for Risk Stratification in Experimental Ischemic Stroke
Lückl Janos

Prophylactic Treatment of Migraine With (100%) Aura: Evaluating The Efficacy of Lamotrigine in Preclinical and Clinical Settings
Buket Nebiye Demir

Impact of Nimodipine on Hemodynamic Fluctuations and Connectivity Dynamics Following Cortical Spreading Depolarizations in a Gyrencephalic Swine Model
Diego Alberto Sandoval Lopez

Inhibition of Nitric Oxide Synthase Transforms Carotid Occlusion-Mediated Benign Oligemia into Large Cerebral Infarction
Dong-Eog Kim

10:30-10:45 Coffee Break

Hyperosmotic Treatment for Neuroprotection: In Vitro Effects of Mannitol
Rita Frank

Effect of Sın-1 on The Sd-Initiated Nup and The No-Reflow Phenomenon During Forebrain Ischemia and Reperfusion in Rats
Lemale Coline

Investigating the Effects of Nanoencapsulated Ketamine on Cerebral Blood Flow Responses Post Focal Cortical Ischemia Using Functional Ultrasound Imaging
Lorena Figueiredo Fernandes

Blood-Brain Barrier Dysfunction in Abnormal Brain Predicts Epilepsy After Subarachnoid Hemorrhage
Dreier Jens

11:50-12:55 Lunch Break

12:55-14:30 Oral Presentations
Chairs: **Eszther Farkas, Muhammed Miran Öncel**

The Role of an Innate Immune System Pathway in Cortical Spreading Depolarization and Nociception
Kadir Oguzhan Soylu

Does Spreading Depression Rewire Cortical Pain Networks?
Bengisu Solgun

Cortical Spreading Depolarization-Induced Nlrp3 Inflammasome Activation Via P2x7 Receptor Activity in Trigeminal Ganglia
Beyza TÜRKEN

How Spreading Depolarizations Shape Epileptic Activity
Roustem Khazipov

Natural History of Seizures, Spreading Depolarizations And Seizure-Associated Spreading Depolarization in Mouse Models of Epilepsy
Rob Wykes

Seizure Propagation Triggers a Protective Contralesional Spreading Depolarization During Focal Hippocampal Stroke in Freely Behaving Female Mice
Andrew Boyce

Characterization of Spreading Depolarization And Epileptiform Activity Following İnduction of Focal Cerebral Ischemia in Awake Mice
Samuel Flaherty

14:30-16:30 Posters with Coffee+Snacks

The Effect of Noninvasive Cortical Spreading Depolarizations on a Test of Executive Function
Lydia Hawley

Nimodipine Reduces Microglial Activation by Spreading Depolarization and in Response To Lipopolysaccharide, As Evidenced by Morphological Phenotype and RNA Sequencing
István Pesti

Pre-Stroke or Post-Stroke Spreading Depolarization and Ischemia Do Not Affect Stroke Outcomes in a New Mouse Model of Focal Ischemic Stroke, Naim
Kyusun Han

Effects of Metabolic Inhibition on Intracellular CA2+ And ATP in Human Cortical Brain Organoid Slice Cultures (CBOS)
Laura Petersilie

Activation of TRPV4 Channels Promotes The Loss Of Cellular Atp in Mouse Neocortex Exposed to Chemical Ischemia
Nils Pape

Combined Dasatinib and Quercetin Treatment After Carotid Artery Stenosis Limits Spreading Depolarization During Subsequent Acute Ischemic Stroke in Aging Rats
Szilvia Kecskés

Pro-Epileptic Effects of Spreading Depolarizations
Daria Vinokurova

Impact of Cortical Spreading Depolarization on Neural Precursor Dynamics and Neurogenesis in The Adult Dentate Gyrus
Anja Urbach

16:30-17:30 Keynote
Moderator: **Jed Hartings**

Clinical Neuromonitoring in the Intensive Care Unit: Spreading Depolarizations in Real Time and in the Real World
Brandon Foreman

20:00-21:00 Late Night Roundtables

The Potential of Pharmacological Interventions Targeting CSD Pathways **Hülya Karataş, Istvan Pesti**

Carreer Discussions for SD Researchers: Grantsmanship and Promotion **Jed Hartings, Melike Sever Bahçekapılı**

17 NOVEMBER 2024, SUNDAY

09:00-09:30 Recap iCSD 2024
Britta Lindquist

09:30-09:45 Oral and Poster Presentation Awards

09:45-10.00 Concluding Remarks

ORAL PRESENTATIONS

OP-1 (ID:62)

INITIAL RESULTS OF THE INDICT FEASIBILITY TRIAL OF SPREADING DEPOLARIZATION MONITORING TO GUIDE MANAGEMENT OF SEVERE TRAUMATIC BRAIN INJURY

JED HARTINGS [1], LAURA NGWENYA [1], JENNIFER GOLDTHWAIT [1], DANIELLE SANDSMARK [2], JENS DREIER [3], BRANDON FOREMAN [1],

[1] *UNIVERSITY OF CINCINNATI*
[2] *UNIVERSITY OF PENNSYLVANIA*
[3] *CHARITE-UNIVERSITATSMEDIZIN BERLIN*

Introduction:
Clinical studies on spreading depolarizations (SD) in stroke and brain injury have documented that greater SD burden is associated with new lesion development and worse outcomes. Several strategies to mitigate SDs have been proposed, and ketamine in particular has proven efficacy to reduce SD burden in both clinical and animal studies. We therefore developed a protocol as a first attempt to integrate real-time SD monitoring and treatment into neurointensive care of traumatic brain injury. This protocol is being tested in a multi-center, randomized, feasibility trial, "Improving Neurotrauma by Depolarization Inhibition with Combination Therapy" (INDICT). Here we report initial results from the trial.

Methods:
Patients who receive electrocorticography strips as standard care monitoring for surgically treated brain trauma are enrolled after surrogate informed consent. Those who exhibit SD are then randomized 1:1 to (a) standard care with blinding to electrocorticography or (b) a tiered intervention protocol (thee tiers T1-3) aimed at SD prevention and suppression. T1 includes targets for cerebral perfusion pressure (>70mmHg, or SBP>120mmHg) and serum glucose (140-180 mg/dL); T2 adds a P_aCO_2 target of >40mmHg, core temperature target of <37.0°C, and ketamine infusion at 1 mg/kg/hr; T3 increases the ketamine dosing to 2-4 mg/kg/hr in titrated steps. Patients are escalated to higher tiers as soon as 3 SDs are observed on current treatments and are de-escalated to lower tiers after defined periods of complete SD suppression (Tier3àTier2: 12 hr; Tier2àTier1: 24 hr; Tier1àstandard care: 48 hr). Data are reported as median values.

Results:
Since January 2023, 18 patients have been enrolled at 2 sites (Cincinnati and Philadelphia). Five patients (28%) had no SDs and one had difficulties with real-time monitoring; these patients were not randomized. The remainder were randomized 19 hr (median) after the start of electrocorticography when SDs were observed. Five were assigned to treatment and seven to standard care. Those in the treatment group had 2.9 SD/day over 7.6 days of electrocorticography after randomization, while the standard care group had 5.7 SD/day over 2.3 days. The treatment group trended toward longer overall durations of monitoring (8.1 vs. 4.9 days), as the protocol requires continued monitoring until SDs are suppressed for 24 hours. All five treated patients required escalation to T2, and three were escalated to T3. Due to multiple escalations and de-escalations, there were 13 total trials of T1 (cumulative duration: 11.3 days), 13 of T2 (15.6 days), and 5 of T3 (3.6 days). SD rates over these cumulative durations for T1, T2, and T3 were 5.4, 2.3, and 1.7 SD/day, respectively. Individual cases evidenced a strong efficacy of T2 and T3 to block SDs. All patients (5/5) in the treatment group survived to discharge from intensive care, as compared to 43% (3/7) in the standard care group.

Discussion:
Results thus far demonstrate the feasibility of implementing a complex, tier-based neurointensive care protocol for severe brain trauma based on real-time monitoring of SDs. While interim statistical analysis was not planned or conducted, results to date are consistent with the possibility that SD burden will be reduced in treated patients compared to those receiving standard care with blinding to SD course. Initial experience has highlighted the conservative nature of the treatment protocol, with slow escalation of therapeutic intensity and aggressive de-escalation. This approach likely yields less suppression of SDs than might be achieved with other protocols. The study aims to randomize an additional 30 patients to complete the study.

OP-2 (ID:107)

CONTINUOUS MONITORING OF CEREBROVASCULAR AUTOREGULATION USING FUNCTIONAL ULTRASOUND IMAGING IN THE PIGLET BRAIN

DIETVORST SOFIE [1], BRUNNER CLEMENT [2], MONTALDO GABRIEL [2], DEPREITERE BART [1], URBAN ALAN [2],

[1] *KU LEUVEN*
[2] *NERF NEURO-ELECTRONİCS RESEARCH FLANDERS*

Abstract:
Currently, there are no available tools that allow for continuous real-time bedside monitoring of cerebral blood flow (CBF), nor are there validated direct methods to measure cerebrovascular autoregulation (CA) capacity in patients. However, such data would be invaluable for guiding arterial blood pressure (ABP) management in cases of acute brain injury. In this study, we utilized functional ultrasound (fUS) imaging within a porcine cranial window model to monitor and compare CA hemodynamics with measurements obtained using Laser Doppler Flowmetry (LDF) and red blood cell (RBC) flux.

Six 6-week-old piglets were anesthetized and fitted with invasive monitors for arterial blood pressure (ABP), intracranial pressure (ICP), and LDF probes. Cranial windows were created to allow for the measurement of RBC flux in pial arterioles and for brain hemodynamic imaging using fUS. The piglets underwent non-pharmacological manipulation of ABP via the inflation and deflation of intraaortic or intracaval balloons. Hemodynamic parameters derived from fUS, including signal intensity and velocity, were compared with calculated RBC flux from microscopy and LDF measurements during ABP alterations.

fUS imaging successfully provided continuous monitoring of changes in signal intensity and velocity in both arterioles and veins within a 16-mm width by 15-mm depth section of the piglet brain. By calculating the fUS signal intensity and velocity, we were able to obtain robust estimates of CBF, which exhibited a strong correlation with RBC flux measurements. The study demonstrated that ultrasound-based hemodynamic monitoring offers a direct, accurate, and stable method for assessing CA and its limits when compared with both LDF and RBC flux measurements.

In conclusion, fUS imaging has the potential to become a transformative tool for bedside clinical assessment of CBF due to its high accuracy and ease of transferability to patient care. This technology could provide real-time, non-invasive insight into cerebral hemodynamics, enabling clinicians to optimize ABP management in critical care settings.

OP-3 (ID:104)

SPATIAL DYNAMICS OF HUMAN SPREADING DEPOLARIZATIONS: PRELIMINARY RESULTS APPLYING A NEWLY DEVELOPED TWO-DIMENSIONAL STRIP

LIANGCHEN GUO , TRINE HJORSLEV ANDREASEN , KIRSTEN MøLLER , TORBEN ESPENHEIM , MARTIN FABRICIUS ,

RİGSHOSPİTALET, COPENHAGEN

Introduction:

In the injured gyrencephalic brain, spreading depolarizations (SDs) propagate in a complex fashion and may even circulate around the primary cortical lesion. SDs may promote secondary neuronal injury. The linear velocity of SDs is affected by multiple factors, and it is hypothesized that changes in velocity may reflect changes in the condition of the tissue and potentially be a marker of deterioration of the homeostasis of the cortex. Further study of the factors that govern SD propagation velocity could potentially improve future management of patients with acute brain injury.

SDs in the acutely injured human brain are usually monitored using an electrode strip with six platinum electrodes placed in a linear pattern. The SD waves, however, may propagate in any direction rendering it impossible to evaluate the linear velocity of propagation.

Methods:

To further characterize the spread of SDs, we have designed a strip in a two-dimensional pattern while almost maintaining the outer dimensions of the conventional 6-electrode strip. Contact points are printed on silicone as opposed to the conventional linear strip. This allows the strip to be marginally wider than the conventional strip while maintaining high flexibility. The electrode pattern enables two-dimensional measurements (XY-axes) and covers a greater brain area. We expect the new strip design to enable more precise measurement of SD spread and velocity, and to provide useful data in case of suboptimal electrode placements.

We included patients undergoing acute craniotomy due to trauma, spontaneous subarachnoid hemorrhages, or intracerebral hematomas. The novel strip was placed in the same fashion as a conventional strip at the end of the operation. At the end of monitoring, the strip was removed bedside by gentle traction.

Results:

The novel strip has been used on a total of six patients included in the ongoing trial KETA-BID at Rigshospitalet, Copenhagen. The total monitoring time ranged from six to 14 days. No instances of infection or hemorrhage due to the strip was observed; one patient experienced CSF leakage, which stopped after removal of the strip.

The strip contained a newly designed connection section to allow the strip to be tunneled from inside-out before being attached to the amplifier leads. This connection section proved to be unstable for long term recordings and had to be modified several times. Due to this impediment, many recording channels failed during the recording.

So far, we have succeeded in obtaining data of sufficient quality, where SDs recorded from the new strip were comparable in morphology and propagation to SDs recorded from linear strips. We have further characterized the time intervals where data of sufficient quality could be obtained from the novel strip. The longest period with optimal signal from all eight electrodes was 706 minutes.

Conclusion:

The novel electrode appears to be a safe tool for placement in patients to observe SDs. The problems with the strip connection section were unrelated to the design of electrode contacts, However, it has limited the number of data we have obtained so far.

We have demonstrated that it is feasible to produce and place, in a patient, a novel strip with electrodes placed in a two-dimensional pattern. With the strip, we have obtained measurements of SDs similar to conventional, linear strips. We hypothesize that the novel strip may enable more precise measurement of SD spread and velocity. However, this requires further data, modelling, and signal analysis.

OP-4 (ID:58)

CORTICAL SPREADING DEPOLARIZATION DURING SURGICAL MANAGEMENT OF CEREBRAL ARTERIOVENOUS MALFORMATIONS AND ARTERIOVENOUS FISTULAS

PATRICK DOMER [1], SIMEON O. A. HELGERS [1], FRANZISKA MEINERT [1], MARYAM SAID [1], RENAN SACHEZ-PORRAS [1], CHRISTIAN MATHYS [2], JOAHNNES WOITZIK [1],

[1] DEPARTMENT OF NEUROSURGERY, CARL VON OSSİETZKY UNİVERSİTY OLDENBURG, OLDENBURG, GERMANY
[2] DEPARTMENT OF RADİOLOGY AND NEURORADİOLOGY, EVANGELİSCHES KRANKENHAUS OLDENBURG, GERMANY

Introduction:
Cerebral arteriovenous malformations (AVMs) and arteriovenous fistulas (AVF) represent pathological vascular anomalies characterized by abnormal arterio-venous anastomoses, bypassing the typical intervening capillary network. This results in altered hemodynamics, an increased risk of hemorrhage as well as neurological deficits. Despite the description of SDs in acute diseases like ischemic stroke, subarachnoid hemorrhage or traumatic brain injury SD have been also shown in chronic diseases like migraine. Furthermore, a recent publication has shown SDs in moyamoya disease. There is, however, currently no direct evidence for the occurrence of SDs in patients with AVMs or AVFs.

Methods:
Using intraoperative Laser Speckle Contrast Imaging, cortical perfusion was recorded in nine patients undergoing surgical AVM resection and two patients with surgical AVF treatment for at least 5 minutes. Measurements were taken after surgical treatment of the vascular anomality before closing the surgical situs. Cortical perfusion was analyzed across the whole exposed cortical surface the occurrence of SD.

Results:
Spontaneous SD activity was observed in 2 patients. One patient was undergoing AVM resection, whereas the in the other patient, a AVF was surgically treated. Within those two patients, four SDs were observed. The hemodynamic response was characterized by a traveling wave of local hyperperfusion.

Conclusion:
By employing intraoperative laser speckle perfusion measurement, spontaneous intraoperative SD activity was observed for the first time during the treatment of AVM and AVF. SDs could potentially be triggered by the altered hemodynamics induced by surgical interventions. Furthermore, SD might play a role in the pathomechanism of symptoms even related to AVMs and AVFs even before treatment and should be considered in the postoperative phase of these pathologies.

OP-5 (ID:24)

SPREADING DEPOLARIZATION CONTINUUM IN THE AGED NON-HUMAN PRIMATE AFTER FOCAL ISCHEMIC STROKE

JEREMY J. SWORD [1], TYLER SPARKS [2], LUCA H. DEBS [2], SEBASTIAN MAJOR [3], SUASH J. SHARMA [5], MICHAEL A. JENSEN [6], DEBRA MOORE-HILL [7], KAREN BARTON [7], K. ALFREDO GARCIA [7], MANAN SHAH [7], JEFFREY A. SWITZER [7], DAVID T. BLAKE [1], FERNANDO L. VALE [2], JENS P. DREIER [8], JED A. HARTINGS [9], SERGEI A. KIROV [4],

[1] *DEPT. OF NEUROSCİENCE AND REGENERATİVE MEDİCİNE, MEDİCAL COLLEGE OF GEORGİA AT AUGUSTA UNİVERSİTY, AUGUSTA, GEORGİA, USA*

[2] *DEPT. OF NEUROSURGERY, MEDİCAL COLLEGE OF GEORGİA AT AUGUSTA UNİVERSİTY, AUGUSTA, GEORGİA, USA*

[3] *DEPT. OF NEUROLOGY, CENTER FOR STROKE RESEARCH BERLİN AND DEPT. OF EXPERİMENTAL NEUROLOGY, CHARİTE´ UNİVERSİTY MEDİCİNE, BERLİN, GERMANY*

[4] *DEPT. OF NEUROSCİENCE AND REGENERATİVE MEDİCİNE AND DEPT. OF NEUROSURGERY, MEDİCAL COLLEGE OF GEORGİA AT AUGUSTA UNİVERSİTY, AUGUSTA, GEORGİA, USA*

[5] *DEPT. OF PATHOLOGY, MEDİCAL COLLEGE OF GEORGİA AT AUGUSTA UNİVERSİTY AND CHARLİE NORWOOD VA MEDİCAL CENTER, AUGUSTA, GA, USA*

[6] *DEPT. OF MEDİCAL ILLUSTRATİON, MEDİCAL COLLEGE OF GEORGİA AT AUGUSTA UNİVERSİTY, AUGUSTA, GEORGİA, USA*

[7] *DEPT. OF NEUROLOGY, MEDİCAL COLLEGE OF GEORGİA AT AUGUSTA UNİVERSİTY, AUGUSTA, GEORGİA, USA*

[8] *DEPT. OF NEUROLOGY, CENTER FOR STROKE RESEARCH BERLİN AND DEPT. OF EXPERİMENTAL NEUROLOGY, CHARİTE´ UNİVERSİTY MEDİCİNE, BERLİN, BERNSTEİN CENTER FOR COMPUTATİONAL NEUROSCİENCE BERLİN AND EİNSTEİN CENTER FOR NEUROSCİENCES BERLİN, BERLİN, GERMANY*

[9] *DEPT. OF NEUROSURGERY, UNİVERSİTY OF CİNCİNNATİ COLLEGE OF MEDİCİNE AND MAYFİELD CLİNİC, CİNCİNNATİ, OH, USA*

Abstract:

Comprehensive clinical data revealed that spreading depolarization (SD) plays a central role in developing cortical lesions in patients with acute brain injury. However, detailed mapping of the brain's electrical activity in clinics at the onset of focal ischemic stroke and during the initial phase of cortical injury development is lacking because electroencephalography (ECoG) monitoring typically starts hours or days after focal ischemia. Non-human primate (NHP) models are considered the best representation of human stroke due to their genetic, physiological, and anatomical similarities to humans. Craniotomies were performed over the left and right hemispheres on five male and female nemestrina and rhesus macaques aged 23-32 years. Subdural electrode arrays were placed bilaterally over the middle cerebral artery (MCA) territory, recording from 24 electrodes 1 cm apart on the left cortex and 7 electrodes on the right. After 30 minutes of baseline ECoG, the left MCA and, in some cases, also the left internal carotid or anterior cerebral arteries were permanently occluded with aneurysmal clips. Repetitive SDs were recorded during the next 3 hours, followed by terminal SD during euthanization. No epileptiform activity was noted in any of the five animals. Non-spreading electrical silence developed in the ischemic core within seconds of ischemic onset, followed by SD and SD-initiated negative ultraslow potential (NUP) with a substantial delay. These events defined the ischemic core and led to histologically confirmed cell damage. The initial and subsequent transient SDs caused the spreading depression of spontaneous activity at the normally perfused surrounding cortex without any signs of histological damage. Circulatory arrest at the end of experiments first induced non-spreading depression of activity followed by SD and, eventually, the SD-initiated NUP, which indicated brain death. Results in gyrencephalic NHP hold significant implications for understanding the causal role of SD in acute brain injury development alongside the SD continuum as it transitions from persistent depolarization in the severely ischemic cortex to transient depolarization in the normal brain.

Supported by the National Institutes of Health Grants RF1-AG060754 (DTB), NS083858 (SAK), the Intramural Grants Program IGPP00057 (SAK), and funding from the Department of Neurosurgery, Medical College of Georgia at Augusta University. JPD received funding from Deutsche Forschungsgemeinschaft (DFG DR 323/10-2).

OP-6 (ID:22)

HIGH-FREQUENCY OSCILLATIONS DURING CORTICAL SPREADING DEPOLARIZATION

AZAT NASRETDINOV [1], DARIA VINOKUROVA [1], ELVIRA JUZEKAEVA [1], GULSHAT ZAKIROVA [1], BULAT MINGAZOV [1], KARINA TUKHVATULLINA [1], ROUSTEM KHAZIPOV [2],

[1] *KAZAN FEDERAL UNIVERSITY, KAZAN, RUSSIA*
[2] *KAZAN FEDERAL UNIVERSITY, KAZAN, RUSSIA; INMED, INSERM, AIX-MARSEILLE UNIVERSITY, MARSEILLE, FRANCE.*

Introduction:
Spreading depolarizations (SDs) are usually expressed as a slow potential shifts and suppression of activity in the traditional EEG frequency band. Here we show that long-lasting high-frequency oscillations (HFOs) occur during SDs at the rat cortical surface as a counterpoint to the depression of activity, and can serve as a robust marker for SD detection.

Methods:
Multi-channel subdural ECoG arrays, intracortical silicon probes, and Ag EEG wires were used to record full-band cortical activity (0-16kHz) from the somatosensory cortex of urethane-anesthetized head restrained rats. SDs were induced by epipial application of potassium chloride, inhalation of flurothyl in the epilepsy model, pinprick in the injury model, and injection of endothelin-1 or rose bengal in the ischemia models. SD propagation was also monitored using intrinsic optical imaging.

Results:
We found that during ECoG recordings from the cortical surface, potassium-evoked SDs were typically accompanied by HFOs in the range of 60-150 Hz. HFOs were observed at the SD onset and during the negative DC shift of the SD, lasted from a few to tens of seconds, and occurred as a counterpoint to the depression of activity in the traditional EEG bands (0.5-45 Hz). HFOs spread horizontally along the cortex in association with SDs. Interestingly, HFOs were also present during "isoelectric" SDs, occurring at short inter-SD intervals in SD clusters. HFOs could also be detected during high potassium-induced SDs using EEG recordings from the skull surface. HFOs were also characteristic of SDs in several models, including ischemia, epilepsy, and traumatic brain injury. Intracortical recordings revealed that SD-associated HFOs are generated by the pre-SD excitation wave, which synchronizes neuronal network activity in local (~300 micrometers) fast gamma oscillations and propagates vertically through the cortical depth from superficial to deep layers along with vertical SD propagation. In cases of partial SDs that failed to propagate through the entire cortical depth, HFOs were also supported by fast gamma activity in the sub-SD zone through the entire time course of the SD above. The power of HFOs at the cortical surface correlated strongly with the level of neuronal synchronization in fast gamma oscillations in the pre-SD and sub-SD zones.

Conclusions:
Thus, HFOs could serve as a potential marker of SD in addition to the classical SD detection algorithms based on DC shift and suppression of AC-activity.

This research was funded by the Russian Science Foundation grant № 24-75-10054 (https://rscf.ru/en/project/24-75-10054/)

OP-7 (ID:76)

NONINVASIVE OPTICAL DETECTION OF SPREADING DEPOLARIZATION IN RAT

ELYSSA ALBER , QINGLING ZHAI , LYDIA HAWLEY , ANDREIA MORAIS , CENK AYATA , DAVID CHUNG ,

NEUROVASCULAR RESEARCH UNİT, MASSACHUSETTS GENERAL HOSPİTAL

Abstract:

Cortical spreading depolarizations (CSD) are implicated in the pathogenesis of migraine with aura and are associated with neurological decline after acute brain injury. CSDs can be observed in mice noninvasively with light through intact skull. However, rats have thicker skulls and noninvasive optical detection of CSDs has not been reported. Therefore, we sought to detect CSDs optically in rats using a longer wavelength light than previously attempted to penetrate tissue at greater depths. Rats were placed under isoflurane anesthesia. Mineral oil was applied immediately after scalp incision and reapplied during and after periosteum removal. Three burr holes were drilled, one for inducing CSDs and two for recording electrodes to confirm CSD occurrence. CSDs were induced with bipolar electrode stimulation or KCl application. Laser speckle flowmetry (LSF) was performed using an 840nm coherent light source with Basler Ace USB camera. Every second, speckle contrast images were obtained by calculating the mean and standard deviation of reflectance over 50 frames. Relative cerebral blood flow (CBF) maps were computed by solving for the relationship between the speckle time constant (tc) and the speckle contrast where 1/tc is proportional to cerebral blood flow (CBF). Qualitatively, CSDs were more readily detected using a moving reference instead of a static, fixed baseline (Figure A). Region-of-interest-based relative CBF changes due to CSDs were apparent and quantifiable (Figure B). We optically detected all CSDs that were detected with recording electrodes (n = 6 CSDs). In conclusion, noninvasive optical CSD detection is possible in rats and can be used to determine quantifiable changes in cerebral blood flow across the entire dorsal surface of the brain. Additional studies focused on minimally-invasive CSD induction approaches or non-invasive assessment of disease states with spontaneously occurring CSDs are feasible.

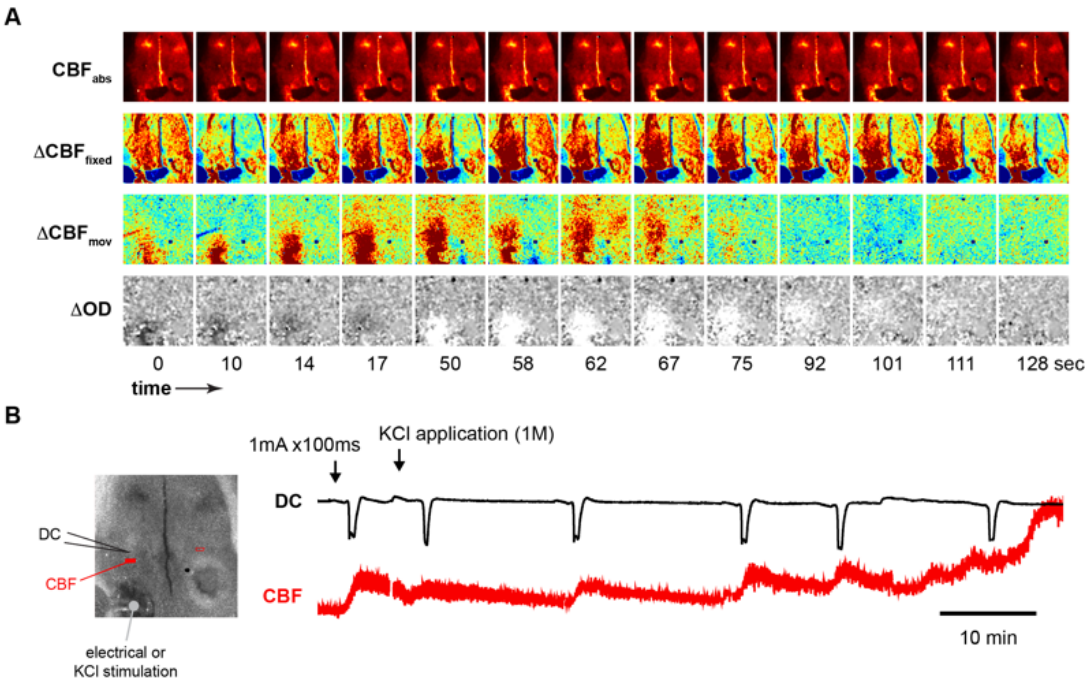

Figure. Cortical spreading depolarizations (CSD) can be detected with near infrared light through intact rat skull. (A) Representative time lapse images of the third CSD in the left hemisphere of a rat post KCl application (1M) to the visual cortex. CBF_{abs} represents a map that is proportional to absolute cerebral blood flow (CBF). delta CBF_{fixed} is a CBF map relative to a baseline before the first CSD. delta CBF_{mov} is a CBF map with a moving reference point. delta OD represents relative reflectance of infrared light with respect to a moving reference point. (B) Direct current (DC) record and CBF tracing from a region of interest (solid red rectangle) which demonstrates electrical (1 mA for 100 ms) or KCl CSDs originating from left visual cortex.

OP-8 (ID:31)

THE INTRODUCTION OF A NOVEL VISUALIZATION METHOD OF CEREBRAL BLOOD FLOW CHANGES IN MICE WITH AN RGB CAMERA: THE EFFECTS OF BOSENTAN ON SPREADING DEPOLARIZATIONS INDUCED BY EXPERIMENTAL AIR-EMBOLI MODEL VIA EXTERNAL CAROTID ARTERY CANNULATION

MEHMET TOLGA DOĞRU [1], TOLGA İNAN [5], HAYRUNNİSA BOLAY BELEN [2], MEHMET YILDIRIM SARA [3], ERGİN DİLEKÖZ [4],

[1] KIRIKKALE ÜNİVERSİTESİ TIP FAKÜLTESİ KARDİYOLOJİ AD.
[2] GAZİ ÜNİVERSİTESİ TIP FAKÜLTESİ NÖROLOJİ AD.
[3] HACETTEPE UNİVERSİTESİ TIP FAKÜLTESİ TIBBİ FARMAKOLOJİ AD.
[4] GAZİ ÜNİVERSİTESİ TIP FAKÜLTESİ TIBBİ FARMAKOLOJİ AD.
[5] TOBB ETU YAPAY ZEKA MÜHENDİSLİĞİ BD.

Abstract:

Since the discovery and definition of cortical spreading depolarizations (CSD) by Leão in 1944, the phenomenon has become one of the most important research topics of experimental migraine studies due to its electrophysiological, electrochemical and vascular features. Besides, the clinical aspects of both migraine and cerebrovascular events such as stroke and hemorrhages and their related complications (i.e. peri-infarct depolarizations) increase the demand for a reliable animal model in order to achieve relevant data regarding pathological features of such incidences.

Hereby, we introduce a novel, practical and relatively inexpensive, yet efficient visualization technique, utilizing an RGB camera and a software to observe the blood flow changes from images obtained from the skulls of mice. This new method provided us with reasonably high resolution images (Figure 1) and reduced some of the physical and economical limitations of previously described modalities such as laser speckle contrast imaging and laser doppler flowmetry. For the assessment of the accuracy of our method in detecting blood flow changes, we compared our results with the data obtained via laser doppler flowmetry and noted that both modalities produced similar outcomes (Figure 2) in response to CSDs induced by potassium chloride administration (Spearman correlation test; $r=0.8694$; $p<0.0001$)

With the help of this new technique, we investigated the effects of non-selective endothelin receptor antagonist bosentan on cortical spreading depolarizations induced by air embolies (0.5 mL air, trapped in filtered saline) delivered through a cannula intruded in to the external carotid artery. Microembolization of the cerebral cortex initiated CSDs in mice with almost no exception. Bosentan application (i.p. 30mg/kg) did not produce a visible variation in basal cortical blood flow nor in arterial blood pressure. Bosentan however, changed the spreading pattern of CSDs and caused prominent and bilateral depolarization waves in mice, whereas bilateral CSDs were rare in control animals. Bosentan administration also altered the depth of the oligemia produced by CSDs. The spreading velocity of CSD waves did not differ significantly within both control and bosentan groups, whereas the measured velocity was slightly lower under bosentan influence.

In electrophysiology setups, the administration of bosentan significantly increased the slope of the recorded DC shifts ($p< 0.01$) whereas the differences in amplitude and the duration of depolarization waves, were insignificant. Similarly bosentan administration increased the slopes and area-under-curves of somatosensorial evoked potentials provoked by the stimulation of whisker pads of the mice ($p<0.05$).

Our results suggested a possible role for endothelins and their contribution to neuro-vascular coupling processes of spreading depolarizations.

OP-9 (ID:)

MEMS-BASED SU-8 NEURAL PROBES FOR ENHANCED NEUROMONITORING

ALİ CAN ATİK [1] LEMAN DİCLE BALCI [1] ÖZLEM TOPÇU [1] AKIN MERT YILMAZ [2] ŞAHİN HANALİOĞLU [3] HÜLYA KARATAŞ [4] HASAN ULUŞAN [1] MAHMUT KAMİL ASLAN [2] HALUK KÜLAH [1]

1- DEPARTMENT OF ELECTRICAL AND ELECTRONICS ENGINEERING, MIDDLE EAST TECHNICAL UNIVERSITY (METU), ANKARA, TURKEY
2- METU MEMS RESEARCH AND APPLICATIONS CENTER, ANKARA, TURKEY
3- DEPARTMENT OF NEUROSURGERY, FACULTY OF MEDICINE, HACETTEPE UNIVERSITY, ANKARA, TURKEY
4- INSTITUTE OF NEUROLOGICAL SCIENCES AND PSYCHIATRY, HACETTEPE UNIVERSITY, ANKARA, TÜRKİYE

In cases of traumatic brain injury (TBI), most patients experience cortical spreading depolarizations (CSDs) waves, with many exhibiting continuous, repetitive series lasting several days or even weeks after the injury. CSD is a wave of neuronal depolarization that spreads slowly across the gray matter of the central nervous system. The sustained depolarization triggers metabolic acidosis, leading to vasoconstriction, which reduces blood supply, increases blood-brain barrier permeability, and results in vasogenic edema. This hemodynamic response creates a pathological feed-forward cycle that drives the recurrence of further CSDs [1,2]. These recurrent CSD waves can lead to secondary brain injury, increased risk of late post-traumatic seizures, and epilepsy. Therefore, the neuromonitoring of CSDs is of great importance for the early diagnosis and treatment of secondary brain injury. In this work, we propose the design and microfabrication of a neural probe for the neuromonitoring of patients with acute brain injury. Despite their widespread use, traditional silicon-based neural probes often lead to tissue inflammation and irreversible brain damage due to their rigidity and are prone to breakage during manipulation because of their brittleness. In contrast, more flexible materials such as polyimide [3], parylene C [4] and SU-8 [5] offer a less invasive alternative thanks to their good biocompatibility, electrical insulation properties, and microfabrication compatibility. Among these polymers, SU-8 offers an adjustable thickness sufficient for improved insertion, while the other polymers remain excellent choices for planar electrode technology. Therefore, a micro-electromechanical system (MEMS)-based SU-8 neural probe is designed for placement on a mouse brain, incorporating a microelectrode array to detect CSDs and determine the rate and direction of their propagation across cortical layers. The microelectrode array, with its closely spaced electrodes, provides more detailed spatial resolution compared to conventional electrodes, allowing for more precise mapping of CSD activity. Additionally, the compatibility with MEMS fabrication techniques could allow for the future integration of various microsensors and microchannels, potentially enhancing the probes functionality. In conclusion, the development of a MEMS-compatible neural probe represents a significant advancement in neuromonitoring, providing more accurate monitoring of CSDs in TBI.

Acknowledgement

This work was funded by The Scientific and Technological Research Council of Turkey (TUBITAK) within the scope of 1004 - Center of Excellence Support Program with the grant number of 22AG008

References

[1] D. R. Kramer, T. Fujii, I. Ohiorhenuan, and C. Y. Liu, "Interplay between cortical spreading depolarization and seizures," Stereotact. Funct. Neurosurg., vol. 95, no. 1, pp. 1-5, 2017, doi: 10.1159/000452841.
[2] J. P. Dreier et al., "Recording, analysis, and interpretation of spreading depolarizations in neurointensive care: Review and recommendations of the COSBID Research Group," Journal of Cerebral Blood Flow & Metabolism, vol. 37, no. 5, pp. 1595–1625, Jul. 2016. doi:10.1177/0271678x16654496.
[3] K. Xie et al., "Portable wireless electrocorticography system with a flexible microelectrodes array for epilepsy treatment," Sci. Rep., vol. 7, no. 1, 2017, doi: 10.1038/s41598-017-07823-3.
[4] X. Wang et al., "A parylene neural probe array for multi-region deep brain recordings," J. Microelectromech. Syst., vol. 29, no. 4, pp. 499-513, 2020, doi:10.1109/jmems.2020.3000235.
[5] A. Altuna et al., "SU-8 based microprobes for simultaneous neural depth recording and drug delivery in the brain," Lab Chip, vol. 13, no. 7, pp. 1422-1430, 2013, doi: 10.1039/C3LC41364K.

OP-10 (ID:77)

NONINVASIVE, AUTOMATED DETECTION OF SPREADING DEPOLARIZATIONS USING SCALP ELECTROENCEPHALOGRAPHY: A MULTICENTER VALIDATION IN PATIEITS WITH AND WITHOUT SKULL DEFECT

ALİREZA CHAMANZAR [1], ERIC S. ROSENTHAL [2], SEBASTIAN MAJOR [4], SHRAVAN SIVAKUMAR [5], JONATHAN ELMER [6], LORI SHUTTER [7], COLINE L. LEMALE [4], AMAN B. PATEL [8], CHRISTOPHER J. STAPLETON [8], JED HARTINGS [9], JENS P. DREIER [4], PULKIT GROVER [1], DAVID Y. CHUNG [3],

[1] *DEPARTMENT OF ELECTRİCAL AND COMPUTER ENGİNEERİNG, CARNEGİE MELLON UNİVERSİTY, PİTTSBURGH, PA*
[2] *DEPARTMENT OF NEUROLOGY, MASSACHUSETTS GENERAL HOSPİTAL, BOSTON, MA*
[3] *NEUROVASCULAR RESEARCH UNİT, DEPARTMENT OF RADİOLOGY, MASSACHUSETTS GENERAL HOSPİTAL, HARVARD MEDİCAL SCHOOL, CHARLESTOWN, MA*
[4] *CHARİTé UNİVERSİTäTSMEDİZİN BERLİN, FREİE UNİVERSİTäT BERLİN AND HUMBOLDT-UNİVERSİTäT ZU BERLİN, CENTER FOR STROKE RESEARCH BERLİN, CHARITé UNIVERSITäTSMEDIZIN BERLIN, GERMANY*
[5] *DEPARTMENT OF NEUROLOGY, BETH ISRAEL DEACONESS MEDİCAL CENTER, BOSTON, MA*
[6] *DEPARTMENTS OF EMERGENCY MEDİCİNE, CRİTİCAL CARE MEDİCİNE AND NEUROLOGY, UNİVERSİTY OF PİTTSBURGH SCHOOL OF MEDİCİNE, PITTSBURGH, PA*
[7] *DEPARTMENTS OF CRİTİCAL CARE MEDİCİNE, NEUROLOGY AND NEUROSURGERY, UNİVERSİTY OF PİTTSBURGH SCHOOL OF MEDİCİNE, PITTSBURGH, PA*
[8] *DEPARTMENT OF NEUROSURGERY, MASSACHUSETTS GENERAL HOSPİTAL, BOSTON, MA*
[9] *DEPARTMENT OF NEUROSURGERY, UNİVERSİTY OF CİNCİNNATİ, CİNCİNNATİ, OH*
*Co-first authors

Background:
Each year, more than 3.6 million Americans suffer an acquired brain injury (ABI) related to traumatic brain injury (TBI) or stroke[1]. TBI, as the major group of ABI, affects 2.5 million people in the US[2] and is a principal cause of mortality and lifelong disability[3,4]. More than 50% of patients with moderate or severe TBI experience neurological worsening or death[5,6]. Growing evidence over the past two decades shows that *spreading depolarizations* (SDs) reliably predict poor outcomes after TBIs[7] and stroke[8–13].Clinical detection of SDs requires intracranial electroencephalography (EEG), an invasive method with limited spatial coverage. We previously established in a single center cohort the feasibility of noninvasive detection and tracking of SD from scalp EEG in patients with a skull defect after craniectomy. Here, we used advances in deep learning and signal processing to assess the external validity of our approach in a multicenter cohort of patients, including those with intact skulls and those who have undergone craniectomy.

Methods:
We tested the performance of our previously developed WAVEFRONT algorithm on three cohorts of patients: (i) Cincinnati dataset[14]: a cohort of 12 severe TBI patients with a total of 700 SDs (including 2 control patients without any SDs) who underwent simultaneous scalp EEG monitoring and gold standard invasive monitoring from a subdural electrode strip placed on a pericontusional gyrus during decompressive hemicraniectomy. The skull was surgically absent at the site of intracranial recording for all patients, (ii) MGH dataset[13]: a cohort of 12 TBI and subarachnoid hemorrhage (SAH) patients with a total of 124 SDs (including 6 control patients without any SDs), who underwent simultaneous scalp EEG monitoring and gold standard invasive monitoring from a subdural electrode strip placed at the site of injury during craniotomy. The bone flap was replaced before the recording from these patients, and (iii) Berlin dataset[15]: a cohort of 5 SAH (intact skull) and 3 malignant hemispheric stroke (MHS, skull defect) patients with a total of 453 SDs, who underwent simultaneous scalp EEG monitoring and gold standard invasive monitoring from a subdural electrode strip placed at the site of injury on a viable tissue in SAH patients during craniotomy or on a viable peri-infarct tissue in MHS patients during hemicraniectomy. The bone flap was replaced before the recording of the SAH patients, while the skull was surgically absent for the MHS patients. EEG electrodes were placed at standard 10-20 locations in the Cincinnati and MGH datasets. For the Berlin EEG data, partial scalp coverage was performed mostly over the side ipsilateral to subdural strip. We assessed the generalizability of WAVEFRONT in two different ways (summarized in Fig. 2): (i) from one center to the other, and (ii) one group of patients (i.e., with or without skull defect) to the other. We used true positive rate (TPR) and false positive rate (FPR) as two main performance metrics, defined in 2min overlapping time windows (with 30s overlap), closely following the steps in our previous work[14].

Results:
WAVEFRONT detects SDs in the intact skull cohort (17 patients from MGH and Berlin) with an average validation TPR of 79% with less than 1.5% FPR. WAVEFRONT achieves the best performance on the MGH cohort with 82% TPR and less than 2% FPR, followed by Berlin and University of Cincinnati (UC) cohorts (see Fig.1 A for details). WAVEFRONT, once trained on the MGH cohort, shows a unidirectional generalizability to the other two cohorts with an average TPR of more than 76% and less than 5% FPR (see Fig. 2A). Training on both intact and skull defect patients achieves a more generalizable model with a TPR of 76% with less than 2% FPR across all the 32 patients in this multicenter cohort (see Fig. 1B).

Conclusions:
These results, for the first time, show the feasibility of noninvasive SD detection in a diverse cohort of ABI patients, with generalizability to new patients (e.g., from different centers) and monitoring conditions (e.g., with or without skull defects). The results on the intact skull cohort highlights the performance of our noninvasive technique in the most challenging scenario where the skull is present during the monitoring of patients. Training on the intact skull cohort, generalizes to the patients with skull defects, but not in the other direction (Fig. 1B). This unidirectional generalizability might be because the presence of the skull makes the algorithm learn more subtle signatures of SDs on the scalp. More patients with a wider range of injury types are needed to further improve and validate our noninvasive technique.

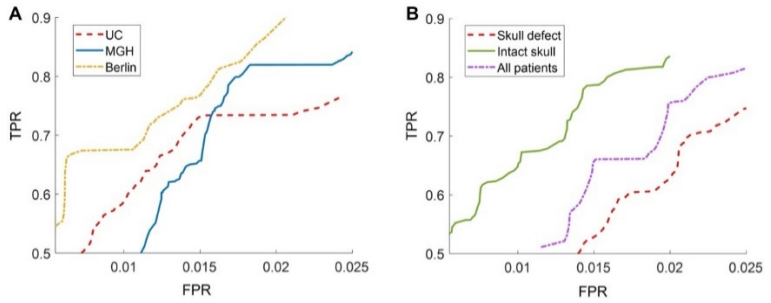

Fig. 1. Average cross validation ROC curves across A) centers, and B) groups of patients with and without skull defect.

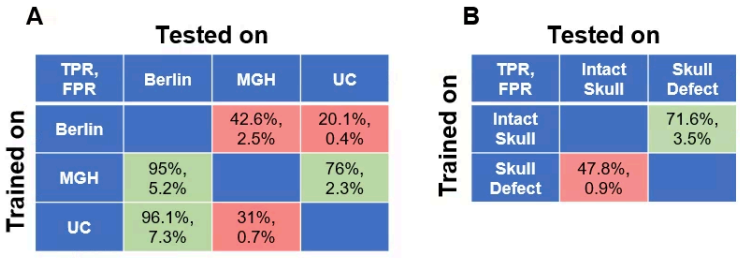

Fig. 2. WAVEFRONT generalizability to different A) centers, and B) groups of patients with and without skull defect.

1. Goldman, L. *et al.* Understanding Acquired Brain Injury: A Review. *Biomedicines* **10**, (2022).
2. Centers for Disease Control and Prevention (CDC). Preprint at https://www.cdc.gov/traumaticbraininjury/pubs/congress_epi_rehab.html.
3. Giustini, A., Pistarini, C. & Pisoni, C. Chapter 34-Traumatic and nontraumatic brain injury. in *Handbook of Clinical Neurology* (eds. Barnes, M. P. & Good, D. C.) vol. 110 401–409 (Elsevier, 2013).
4. Bramlett, H. M. & Dietrich, W. D. Long-term consequences of traumatic brain injury: Current status of potential mechanisms of injury and neurological outcomes. *J. Neurotrauma* **32**, 1834–1848 (2015).
5. Moderate and severe TBI. https://www.cdc.gov/traumaticbraininjury/moderate-severe/index.html (2022).
6. Levant, S., Chari, K. & DeFrances, C. National Hospital Care Survey Demonstration Projects: Traumatic Brain Injury. *Natl. Health Stat. Report.* 1–16 (2016).
7. Hartings, J. A. *et al.* Surgical management of traumatic brain injury: a comparative-effectiveness study of 2 centers. *J. Neurosurg.* **120**, 434–446 (2014).
8. Dreier, J. P. The role of spreading depression, spreading depolarization and spreading ischemia in neurological disease. *Nat. Med.* **17**, 439–447 (2011).
9. Lauritzen, M. *et al.* Clinical relevance of cortical spreading depression in neurological disorders: migraine, malignant stroke, subarachnoid and intracranial hemorrhage, and traumatic brain injury. *J. Cereb. Blood Flow Metab.* **31**, 17–35 (2011).
10. Dreier, J. P. *et al.* Cortical spreading ischaemia is a novel process involved in ischaemic damage in patients with aneurysmal subarachnoid haemorrhage. *Brain* **132**, 1866–1881 (2009).

11. Hartings, J. A. *et al.* Spreading depolarizations and late secondary insults after traumatic brain injury. *J. Neurotrauma* **26**, 1857–1866 (2009).
12. Dreier, J. P. *et al.* Recording, analysis, and interpretation of spreading depolarizations in neurointensive care: Review and recommendations of the COSBID research group. *J. Cereb. Blood Flow Metab.* **37**, 1595–1625 (2017).
13. Sivakumar, S. *et al.* Cortical Spreading Depolarizations and Clinically Measured Scalp EEG Activity After Aneurysmal Subarachnoid Hemorrhage and Traumatic Brain Injury. *Neurocrit. Care* **37**, 49–59 (2022).
14. Chamanzar, A., Elmer, J., Shutter, L., Hartings, J. & Grover, P. Noninvasive and reliable automated detection of spreading depolarization in severe traumatic brain injury using scalp EEG. *Commun. Med.* **3**, 113 (2023).
15. Drenckhahn, C. *et al.* Correlates of spreading depolarization in human scalp electroencephalography. *Brain* **135**, 853–868 (2012).

OP-11 (ID:97)

STANDARDISING DIRECT CORTICAL RESPONSE MONITORING OF SPREADING DEPOLARISATIONS: A MATLAB-BASED APPROACH FOR AUTOMATING OPTIMAL STIMULATION CHANNEL SELECTION

KHEVNA VASANI[A,B], TOMAS WATANABE[C], JOSE-PEDRO LAVRADOR[D], JOEL WINSTON[A], AHILAN KAILAYA-VASAN[D], MARTYN BOUTELLE[B], ANTHONY STRONG[A], SHARON JEWELL[A].

[a]Department of Basic and Clinical Neuroscience, Kings College London, London, UK;
[b]Department of Bioengineering, Imperial College London, London, UK;
[c]Vagalume LLC, Palo Alto, California, USA;
[d]Department of Neurosurgery, Kings College Hospital, London, UK.

Introduction:

Direct Cortical Response (DCR) monitoring in severe acute brain injury has shown promise as a means of objectively quantifying key Spreading Depolarisation (SD) properties; notably duration and burden. It has also revealed novel insights into neuronal behaviour in the in-vivo human brain during the passage of the SD wavefront: Findings from the first major study of DCR monitoring during SDs were presented at 2023 COSBID meeting and this study now follows on from those. We believe that DCR monitoring may both pave the way for a more nuanced management of SDs in critically injured patients and enhance our understanding of this complex process. We thus aim to make this technique readily available to other researchers in the field as soon as feasibly possible. A first approach to this, is to build a means of automating optimal stimulation channel selection:

Effective DCR monitoring relies on capturing optimal amplitude DCR responses from the greatest number of electrodes possible, as this enables accurate assessment of the impact of SDs on neuronal excitability across multiple brain regions. Given the complexity of brain anatomy and the heterogeneity of injuries in our patient cohort, predetermining which electrode stimulation pair will yield the optimal number and amplitude of DCR responses is challenging. Currently, the process of selecting electrode stimulation pairs is empirical and undertaken subjectively. It involves testing each contiguous pair consecutively in both polarities (anode-cathode/cathode-anode) and then visually comparing responses on moving charts that cannot easily be re-reviewed at the bedside. Time is also of the essence, since this process must be undertaken between SDs or other swings in systemic physiology. One way to address this setup challenge is to automate the stimulation channel selection process. Here we describe our approach based on MATLAB app development, which can easily be deployed at the bedside and distributed to other centres.

Objective:

To develop a software tool that automates the process of optimal stimulation channel selection with the aim of making DCR monitoring setup more efficient and reliable.

Method:

To automate stimulation pair selection, we developed a MATLAB-based tool on post-hoc data sets. The preprocessing stage involved bandpass filtering to isolate the frequency range of interest.

The automation process was then subsequently divided into two key stages:

1. *Identification of stimulation channels:* Stimulation intervals (when stimulation was being undertaken) were identified using root mean square (RMS) signal analysis across data samples. Stimulation channels were identified by calculating the rolling standard deviation across each individual channel. Within each stimulation time block, the two channels exhibiting the highest standard deviation were designated as stimulation channels. This approach accurately distinguished stimulation channels from recording channels based on their characteristic signal variability.
2. *Analysis of response channels:* We analysed each stimulation interval individually for all the response channels, detecting stimulus artifacts and DCR components N1 and P2 (figure 1) using thresholding and specified latency criteria based upon averages taken from 98k responses analysed in the initial study. This approach allowed for amplitude measurement of individual DCR components. The algorithm then stacked and aligned multiple responses for each channel facilitating visual identification of outliers. Mean peak-to-peak amplitudes were then calculated for each channel, enabling quantitative comparison to determine optimal stimulating channels.

Results:
Preliminary results indicate that our proposed logic effectively segregates stimulation channels from recording channels as these are changed by the researcher during the setup. The thresholding and latency criteria successfully detect stimulus artifacts in response channels. Detection of N1 and P2 components using latency range and absolute maxima allow for reliable, objective measurement of peak-to-peak amplitude across all channels showing DCR. Development of a summary measure for the comparison of best stimulation pair and a user interface is underway.
While comprehensive validation across a larger dataset is on-going, our preliminary results suggest this automated approach has the potential to significantly streamline DCR monitoring setup. Future work will involve implementing quantitative performance metrices, such as accuracy in stimulation pair identification and DCR component detection against ground truth. These metrices will be crucial for a robust and reliable tool that can be shared among other researchers in the field.

Conclusion:
This study introduces a structured approach for automating stimulation pair selection in DCR setup and monitoring. Preliminary results affirm its effectiveness, with further validation promising to enhance reliability and facilitate broader adoption, making DCR monitoring more accessible for researchers and clinicians alike with the ultimate aim of enhancing understanding and improving management of SDs using a tool with unapparelled translatability.

OP-12 (ID:12)

NONINVASIVE VS. INVASIVE DETECTION OF CORTICAL SPREADING DEPOLARIZATION VIA DC-SHIFT COMPARISON

BENJAMIN BROWN [1], SAMUEL HUND [2], KIRK EASLEY [3], ERIC SINGER [1], WILLIAM SHUTTLEWORTH [4], ANDREW CARLSON [4], STEPHEN JONES [1]

[1] *CEREBROSCOPE*
[2] *SİMULATİON SOLUTİONS LLC*
[3] *EMORY UNİVERSİTY*
[4] *UNİVERSİTY OF NEW MEXİCO*

Background/Objective:

Cortical spreading depolarization (SD) is increasingly recognized as a major contributor to secondary brain injury[1]. Monitoring SDs could be used to institute and guide SD-based therapeutics if noninvasive detection methods were available. Noninvasive SD detection attempts have not been completely successful[2-9], but simulation studies have suggested several possibilities[10,11]. Here, we explore the premise that DC-EEG with closely-spaced electrodes can provide viable scalp detection of the primary SD event, the electric-field from the en-mass cortical depolarization, based on cortical voltage and extent estimates from a finite-element model simulation of concussive SD[10]. To be clear, this approach is distinct compared to those efforts to provide algorithms using clinical frequency EEG with "ultra-low-density EEG[5], ~2.5 cm electrode spacing with the 10-20 system[4], or high-density EEG[12] to detect SD's secondary EEG suppression. Our objective is to compare the DC-shifts from ECoG-coded SDs and DC-shifts detected from scalp electrodes from acute brain injury patients in the neurointensive care unit to establish proof-of-concept validation that scalp DC-potentials can provide noninvasive SD detection with the caveat that the artifact burden must be minimal.

Methods:

An 83x58 mm thermoplastic elastomer array with 29 embedded 6-mm diameter Ag/AgCl 1-cm spaced electrodes, the CerebroPatch™ Proof-of-Concept Prototype (the Prototype Device), was adhesively placed on the forehead with an intervening electrode gel interface to record 2 hours to 12 days of DC-EEG in normal volunteers and severe acute brain injury Neuro-ICU patients with and without invasive brain-surface ECoG electrodes. Data analysis focused on one patient with sub-arachnoid hemorrhage whose ECoG recordings displayed SDs during artifact-free scalp recording periods. The scalp and ECoG voltages were collected by a Moberg® Advanced ICU Amplifier. ECoG recordings were coded by an experienced investigator (APC) for SDs using LabChart software. Data was then processed using lab-designed Python scripts by first determining the mean voltage within 8-sec non-overlapping segments, reducing the signal sample rate to 0.125 Hz. Time-course ECoG and scalp electrode detrended channel plots and heat-map movies produced with Python scripts allowed the classification of SD associated DC-shifts (by SCJ) into five groups. These five groups included combinations of: 1) propagation as evidenced by the lab-derived ECoG channel plots; 2) simultaneous DC-shifts occurring in several channels at once; and 3) "Twin-Peaks" as described by Drenckhahn et al.[2] (see caption of Figure 3). Four or 12 minute epochs were selected where ECoG-coded SDs occurred in regions of readable scalp DC-shift voltages that satisfied the voltage and spatial-spread extent boundaries estimated from numerical simulations[10,13] and experimental[10] scalp/brain-surface voltage ratios. The 8-sec averages of ECoG and non-invasive Prototype Device voltages in these chosen epochs were least-squares fitted to a Gaussian plus quadratic six-parameter model. The Gaussian parameters of maximum voltage extent, time of peak signal, and width as full-width-half-maximum (FWHM) were used to compare the scalp and ECoG DC-shifts. In each epoch the invasive ECoG and scalp channels with maximum DC-voltage extent were compared using the Coefficient-of-Determination: a value of >0.80 was deemed as suggesting acceptable structural similarity. The spatial extent of the scalp DC-shifts was estimated as the area of the contiguous region above the 50% isocontour of the DC-voltage amplitude at the peak voltage time.

Results:

All 140 LabChart-identified ECoG SDs and ISDs over a period of 11 days were visualized using the Python-script depictions of the ECoG voltage time series, with 26 in readable portions of scalp recordings. These ECoG-coded SDs exhibited multi-ECoG electrode DC-shifts with 15 (10.7%) classed as "Propagating", 76 (54%) classed as "Simultaneous", 42 (30%) classed as "Simultaneous & Twin Peaks", six (4.3%) as "Simultaneous & Twin Peaks & Propagating", and one (0.71%) as "Simultaneous & Propagating". Eighty-four percent (54%+30%) were in classes that were not propagating and 15.7% were in those that displayed propagation.

The Table presents the comparison of the fitted parameters between the ECoG and Prototype Device DC-shifts.

Table: Comparison of CerebroPatch™ Proof-of-Concept Prototype (Prototype Device) with ECoG DC-shift parameters					
		Signal origin			
Parameter	Units	Prototype Device	ECoG	Ratio or Difference	n
Voltage	(μV)	-458 ± 67	-3793 [293]	0.120 ± 0.016	26
Duration (FWHM)*	(sec)	70.5 [9.1]	62.7 [5.2]	1.11 ± 0.083	26
Peak Time Difference**	(sec)	-	-	2.89 [2.28]	25
Area	(cm^2)	18.7 ± 2.71			26
Coefficient of Determination (>0.80)	(-)	-	-	0.98 [0.02]	24
Values are mean ± SD or median [interquartile range, IQR]					
* $p < 0.01$					
** With only scalp delayed (excluding one preceding)					

The DC-shift comparison and reconstructed DC-voltage heat-map image of the noninvasive Prototype Device from a typical epoch is shown in the Figure:

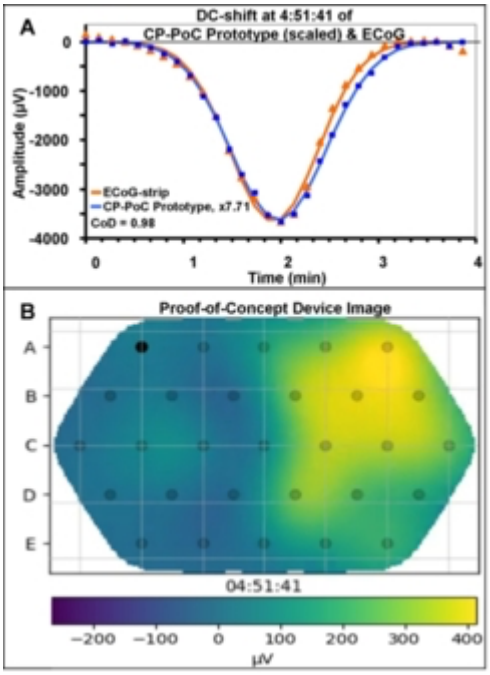

A, The structural similarity of the processed ECoG (red) and the proof-of-concept (PoC) Prototype Device DC-shifts (blue, scaled by the 7.71 ratio of the largest peak signal amplitudes) is shown by a Coefficient-of-Determination (CoD=R^2) of 0.98. B, The 4-5 cm extent of the scalp-visible 400 μV DC-field of an SD (yellow) is shown in a video frame at the 4:51 peak voltage of the DC-potential heat-map image composed from 22 (7 dead channels) of the 29 1-cm spaced electrode voltages (gray dots). At the bottom, the color-map voltage scale (positive and negative are reversed in scale) shows the voltage range from 250 to -410 μV.

The 0.98 [0.02] (median [IQR]) Coefficient-of-Determination between the 24 scalp DC-shifts detected by the Prototype Device and those from ECoG-coded SDs whose coefficients-of-determination >0.80 strongly suggests that the transient voltages (peak -458 ± 67 μV [mean ± SD], FWHM 70.5 [9.1] sec, area 18.7 ± 2.71 cm^2) depicted in the heat-map movies represent noninvasively detected SDs.Many (84%) of the ECoG-coded SDS were classed as non-propagating from our independent analysis. We surmise that non-propagating SDs are underreported by investigators because they are presumed to be traveling perpendicular to the ECoG strip, are classed inappropriately as artifacts, or are dismissed as missing one of the presumed essential identifiers of SDs, although suggestions of cortical non-spreading depolarizations have been made[9,14,15].

The combination of voltage-ratio- and spatial-extent-targeted scalp DC-shifts, scalp DC-visual imaging from closely spaced electrodes, and paired quantitative time-course scalp and ECoG comparison via the Coefficient-of-Determination are the hall-marks of the premise that this data provides proof-of-concept validation of noninvasive SD detection. These noninvasive SD identification criteria are supported by previous studies that used multiple criteria for identifying SDs depending on the detection method[9,15-21]. The CerebroPatch™ Proof-of-Concept Prototype system criteria combining these three analyses suggests an additional method of SD identification. By focusing on a limited, artifact-free period that encompasses a suspected scalp DC-EEG signal of an SD, we suggest that a 4 min epoch can be analyzed to identify a SD via these DC-shift attributes. These results suggest that noninvasive SD detection is possible using scalp DC-potential signals if artifact-free DC-EEG detection can be realized

Conclusions:
By comparing the maximum extent DC-shifts from the scalp and the brain-surface channels, we show that the scalp DC-shifts are a virtual replica of those from brain-surface SDs, a novel finding not previously reported. This numerical comparison of invasively and noninvasively detected DC-shifts and the visualization and spatial characterization as enabled by the closely-spaced 1-cm electrode array of the noninvasive Prototype Device distinguishes our results from previous scalp DC-shift recordings[2,3]. The limited scalp electrode spacing of these publications did not permit the reconstruction and visualization of the scalp electric field or allow the optimal alignment of the scalp and brain surface electrodes for the quantitative comparison of their DC-shifts.
Many (84%) of the ECoG-coded SDS were classed as non-propagating from our independent analysis. We surmise that non-propagating SDs are underreported by investigators because they are presumed to be traveling perpendicular to the ECoG strip, are classed inappropriately as artifacts, or are dismissed as missing one of the presumed essential identifiers of SDs, although suggestions of cortical non-spreading depolarizations have been made9,14,15.

The combination of voltage-ratio- and spatial-extent-targeted scalp DC-shifts, scalp DC-visual imaging from closely spaced electrodes, and paired quantitative time-course scalp and ECoG comparison via the Coefficient-of-Determination are the hall-marks of the premise that this data provides proof-of-concept validation of noninvasive SD detection. These noninvasive SD identification criteria are supported by previous studies that used multiple criteria for identifying SDs depending on the detection method9,15-21. The CerebroPatch™ Proof-of-Concept Prototype system criteria combining these three analyses suggests an additional method of SD identification. By focusing on a limited, artifact-free period that encompasses a suspected scalp DC-EEG signal of an SD, we suggest that a 4 min epoch can be analyzed to identify a SD via these DC-shift attributes. These results suggest that noninvasive SD detection is possible using scalp DC-potential signals if artifact-free DC-EEG detection can be realized.

References

1. Lemale C.L. et al., (2022), PM:35237133.
2. Drenckhahn C. et al., (2012), PM:22366798.
3. Hartings J.A. et al., (2014), PM:25154587.
4. Chamanzar A. et al., (2023), PM:37598253.
5. Wu Y. et al., (2024), PM:38412076.
6. Hofmeijer J. et al., (2018), PM:29422883.
7. Hartings J.A. et al., (2018), PM:29869634.
8. Robinson D. et al., (2021), PM:34617254.
9. Bastany Z.J.R. et al., (2020), PM:33152524.
10. Hund S.J. et al., (2022), PM:35233716.
11. Chamanzar A. et al., (2019), PM:30176578.
12. Wang H.Y. et al., (2023), PM:38082965.
13. Hund S.J. et al., (2024), In preparation.
14. Dohmen C. et al., (2008), PM:18496842.
15. Strong A.J. et al., (2002), PM:12468763.
16. Mayevsky A. et al., (1996), PM:8973824.
17. Hadjikhani N. et al., (2001), PM:11287655.
18. Woitzik J. et al., (2013), PM:23446683.
19. Strong A.J. et al., (1996), PM:8621741.
20. Takano K. et al., (1996), PM:8602749.
21. Yushmanov V.E. et al., (2012), https://archive.ismrm.org/2012/3063.html

OP-13 (ID:98)

STEP RESPONSE OF METALLIC ELECTRODES

KEVAN HASHEMI , CALVIN DAHLBERG ,

OPEN SOURCE INSTRUMENTS INC.

Introduction:

Spreading depolarizations (SDs) produce slow, distinctive, solitary waves in local field potential (LFP). These waves evolve over hundreds of seconds. In mouse and rat brains, the SD potential we record with metallic electrodes can be as small as 2 mV and as large as 10 mV. The ideal pair of electrodes would convey the SD potential in the cerebrospinal fluid to our amplifier without attenuation or distortion. We studied the performance of a variety of metals as electrodes for recording SD potentials, hoping to identify some that will be suitable for use with our implantable telemetry devices.

Methods:

We measured the response of a variety of electrodes to a 20-mV, 0.0025-Hz square wave applied to 1% saline. We recorded the electrode potentials with a 10-MΩ, 0.0-80 Hz amplifier. We varied the electrode metal and surface area. We noted the amplitude, offsets, and decay constants of the response of each electrode.

Results:

Stainless steel produces significant attenuition of very low frequencies due to a decay constant in its response. Silver wire coated with silver chloride provides faithful representation of low frequencies. Stainless steel wires may be combined with stainless steel fastening screws without any loss of amplitude or introduction of galvanic potential. Silver chloride wires combined with stainless steel screws generate a substantial galvanic potential and suffer the same attenuition of low frequencies as stainless steel.

Conclusion:

Silver-chloride coated silver wire, secured with cement, offers the highest amplitude and fidelity for SD recordings. Stainless steel electrodes attenuate SD waves, but this attenuation is consistent, and stainless steel wires are more convenient for implantation because they may be secured with steel screws without generating a galvanic potential.

OP-14(ID:92)

MONITORING HIGH-RESOLUTION ELECTROPHYSIOLOGICAL ACTIVITY OF BRAIN SLICES WITH A MULTI-FUNCTIONAL HIGH-DENSITY MICROELECTRODE ARRAY

HASAN ULUŞAN [1], JULIAN BARTRAM [2], TOBIAS GAENSWEIN [2], SREEDHAR KUMAR [2], ANDREAS HIERLEMANN [2],

[1] *DEPARTMENT OF ELECTRİCAL-ELECTRONİCS ENGİNEERİNG, MİDDLE EAST TECHNİCAL UNİVERSİTY, ANKARA, TÜRKİYE*
[2] *DEPARTMENT OF BİOSYSTEMS SCİENCE AND ENGİNEERİNG, ETH ZÜRİCH, BASEL, SWİTZERLAND*
[3] *METUMEMS RESEARCH AND APPLİCATİONS CENTER, ANKARA, TÜRKİYE*

Abstract:
Many neuroscientific questions can be addressed by studying highly interdependent processes and features, such as the exact timing and occurrence of single-cell action potentials, their propagation speed and trajectories along axons, the release of neurotransmitters at synapses, cell densities, tissue properties, and surface adhesion. Measuring these properties simultaneously at sufficient spatial and temporal resolution poses significant challenges. CMOS-based high-density microelectrode array (HD-MEA) systems enable the measurement of various features of biological tissues at subcellular resolution [1], [2]. The multi-functional HD-MEA chip, developed by the Bio Engineering Laboratory at ETH Zurich, features 59,760 electrodes at a pitch of 13.5 µm [3], [4]. The electrodes can be arbitrarily connected to voltage recordings, impedance measurements, neurotransmitter detection, and extracellular voltage- or current-stimulation units.

In this research, we use the specifically developed HD-MEA platform to visualize the position and attachment of brain slices on the HD-MEA with impedance imaging and precisely monitor the electrophysiological activity of the slices. It allows for studying the correlation between tissue-to-electrode adhesion and properties, as well as measuring the spiking activity of neuronal cells on the HD-MEA. For monitoring single cell and network level activity of an acute brain slice of mouse cortex was pressed on the HD-MEA, and electrophysiology and impedance recording protocols were applied. The cell viability was maintained by continuously superfusing the chip with carbogen-bubbled artificial cerebrospinal fluid (aCSF) at 36°C. As the first, slices were localized on the HD-MEA with impedance imaging where the impedance measurements were carried with less than 30 µm resolution. Then, single-cell action potentials and network-level activities were monitored with the HD-MEA system. The electrophysiological activities were recorded by scanning all of the 59,760 electrodes to achieve the overall activity scheme of the slice and then recorded with a high-density configuration with 45 x 45 electrodes (600 x 600 μm^2) to characterize specific areas of the tissue. We extracted the single-cell activity of individual neurons through automatic spike sorting and established their electrical "footprints" in the recording area. The analyzed data show that the spiking response of multiple neurons can be recorded at very high resolution and then used for further analysis, such as connectivity inference between neurons or analysis of action potential propagation. Furthermore, the high-resolution propagation of electrophysiological wave activity through the tissue was observed with the unique performance of the multi-functional HD-MEA platform. Simultaneous high-density impedance imaging and electrophysiological recordings enable the identification and high-resolution monitoring of electrophysiological activities of specific locations of brain slices.

Acknowledgements:
All use of animals and all experimental protocols were approved by the Basel Stadt veterinary office according to Swiss federal laws on animal welfare. This work was supported by the European Union through the European Research Council (ERC) Advanced Grant 694829 'neuroXscales' and the Swiss National Science Foundation under contract 205320_188910 / 1.

References:
[1] M. Ballini et al., "A 1024-Channel CMOS Microelectrode Array With 26,400 Electrodes for Recording and Stimulation of Electrogenic Cells In Vitro," *IEEE J. Solid-State Circuits*, vol. 49, no. 11, pp. 2705–2719, 2014.
[2] A. Hierlemann, U. Frey, S. Hafizovic, and F. Heer, "Growing cells atop microelectronic chips: Interfacing electrogenic cells in vitro with CMOS-based microelectrode arrays," *Proc. IEEE*, vol. 99, no. 2, pp. 252–284, 2011.
[3] J. Dragas et al., "In Vitro Multi-Functional Microelectrode Array Featuring 59 760 Electrodes, 2048 Electrophysiology Channels, Stimulation, Impedance Measurement, and Neurotransmitter Detection Channels," *IEEE J. Solid-State Circuits*, vol. 52, no. 6, pp. 1576–1590, 2017.
[4] V. Viswam et al., "Impedance Spectroscopy and Electrophysiological Imaging of Cells with a High-Density CMOS Microelectrode Array System," *IEEE Trans. Biomed. Circuits Syst.*, vol. 12, no. 6, pp. 1356– 1368, 2018.

OP-15 (ID:13)

THE IMPACT OF CORTICAL SPREADING DEPOLARIZATION ON THE AUTONOMOUS NERVOUS SYSTEM IN CRITICALLY BRAIN INJURED PATIENTS

GWENDAN PERCEVAULT [1], VALENTIN GHIBAUDO [1], SAMUEL GARCIA [1], BAPTISTE BALANÇA [1],

[1] *CENTRE DE RECHERCHE EN NEUROSCİENCES DE LYON (CRNL)*
[2] *HOSPİCES CİVİLS DE LYON (HCL)*

Introduction:
Spreading Depolarizations (SDs) are a marker of poor prognosis after acute brain injuries. They may lead to secondary brain injuries through different mechanisms and are associated with increased mortality in critically ill patients. Their detection using electrocorticography (ECoG) integrated into a multimodal monitoring strategy in critical care may allow clinicians to tailor individual care. However, the consequence of SDs on the autonomous nervous system by affecting the brainstem is still sparsely studied in the literature. We hypothesize that the propagation of SDs to the brainstem could have an impact on cardiorespiratory centers, thereby affecting cardiovascular and respiratory functions in critically ill brain-injured patients.

Methods:
We analyzed multimodal neuromonitoring data from the CNS-MOBERG (Multi-ICU trial, CNIL=25_5713). This database include data from patients with severe traumatic brain injury or poor grade subarachnoid hemorrhage admitted in the neurocritical care unit of the Hospices Civils de Lyon (France). The CNS Monitor (MICROMED NATUS) was used to continuously monitor SD and other physiological parameters such as intracranial pressure, ventilation and cardiovascular monitoring. We extracted and analyzed physiological signals using the pycns and physio toolboxes in the Python programming language. Heart rate variability, respiratory rate variability, respiratory sinus arrythmia, arterial blood pressure and intracranial pressure were processed and analyzed 15 minutes before (baseline window), during (per-SD window), and after a SD at 5, 10 and 15minutes (post-SD windows). Statistical analyses were performed using a linear mixed effect model.

Results:
Of 19 patients included in our study we analyzed 318 SD events. Median age was 49 years old and 31% had a severe traumatic injury. Median ECoG recording duration was 7 days. Compared to the baseline window, we observed a decrease of 3.01ms [-5.86, -0.16] p=0.038 in the heart rate median absolute deviation during the 10min post-SD window. There was also an increase of 0.96bpm [0.29 – 1.62] p=0.005 of the median respiratory sinus arrythmia during the 15min post-SD window. No statistical difference was observed when analyzing the respiratory rate variability.

Discussion:
We extracted and analyzed physiological data from brain-injured patients hospitalized in neurocritical care to study whether SD could have an impact on the autonomous nervous system. Here we found there was a small decrease in the heart rate median absolute deviation during the 10min post-SD window, and an increase of the median respiratory sinus arrythmia during the 15min post-SD window. No effect was observed when analyzing the respiratory rate variability. Those changes in the heart rate variability and respiratory sinus arrythmia might be explained by the impact of SD on cardiorespiratory centers in the brainstem. We plan to perform the same analyses in a model of traumatic brain injury in rats under general anesthesia to corroborate our findings

OP-16 (ID:26)

IMPACT OF SD INITIATION SITE ON OUTCOME OF TRANSIENT FOCAL ISCHEMIA

MICHAEL BENNETT [1], RUSSELL MORTON [1], ANDREW CARLSON [2], C. WILLIAM SHUTTLEWORTH [1]

[1] UNİVERSİTY OF NEW MEXİCO, DEPARTMENT OF NEUROSCİENCES, ALBUQUERQUE, NM, USA
[2] UNİVERSİTY OF NEW MEXİCO, DEPARTMENT OF NEUROSURGERY, ALBUQUERQUE, NM, USA

Keywords. Postconditioning, laser speckle contrast imaging, stroke, MCAO, ischemic penumbra

Background:
A large body of literature has focussed on damaging effects of spreading depolarization (SD), and mechanisms by which SDs contribute to secondary enlargement of acute brain injuries. However, SDs initiated in healthy tissues can lead to significant ischemic preconditioning. We, and others, have shown increased expression of genes associated with neuronal plasticity and cell survival when SDs are produced in non-injured brain. A recent study found that there was no effect on infarct size when SDs were initiated experimentally in a model of focal stroke in mice (Stroke. 2023 54(4): 1110 – 19). We tested the hypothesis that experimentally-induced SDs can have both damaging and protective functions in the context of stroke, and that the balance of these effects depends on the location of the SD initiation site. Experimental SD initiation sites were chosen based on degree of perfusion deficit in a focal stroke model, and compared with animals with focal stroke alone.

Materials & Methods:
Mice aged 8 – 12 weeks were deeply anesthetized using isoflurane (3.5% induction, 1.5 % maintenance). Transient middle cerebral artery occlusion (MCAO) was achieved by microvascular clipping of the distal branch of the MCA for one hour. Cerebral blood flow was monitored via laser speckle contrast imaging (LSCI) through the intact skull. The perfusion deficit produced by MCAO was mapped, and reperfusion confirmed after removal of the vascular clip. Three experimental groups were compared; MCAO alone, or MCAO with a superimposed cluster of experimentally-induced SDs, initiated at one of two locations. In each animal, the SD initiation site was chosen based on relationship to the perfusion deficit. "Proximal SD" initiation sites were defined as being close to the infarct core, at sites with perfusion deficits measured as ≥ 50 percent reduction from baseline. "Remote SDs" were initiated in a location in the same hemisphere, but with perfusion deficits ≤ 25% of baseline. SDs were induced every 10 minutes throughout the 60 min of occlusion. Initiation and propagation of SDs were confirmed through analysis of cerebral blood flow changes (CBF) by LSCI imaging. SDs were initiated either by topical KCl application (1M, 60 sec) in wild type mice or optogenetic stimulation (3mW, 30 sec) in transgenic mice expressing channel rhodopsin under the Thy1 promoter. After the 60 min occlusion (with or without superimposed SDs) the clip was removed, reperfusion confirmed, and mice allowed to recover for 48 hours. Animals were then euthanized, and brains extracted for assessment of infarct volume using triphenyl tetrazolium chloride (TTC) staining. Infarct volumes were analysed using ImageJ software and measured with a correction for oedema.

Figure 1:

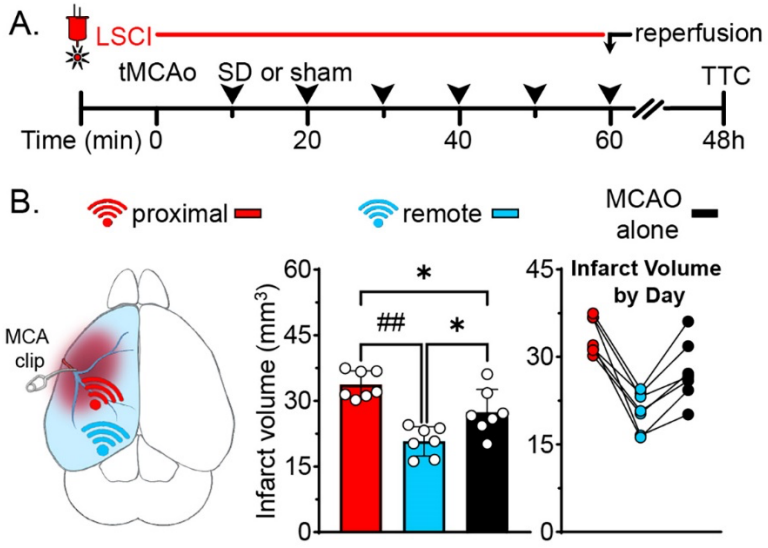

Results:
LSCI mapping confirmed successful experimental initiation of clusters of SDs during the 1-hour recording period, when initiated in either remote or proximal locations. Regardless of the initiation site, SDs propagated through the entire hemisphere including through the ischemic penumbra and infarct core. In a first set of experiments with KCl-evoked SDs, infarct volumes at 48 hours were significantly decreased when SDs were initiated in remote locations, when compared with both MCAO alone and MCAO + proximal SDs ($p < 0.02^{*}$ and $0.0001^{\#\#}$, respectively; n = 7/group, Fig. 1B, middle panel). SDs initiated in proximal regions increased infarct size when compared with MCAo alone ($p < 0.01^{*}$; n = 7/group, Fig. 1B). The right-hand panel of Figure 1B shows the same data, but with lines connecting animals tested with each of the three experimental conditions on a single experimental day. There was no significant difference in results by experimental day and only a significant difference seen with SD initiation location. Preliminary studies in optogenetic mice showed similar results with infarct size being significantly smaller following experimentally-induced SDs initiated in remote locations as compared with initiation in proximal locations ($p < 0.001$, n = 3/group).

Conclusions:
These results are consistent with a protective effect of SDs when they are experimentally-initiated in less vulnerable tissue. Conversely, SDs experimentally-initiated close to the core of the perfusion deficit worsened outcomes. The mechanism of SD initiation (KCl vs optogenetic) did not appear to be important in these phenomena, as compared with the initiation site. Experimental initiation of SD at remote locations may not be relevant to clinical conditions, as spontaneously occurring SDs recorded in brain injured patients are expected to be initiated in vulnerable regions close to ischemic tissue. However, these results help reconcile mixed effects that have been reported for experimentally-induced SDs in the context of stroke, and are consistent with prior reports of protective preconditioning effects when SD is applied to non-ischemic tissue.

Funding: NS129351, NS106901, GM109089

OP-17 (ID:21)

REPETITIVE CORTICAL SPREADING DEPOLARIZATIONS EXACERBATE TISSUE DAMAGE AND NEUROLOGICAL DEFICITS FOLLOWING TRAUMATIC BRAIN INJURY

FAITH BEST , JED HARTINGS , LAURA NGWENYA ,

UNİVERSİTY OF CİNCİNNATİ

Introductıon:

Cortical spreading depolarizations (CSDs), mass depolarizations of neurons and glia that result in near-complete loss of ion homeostasis, occur in >60% of patients with moderate-severe traumatic brain injuries (TBIs) and are associated with poor outcomes 6 months after injury. Laboratory studies have shown effects of a single CSD induced by a mild concussive-like impact in rodents, but studies that replicate the clinical scenario of moderate-severe injury, repetitive CSDs, and subacute time points are lacking. Previous work in our lab has shown that repetitive CSDs induced on the same day as moderate TBI have prolonged depolarization durations, suggesting adverse effects and impaired recovery mechanisms. Here, we further investigated the impact of repetitive CSDs after moderate TBI, focusing on subacute neurologic function as well as histologic damage. We hypothesized that repetitive CSDs would negatively affect behavioral performance, increase lesion size, and cause reactive microglia morphology after experimental TBI. Microglia play a crucial role in CSD and TBI but have not yet been studied in a combined model.

Methods:

Adult Sprague-Dawley male and female rats were subjected to either a moderate lateral fluid percussion (2.11±0.09 atm) or sham injury. Within 35 minutes of injury, CSDs were induced every 15 minutes for 2 hours via 1M KCl or saline (control) application to the cortex. Animals (n=12 per group) underwent modified neurological severity score (mNSS) tasks on 1-day post-injury (dpi), open field test on 2 dpi, radial arm maze (RAM) test on 2 dpi, and novel object recognition (NOR) test on 3 dpi to analyze general neurologic function, locomotor activity, working memory, and short-term memory respectively. Tissue was collected 3 days after injury. Cresyl violet staining was semi-quantitatively analyzed for tissue loss, micro-hemorrhaging, and tissue herniation at the CSD induction site (frontal cortex) and the TBI site (parietal cortex) to investigate potential gross tissue damage that might impact behavior after TBI and CSDs. Ionized calcium-binding adaptor molecule 1 (Iba1) positive microglia were analyzed in the frontal and motor cortices for morphology changes using the ImageJ Skeleton plug-in. All statistical analyses were run on GraphPad Prism 10.2.3 as 2-way analysis of variances (ANOVA) unless otherwise noted.

Results:

TBI+CSD animals had significantly worse mNSS scores than the sham+no CSD, sham+CSD, and TBI+no CSD animals (2-way ANOVA, $p=0.0011$). Of the 10 mNSS tasks, acoustic startle and balance tasks were most affected. During open field testing, no differences in locomotor activity between groups were observed ($p=0.1064$). RAM performance did not differ between groups ($p=0.1381$), though TBI+CSD animals used an egocentric strategy significantly more than the others to complete the task ($p<0.001$). During the NOR test, sham+CSD, TBI+no CSD, and TBI+CSD animals spent significantly less time interacting with either object ($p=0.0247$). TBI animals had more cortical micro-hemorrhaging at the injury site than sham animals, with TBI+CSD animals showing the most micro-hemorrhaging. TBI+CSD animals also had more tissue herniation compared to the other groups. TBI+CSD Iba1-positive microglia had significantly fewer branches per microglia ($p<0.0001$; $p=0.0454$) and endpoints per microglia ($p=0.0006$; $p=0.0454$) in both frontal and motor cortex.

Conclusıons:

Our study revealed worsened general neurological dysfunction, but no deficits in locomotion or memory performance, after the combination of repetitive CSDs and TBI. Additionally, we found more ameboid and reactive microglia in brain regions that correspond with behavioral deficits after TBI and CSDs, as well as increased micro-hemorrhaging and tissue herniation at the site of injury despite no differences in injury severity. These findings suggest that repetitive CSDs aggravate acute reactive responses to TBI, further exacerbating neurological deficits.

OP-18 (ID:83)

EVERY CLOUD HAS A SILVER LINING: SPREADING DEPOLARIZATION INDUCTION OF NEUROPROTECTIVE PATHWAYS THROUGH GENE EXPRESSION CHANGES

MICHELA DELL'ORCO , MICHAEL C BENNETT , LEE ANNA CUNNINGHAM , ANDREW P CARLSON , C. WILLIAM SHUTTLEWORTH ,

[1]Department of Neurosciences, [2]Department of Neurosurgery; University of New Mexico School of Medicine, Albuquerque, New Mexico, 87131, USA.

Keywords: spreading depression, ischemia, enrichment pathway analysis.

Background:
Stroke is one of the most common causes of death and disability in adults but there are limited therapeutic interventions to limit infarction and promote functional recovery and repair. Spreading depolarization (SD) occurs in stroke brain, usually originating near ischemic foci and propagating relatively widely throughout peri-infarct and surrounding tissues. There is strong evidence that SD contributes to progressive infarct expansion, but less is known of effects of SD in surviving peri-infarct tissues. Previous studies of SD induced in healthy brain have shown changes in expression levels of genes known to regulate synaptic activity and neurogenesis.
In this study, we combined gene expression analyses and enrichment pathway analysis to identify the range of biological pathways modified by SD and their predicted effects on peri-infarct tissue survival.

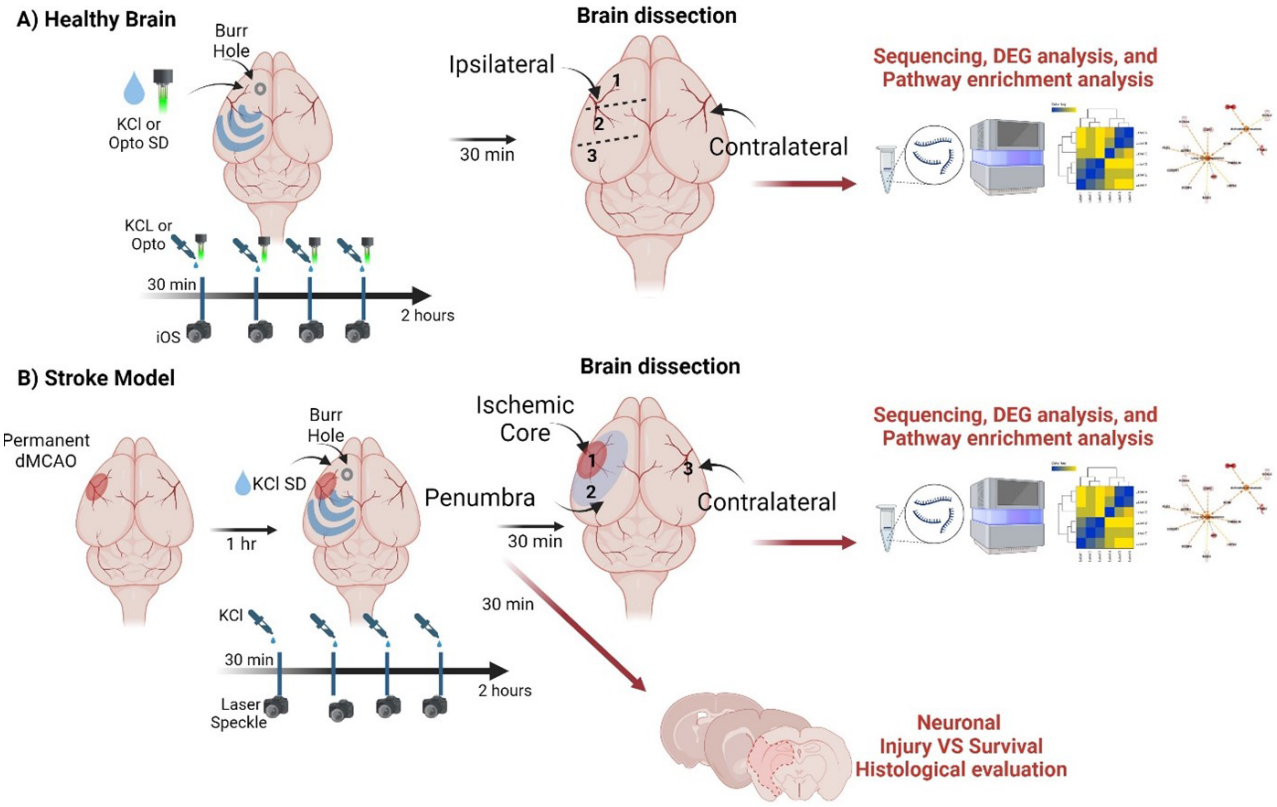

Figure 1. Experimental model A) healthy tissues, and B) dMCAO stroke model.

Methods:
In initial studies, SDs were induced repetitively (4 SDs in 2 hours at 30 min intervals) in healthy mice and confirmed with intrinsic optical imaging (Figure1A). SD induction was with either focal application of KCl in C57Bl/6 mice or with optogenetic stimulation (2 mW for 20 seconds) in Thy1-ChR2-YFP mice. 30 minutes after the last SD, cortical slices were collected and RNA was extracted from total hemispheres (to compare ipsilateral and contralateral), or from punches in 3 different regions of the ipsilateral hemisphere: 1) SD initiation site; 2) intermediate site > 3mm from initiation, 3) remote site >5 mm from initiation (Figure 1A). In the second set of studies, SDs were induced experimentally after induction of stroke (dMCAO) in C57Bl/6 mice; Figure 1B). A

series of SDs were induced repetitively with focal KCl (4 SDs in 2 hours), beginning 30 min after the onset of occlusion. RNA was extracted from total hemispheres (to compare ipsilateral and contralateral), or from punches from 1) SD initiation site 2) infarct core 3) intermediate and 4) remote site. Aliquots of RNA were sent to Arraystar, Inc. for Illumina paired-end RNA-seq or reverse transcribed for qPCR validation to identified differentially expressed genes (DEGs).

Results:
Consistent with previous studies, top DEGs induced by SD in both healthy and stroke tissues include genes encoding the neurotrophic factor BDNF, intermediate early genes FOS, and JUNB. We also found significantly increased levels of other cell proliferation related genes such as DUSP6; plasticity related genes as Homer1a and c and ARC, and inflammation related genes including PTGS2, EGR2 and NR4A1. Pathway analysis of DEGs revealed significant SD-induced increases in the expression of genes associated with axogenesis, branching of axons, neuritogenesis, dendritic growth, and regeneration of neurites when comparing SDs vs sham in both healthy tissues and stroke, and between the infarct core and the intermediate or remote sites. We also found a significant decrease in expression in genes associated with cell death, apoptosis and neuronal degeneration after SD in ischemic core compared with sham (stroke without SD). In the stroke core, NPAS4, previously associated with ischemic preconditioning, was also overexpressed following experimental induction of SD.
When comparing the penumbra with the ischemic core area we found experimentally induced SD resulted in differential expression of genes related to synaptic activity rather than proliferation, such as: SCN4, DRD2, ADORA2A and CamKIIb. When comparing stroke penumbra with contralateral tissues after experimentally induced SD, we found increased levels of plasticity and proliferation associated genes (BDNF, NPAS4, ARC, FOS, EGR1, and PTGS2) and decreased levels of neuronal activity related genes (SCN4, ADORA2A, and DRD2) (Figure 2).

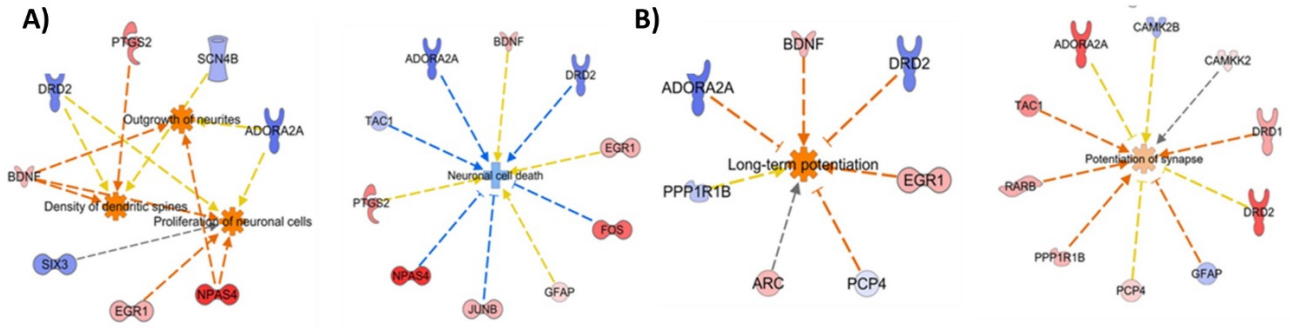

Figure2. Representative networks with DEGs after repetitive SDs showing predicted decrease in neuronal cell death and increases in neuronal development and differentiation (A), and increased synaptic activity (B) in the stroke penumbra vs the ischemic core and contralateral cortex. The intensity of the color red (upregulated) or blue (downregulated) for each molecule is proportional to the FC of the gene. Orange arrows indicate activation of the gene on the related pathway, and the pathway's name highlighted in orange indicates its activation.

Conclusions:
This study identified gene expression changes after repeated spreading depolarizations (SDs) in both healthy and injured brain. While the focus of SD effects in stroke is often on damaging consequences, here we showed that multiple SDs are predicted to induce activation of pathways leading to increase cell differentiation and decreased cell death. These results suggest SDs are may be capable of regulating gene expression changes related to long-term repair process in the stroke penumbra, as well as favoring short-term survival in the core These studies identify novel targets that could be used to guide tests of molecular mechanisms involved in both preconditioning and postconditioning effects of SD and stroke outcomes.

Funding: NIH grants NS106901, P206GM109089

OP-19 (ID:94)

CORRELATION OF BDNF LEVELS WITH CONCUSSION SYMPTOMS AND NEUROBEHAVIOR DEFICITS ASSOCIATED WITH A MILD TRAUMATIC BRAIN INJURY

VENENCIA ALBERT , ARULSELVI SUBRAMANIAN , SHIVANI SHARMA , ASHIMA NEHRA , RAJESH SAGAR

ALL INDİA INSTİTUTE OF MEDİCAL SCİENCES, NEW DELHİ, INDİA

Background:
The relationship between concussive symptoms and neurological as well as neurobehavioural deficits in mild traumatic brain injury (mTBI) is increasingly acknowledged; however, the underlying mechanisms remain inadequately understood, and effective therapeutic interventions are limited. Recent research suggests that perturbations in brain physiology may exacerbate secondary injuries, thereby contributing to these neuropsychiatric outcomes.

Objective:
This study aims to assess the incidence of neurobehavior outcomes, including concussion, depression, anxiety, and stress following mTBI, and to explore their correlation with brain-derived neurotrophic factor (BDNF) levels.

Methods:
A prospective cross-sectional analysis was conducted on mTBI patients. Neurobehavioral assessments were performed within 12 hours of injury and subsequently at 2 weeks and 3 months post-injury, using the Acute Concussion Evaluation (ACE)-ED, Rivermead Post-Concussion Symptoms Questionnaire (RPQ), and Depression Anxiety Stress Scales (DASS-21). Serum BDNF levels were measured at the time of injury, at 2 weeks, and at 3 months.

Results:
A total of 100 mTBI patients (mean age 30.65±9.5 years; 60% male) were recruited from the emergency department. The majority of cases resulted from assault (59%), followed by road traffic accidents (28%) and falls (13%). The average ACE-ED score was 7.72±3.5, with impairments noted across physical, cognitive, emotional, and sleep domains. Within 12 hours post-injury, 90% of patients reported headaches, 23% experienced difficulty concentrating, and 5% had memory difficulties. At 2 weeks post-injury, the median RPQ score was 7.5 (range 0-50), with 14% of patients meeting the criteria for post-concussion syndrome (PCS) and 2% exhibiting moderate to severe functional limitations. DASS-21 scores revealed that 34% of patients experienced depression, 31% anxiety, and 16% stress. By 3 months (n=36), symptom severity had decreased, with a median RPQ score of 5 (range 0-36), 6% of patients still presenting with PCS, and 3% with moderate to severe functional limitations. At this time point, 9% of patients reported depression, 18% anxiety, and 5% stress. Serum BDNF levels were 980.52 pg/ml (range 539.32-1174.12) at injury onset, significantly declining by 2 weeks [869.32 pg/ml (range 414.52-1999), $p < 0.0001$] and remaining reduced at 3 months [897.31 pg/ml (range 416.92-1403.42), $p = 0.01$], although slightly elevated from the 2-week level ($p = 0.02$). An inverse correlation was observed between depression scores and BDNF levels.

Conclusion:
In this cohort, over 20% of patients exhibited concussion symptoms within 12 hours of injury. At 2 weeks post-injury, 34% of mTBI patients showed symptoms of depression, and 14% met the criteria for post-concussion syndrome, with some symptoms persisting up to 3 months. These findings suggest that following mTBI, secondary mechanisms, such as neuronal depolarization, release of excitatory neurotransmitters, altered cerebral blood flow, disrupted axonal function, and metabolic changes may contribute to the onset of neurobehavioral impairments and delayed recovery. The temporal decrease in neurotrophic factors suggests impaired neuroplasticity. The acute deficits observed in mTBI patients, despite normal neuroimaging, highlight the complexity of post-injury recovery. Further studies are required to elucidate the underlying mechanisms contributing to these outcomes, which may guide the development of more effective management strategies for mTBI patients.

Keywords: Mild Traumatic Brain Injury, Neurobehavioral Outcomes, Brain-Derived Neurotrophic Factor (BDNF), Post-Concussion Syndrome (PCS), Neuroplasticity

OP-20 (ID:79)

MIGRAINOUS INFARCTION: MYTH OR REALITY? A SYSTEMATIC REVIEW

EMILIE SCHOU [1], ANDREA M. HARRIOTT [2], CENK AYATA [2], ANDERS HOUGAARD [3],

[1] *DEPARTMENT OF NEUROLOGY, COPENHAGEN UNİVERSİTY HOSPİTAL - RİGSHOSPİTALET, COPENHAGEN, DENMARK*
[2] *NEUROVASCULAR RESEARCH LABORATORY, DEPARTMENT OF RADİOLOGY, MASSACHUSETTS GENERAL HOSPİTAL, CHARLESTOWN, MA, USA*
[3] *DEPARTMENT OF NEUROLOGY, COPENHAGEN UNİVERSİTY HOSPİTAL – HERLEV AND GENTOFTE, COPENHAGEN, DENMARK*

Background:
Migrainous infarction is a rare complication of migraine with aura where an ischemic stroke occurs during a migraine attack. Despite being a recognized entity, the causal relationship between migraine aura and cerebral infarction remains uncertain.
Currently, there is no established mechanism that explains how migraine causes stroke. The prevailing hypothesis holds that the hypoperfusion associated with spreading depolarization (SD), the presumed underlying mechanism of the migraine aura, in rare cases intensifies and leads to ischemia. Conversely, however, consistent evidence indicates that ischemia can trigger SD in animal and human cortex. Numerous cases of symptoms clinically indistinguishable from migraine aura resulting from brain pathology, including ischemia, have been reported.
This systematic review aimed to evaluate the clinical and neuroimaging characteristics of cerebral infarctions attributed to migraine with aura, assess the fulfillment of current diagnostic criteria for migrainous infarction in reported cases, and explore the evidence supporting causality between migraine aura and subsequent brain infarction. We specifically looked for neuroimaging evidence of spreading ischemia and ischemia overlapping adjacent cerebral arterial territories since these features would support SD as the cause.

Methods:
A systematic literature review following PRISMA guidelines was conducted to identify reports of ischemic stroke attributed to attacks of migraine with aura (PROSPERO: CRD42022354253). PubMed and Embase databases were searched without restrictions on publication date or language. Articles were screened for eligibility, and data were extracted regarding patient demographics, migraine characteristics, neuroimaging findings, and diagnostic workups.

Findings:
The search retrieved 3581 records, with 156 individual case reports included after screening. The mean age at the time of infarction was 35.5 years, with a female predominance (102 females, 53 males). Only 35% of cases had a previous history of migraine with aura according to the criteria of the International Classification of Headache Disorders (ICHD). Neuroimaging showed ischemic infarction in relevant brain areas in 84% of cases. Three cases showed signs of ischemia in overlapping vascular territories, but all were cases of cortical laminar necrosis and not classic ischemic stroke. None of the cases demonstrated spreading ischemia. A basic diagnostic workup was performed in 21% of cases, but no cases met the workup standards recommended by major scientific stroke societies. Ultimately, 39% of cases met the diagnostic criteria for migrainous infarction according to any version of the ICHD. A venn diagram of the prevalence of
clinical and neuroimaging characteristics supporting SD-induced ischemia is shown in Figure 1.

Interpretation:
We did not find evidence from clinical cases clearly supporting the occurrence of cerebral infarction as a consequence of an attack of migraine with aura. Co-occurring migraine with aura and cerebral infarction is likely better explained by ischemia-induced SD.
Patients diagnosed with migrainous infarction may receive receive insufficient diagnostic evaluation. Currently, the concept of migrainous infarction is not beneficial but rather may be harmful to stroke patients. Evidence of clinically relevant SD-induced ischemia is required to confirm the existence of migrainous infarctions.

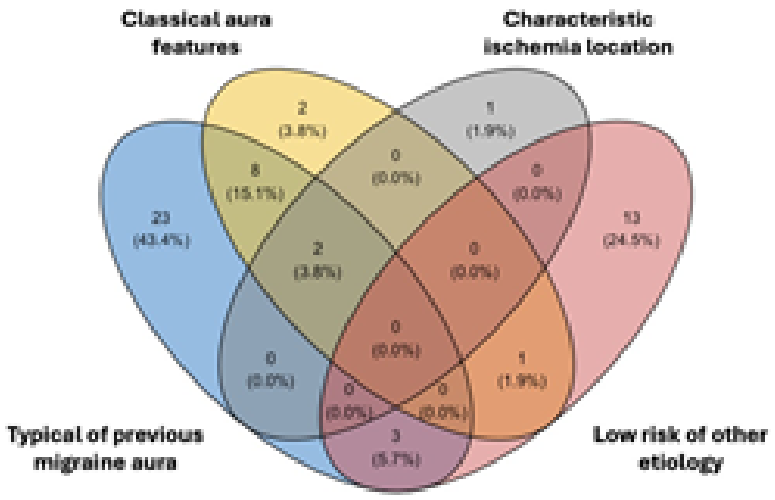

Figure 1: Venn diagram of the clinical and neuroimaging characteristics of cases with migrainous infarction.
Typical of previous migraine aura: Previous history of Migraine with aura (according to ICHD-criteria) AND current attack typical of previous MA attacks – with or without additional symptoms.
Classical aura features: Current attack includes at least one positive symptom AND at least one symptom spreading over >5 minutes or different symptoms occurring in succession.
Characteristic ischemia: Neuroimaging demonstrates ischemic infarction in a relevant area (Corresponding to one or more of the symptoms) AND overlapping adjacent vascular territories.
Low risk of other etiology: No major vascular event before episode AND basic workup without findings supporting likely alternative etiology (A level of 1 or higher for each of the diagnostic work up categories without the finding of an alternative etiology.

OP-21 (ID:99)

A NOVEL MODEL OF IN VITRO CORTICAL SPREADING DEPOLARIZATION

SELİN SAPANCI , ESRA ÖZKAN , YASEMİN GÜRSOY-ÖZDEMİR ,

KOÇ UNIVERSITY, KUTTAM (KOÇ UNIVERSITY RESEARCH CENTER FOR TRANSLATIONAL MEDICINE), SCHOOL OF MEDICINE, İSTANBUL, TÜRKİYE

Introduction:

Most of the studies in spreading depolarisation utilize in vivo animal models. Although these models are efficient and useful for pathophysiological mechanism research, there is a need for high throughput methods for drug screening. Hence, we aimed to develop an in vitro CSD model. This study aimed to induce cortical spreading depolarization directly on human neurons in a human neuroblastoma cells (SH-SY5Y) via converting them into neurons.

Materials and Methods:

In order to establish an in vitro model of cortical spreading depolarization, SH-SY5Y cells were differentiated into neurons. After 18 days, the differentiation process was verified by analyzing neurons via markers with immunofluorescence (IF) and western blot methods. The induction of CSD was initiated by the application of either needle scratching, or microneedle, and or KCL applied to neurons in specifically prepared plates for the model. PI positivity and inflammatory indicators have been compared between the groups.

Results:

Propidium iodide has been identified within the cell in the three CSD mimic techniques. The expression of neurogenic inflammatory markers IL-1β and TLR4 was detected in neurons with the cortical spreading depression (CSD) models compared to normal culture using the western blot method.

Conclusion:

In this study, CSD models were created on human neuronal cells in vitro. Establishing a greater understanding of the mechanisms behind cortical spreading depolarization is crucial to develop a fresh outlook on the identification of novel and individualized therapeutic objectives. This model can be a high throughput screen for drug research.

Keywords: In-vitro model, Cortical Spreading Depression, SH-SY5Y, Differentiation

OP-22 (ID:85)

OLFACTORY BULB INDUCTION OF CORTICAL SPREADING DEPOLARIZATION

MUHAMMED MİRAN ONCEL [1], MICHAEL J. DORA [1], LYDIA HAWLEY [1], DİLARA BAHADİR [1], JAMES H. LAI[1], ELYSSA M. ALBER [1], JOANNA YANG [1], ANDREIA MORAIS [1], ANDREA HARRIOTT [1], KATHLEEN F. VINCENT [2], KEN SOLT [2], SAVA SAKADŽIĆ [3], CENK AYATA [1], DAVID Y CHUNG [1],

[1] 1NEUROVASCULAR RESEARCH UNİT, DEPARTMENT OF RADİOLOGY, MASSACHUSETTS GENERAL HOSPİTAL, HARVARD MEDİCAL SCHOOL, CHARLESTOWN, MA, USA

[2] DEPARTMENT OF ANESTHESİOLOGY, MASSACHUSETTS GENERAL HOSPİTAL, CHARLESTOWN, MA, USA

[3] ATHİNOULA A. MARTİNOS CENTER FOR BİOMEDİCAL IMAGİNG, DEPARTMENT OF RADİOLOGY, MASSACHUSETTS GENERAL HOSPİTAL, CHARLESTOWN, MA, USA

Background:

Cortical spreading depolarization (CSD) is an electrophysiological phenomenon associated with migraine with aura and stroke, among other neurological disorders[1,2]. CSD consists of a spreading wave of depolarization associated with a prolonged depression of electrical activity over the cortical surface[1,2]. Traditionally, preclinical models using CSD induction have used three methods directly affecting the cortex[3]: pinprick through a burr hole, application of concentrated K+, or electrical stimuli. However, these methods are highly invasive and can alter the pial environment[4], contributing to alterations in physiological events such as neurovascular coupling independent of the CSD[4,5,6,7]. Recently, a CSD induction approach to minimize K+ exposure has been described, using a skull-thinning procedure that allows an experimentalist to preserve cortical integrity while causing a CSD[8]. However, this method requires manipulation over the cortical surface and can cause unwanted signals in the field of view when performing in-vivo imaging. Another novel method of CSD induction that is noninvasive utilizes optogenetics through an intact skull in channelrhodopsin (ChR+2) expressing mice[9, 10]. However, optogenetics requires transgenic mice or transfection approaches that can make the approach impractical in some circumstances. Recently, we described unexpected CSD following needle insertion through the olfactory bulb[11]. We hypothesize that inducing CSD through olfactory bulb has the potential to cause a CSD that is minimally invasive with respect to cortical integrity. Herein, we compared the olfactory pinprick method of inducing CSD with KCl application to the cortex. Furthermore, we attempted electrical stimulation of the olfactory bulb to induce CSD.

Methods:

Age and sex-matched C57 animals were securely positioned in a stereotaxic frame. A midline scalp incision was made to expose the skull (Figure 1A). Subsequently, a burr hole with a 1mm diameter was drilled over the right olfactory bulb, 5 mm anterior to bregma and 1 mm lateral to the midline (Figure 1A). On the left cortical surface, a skull thinning procedure was performed 1 mm posterior to the frontal sinus and 2 mm lateral to the midline for KCI application. Intraoperative optical imaging was initiated to identify any inadvertently triggered CSD during the preparation. There were 2 CSDs induced for each animal. In half the animals, KCl was used to induce the first CSD in the left hemisphere. Following a 7-minute wait time for CSD to pass, a needle was inserted into the olfactory bulb to cause a CSD in the right hemisphere. In the other half of the animals, the procedure was reversed so that a needle was used to induce the first CSD in the right olfactory bulb (Figure 1B). The mice were euthanized under 5% isoflurane 24 hours after the experiment. Their brains were preserved in 4% paraformaldehyde for 48 hours, then transferred to 1X PBS until sectioning and staining. Hematoxylin and eosin stain was used to visualize brain tissue. A second set of experiments was conducted to measure the precise minimal depth to cause a CSD by needle insertion (n=6). A final cohort of animals was used to attempt bipolar electrical stimulation at a minimal depth of electrode insertion into olfactory bulb with 6 ms pulses at 8 Hz from 0.1-1.0 mA and 10-30 sec that escalated in charge delivery in a stepwise manner.

Results:

We saw CSDs for every needle-insertion attempt (n = 19). KCl application did not always result in a CSD (n = 12 of 13 KCl attempts). In animals where both approaches resulted in a CSD, we found that KCl-induced CSD was slower than needle-induced CSD (3.8 ± 0.4 vs 4.4 ± 0.5 mm/min, p = 0.0008, n = 12, Figure 2). The order of CSD induction did not matter. The average minimum depth required to induce a CSD using the needle insertion method was 2.9 mm ± 0.6 (n=6) (Figure 3A). In a separate cohort, electrical stimulation of olfactory bulb caused CSD in all attempted mice at needle insertion lengths between 3-4 mm (n = 6, Figure 3B). No CSD occurred with electrical stimulation at superficial depths (0-1 mm). H&E staining demonstrated disruption of the dorsal olfactory bulb with extravasation of red blood cells along the needle tract (Figure 3C-D).

Conclusions:
Olfactory induction of CSD through mouse olfactory bulb is a reliable, minimally invasive method to induce CSD without requiring manipulation of the cortical surface. The mechanism of CSD propagation from olfactory bulb may involve a contiguous tissue tract connecting the dorsal olfactory bulb to the prefrontal cortex. The olfactory bulb approach may be helpful for future CSD studies that require full preservation of cortical integrity.

Figure 1. Experimental setup for olfactory pinprick and KCl studies. **(A)** Field of view over mouse skull showing needle and KCI application sites. **(B)** Experimental protocol for CSD induction. In half of animals, the first CSD was induced with KCl. The order of CSD induction approach was reversed in the other half of animals.

Figure 2. Olfactory needle-induced CSD propagates through cortex faster than KCl-induced CSD. (A) Optical intrinsic signal (OIS) and changes in total hemoglobin r[HbT] from CSDs induced with KCl (left hemisphere) and needle insertion (right hemisphere). (B) Total hemoglobin changes in an anterior-posterior line of interest (LOI) and the power of cerebral blood volume fluctuations are plotted over time. The slope of the line across the CSD wavefront is used to calculate the speed of the CSD (mm/min). (C) Group analysis for the speed of the CSD, with time sequence subdivision.

Figure 3. Needle insertion and electrical stimulation initiates CSD from dorsal olfactory bulb. (A) Minimal depths required to induce a CSD. (B) Charge needed to cause a CSD calculated by the product of current amplitude of stimulation and duration of pulse protocol. (C) Midline sagittal mouse atlas with trajectory of needle tract (black line, 3 mm from the cortical surface, (α = 35°). (D) Sagittal section of an H&E stained brain demonstrates the result of needle insertion and structurally analogous tissue from the tip of the needle tract in dorsal olfactory bulb to the prefrontal cortex.

References

1. Ayata C, Lauritzen M. Spreading Depression, Spreading Depolarizations, and the Cerebral Vasculature. Physiological reviews 2015;95(3):953-93. DOI: 10.1152/physrev.00027.2014.
2. Leão A. Spreading depression of activity in the cerebral cortex. Journal of Neurophysiology 1944;7(6):359-390.
3. Pietrobon D, Moskowitz MA. Chaos and commotion in the wake of cortical spreading depression and spreading depolarizations. Nature reviews Neuroscience 2014;15(6):379-93. DOI: 10.1038/nrn3770.
4. Zhao HT, Tuohy MC, Chow D, et al. Neurovascular dynamics of repeated cortical spreading depolarizations after acute brain injury. Cell Rep 2021;37(1):109794. DOI: 10.1016/j.celrep.2021.109794.
5. Longden TA, Dabertrand F, Koide M, et al. Capillary K(+)-sensing initiates retrograde hyperpolarization to increase local cerebral blood flow. Nature neuroscience 2017;20(5):717-726. DOI: 10.1038/nn.4533.
6. Chang JC, Shook LL, Biag J, et al. Biphasic direct current shift, haemoglobin desaturation and neurovascular uncoupling in cortical spreading depression. Brain : a journal of neurology 2010;133(Pt 4):996-1012. DOI: 10.1093/brain/awp338.
7. Ayata C. Pearls and pitfalls in experimental models of spreading depression. Cephalalgia : an international journal of headache 2013;33(8):604-13. DOI: 10.1177/0333102412470216.
8. Tamim I, Chung DY, de Morais AL, et al. Spreading depression as an innate antiseizure mechanism. Nat Commun 2021;12(1):2206. DOI: 10.1038/s41467-021-22464-x.
9. Chung DY, Sadeghian H, Qin T, et al. Determinants of Optogenetic Cortical Spreading Depolarizations. Cereb Cortex 2018. DOI: 10.1093/cercor/bhy021.
10. Chung DY, Sugimoto K, Fischer P, et al. Real-time non-invasive in vivo visible light detection of cortical spreading depolarizations in mice. Journal of neuroscience methods 2018. DOI: 10.1016/j.jneumeth.2018.09.001.
11. Lai JH, Qin T, Sakadzic S, Ayata C, Chung DY. Cortical Spreading Depolarizations in a Mouse Model of Subarachnoid Hemorrhage. Neurocrit Care 2022;37(Suppl 1):123-132. DOI: 10.1007/s12028-021-01397-9.
12. Chung DY, Oka F, Jin G, et al. Subarachnoid hemorrhage leads to early and persistent functional connectivity and behavioral changes in mice. Journal of cerebral blood flow and metabolism : official journal of the International Society of Cerebral Blood Flow and Metabolism 2021;41(5):975-985. DOI: 10.1177/0271678X20940152.

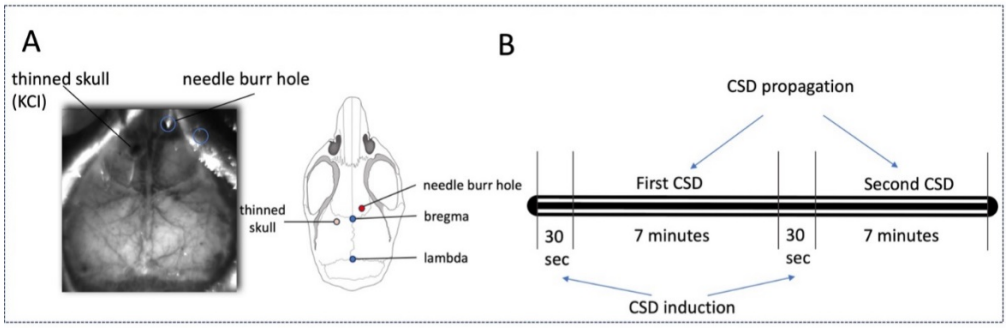
A
thinned skull
(KCl)
needle burr hole
thinned
skull
needle burr hole
bregma
lambda
B
CSD propagation
First CSD
Second CSD
30
sec
7 minutes
30
sec
7 minutes
CSD induction

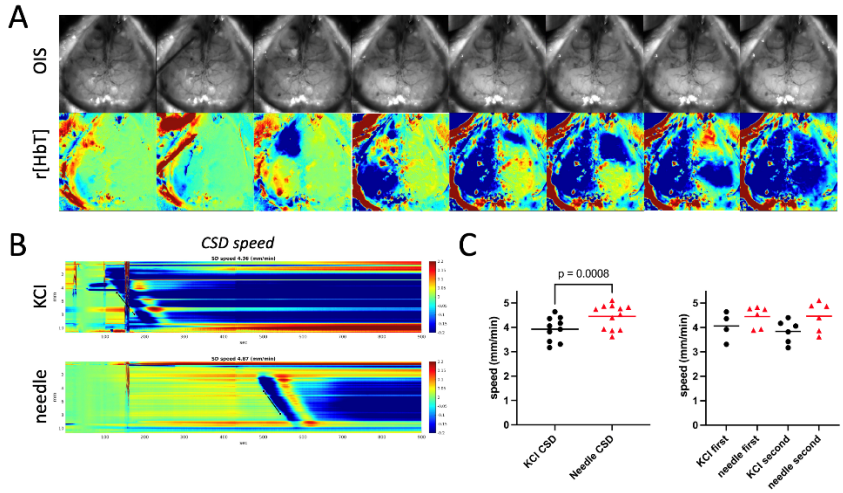
A
OIS
r[HbT]
B
CSD speed
KCl
needle
C
p = 0.0008
speed (mm/min)
KCl CSD
Needle CSD
KCl first
needle first
KCl second
needle second

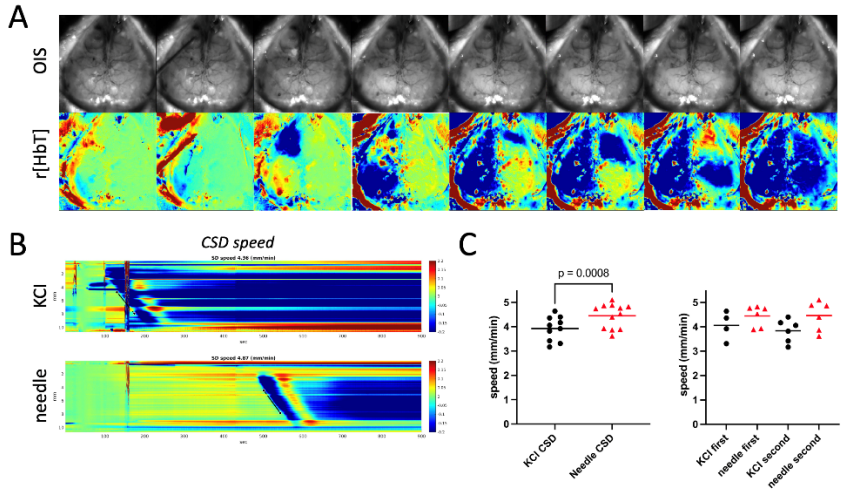
A
OIS
r[HbT]
B
CSD speed
KCl
needle
C
p = 0.0008
speed (mm/min)
KCl CSD
Needle CSD
KCl first
needle first
KCl second
needle second

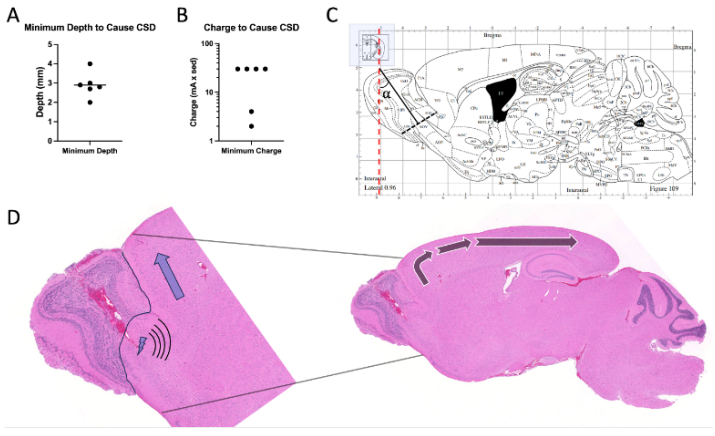
A
Minimum Depth to Cause CSD
Depth (mm)
Minimum Depth
B
Charge to Cause CSD
Charge (mA x sec)
Minimum Charge
C
D

OP-23(ID:45)

EFFECT OF LONG-TERM OPTOGENETIC STIMULATION ON ELECTROPHYSIOLOGICAL SPREADING DEPOLARIZATION PARAMETERS IN MICE

ANNIKA KOHNE , PATRICK DOMER , SIMEON OA HELGERS , FRANZISKA MEINERT , RENáN SáNCHEZ-PORRAS , JOHANNES WOITZIK

DEPARTMENT OF NEUROSURGERY, CARL VON OSSİETZKY UNİVERSİTY OLDENBURG, OLDENBURG, GERMANY

Introduction:
Despite increased research efforts, the pathophysiological mechanisms of spreading depolarizations (SDs) are still unclear. Moreover, investigation of SD effects in animal experiments so far was mainly limited to an acute short-term set-up. However, this scheme does not fully translate to the clinical situation. For translational purposes, we developed a long-term experimental schedule with wireless optogenetic SD induction in freely moving mice of different ages after an initial insult (occlusion of the internal carotid artery or a distal branch of the middle cerebral artery).

Methods:
To test the reliability and comparability of our optogenetic stimulation, preliminary experiments were performed in a final setting on mice without vessel occlusion (Thy1-ChR2) of two different age groups (3-5 months; ~1 year). These mice received surgical implantation of a wireless optogenetic device operating on near-field power transfer. Afterwards, cortical perfusion (assessed by LSI) and neuronal activity (assessed by electrocorticogram (ECoG)) were monitored for several hours with SD triggers being given every 15 minutes.
Chronic experiments were performed in young (3-5 month) and aged mice (~1 year) with chronic cerebral hypoperfusion or distal stroke. In each of these conditions, animals were randomly assigned to a control or stimulation group. After implantation of the optogenetic device, the stimulation groups received a recurrent SD trigger every 6 hours over a period of 3 weeks in their housing cage, the control groups received the same surgical treatments but no SD induction. To assess the effects of this long-term stimulation on electrophysiological SD parameters, simultaneous LSI and ECoG measurement of two SDs was performed on experimental day 14. ECoG measurements of induced SDs in pre- and chronic experiments were analyzed for the following SD parameters: DC-shift duration and amplitude, and duration of depression of spontaneous activity. Additionally, SDs were classified based on their DC-shift waveform (single peak (hyperpolarization), double peak (hyperpolarization)).

Results:
ElectrophysiologicalSD parameters of our pre-experimental groups were comparable to SDs induced by KCl or optogenetics in other recent studies. Proportional distribution of DC-shift waveform, with a high amount of single peak (hyperpolarization) SDs, was also similar to results found before in diseaseless mice. SDs of the single peak type had a shorter duration and smaller amplitude than SDs of the double peak type.
Regarding our chronic experiments, in both age groups of mice with chronic hypoperfusion, there was a significant difference between the stimulated and non-stimulated animals in terms of DC-shift parameters. The control groups showed prolonged SDs with larger amplitudes. These differences were also represented in a different distribution of waveforms for stimulation and control groups, with stimulation groups being similar to the pre-experiments, whereas the control groups showed a higher amount of double peak SDs. A similar trend was also observed for the experimental groups with a distal stroke.

Conclusions:
Our results suggest that medical conditions like chronic hypoperfusion or distal stroke induce a change in the SD waveform features, from single peak forms that are mainly found in diseaseless mice, towards double peak forms. On the other hand, a recurrent SD stimulation seems to shift the waveform distribution back to more single peak SDs.

OP-24 (ID:49)

LOSS OF AROUSAL FOLLOWING INDUCTION OF CORTICAL SPREADING DEPOLARISATION IN AWAKE MICE

KAĞAN AĞAN [1], KAĞAN AĞAN [2], NEELA K. CODADU [1], DAMAN RATHORE [1], EDUARD MASVIDAL-CODINA [3], ENRIQUE FERNáNDEZ-SERRA [4], RANDY GYIMAH [1], ANTON GUIMERA-BRUNET [4], ROB C. WYKES [1], ROB C. WYKES [5],

[1] *DEPARTMENT OF CLINICAL & EXPERIMENTAL EPILEPSY, UCL QUEEN SQUARE INSTITUTE OF NEUROLOGY, UNITED KINGDOM*
[2] *EXPERIMENTAL ANIMAL APPLICATION AND RESEARCH CENTER, DÜZCE UNIVERSITY, DÜZCE, TÜRKIYE*
[3] *CATALAN INSTITUTE OF NANOSCIENCE AND NANOTECHNOLOGY (ICN2), BARCELONA, SPAIN*
[4] *INSTITUT DE MICROELECTRÒNICA DE BARCELONA, IMB-CNM (CSIC), BELLATERRA, SPAIN*
[5] *CENTER FOR NANOTECHNOLOGY IN MEDICINE & DIVISION OF NEUROSCIENCE, UNIVERSITY OF MANCHESTER, UNITED KINGDOM*

Introduction:
Anaesthesia is known to influence not just cortical spreading depolarisation (CSD) properties itself, but also many downstream responses to CSD. The aim of this study is to apply pupillometry as a proxy of arousal state to determine the impact of CSD in awake brain.

Methods:
Mice were injected with viral vectors to express channelrhodospin (ChR2) in the right motor cortex and to attach headbars. Animals were habituated to a Neurotar Mobile Homecage. 6 weeks following injection of virus, acute awake head-fixed experiments were performed. gSGFET arrays were placed either on the dura or on top of intact skull over the ipsilateral cortex. Cameras were focused on the contralateral eye pupil. CSDs were induced using an optogenetic protocol, as previously described (Masvidal E *et al* 2021), briefly; sustained blue light (473nm) to the motor cortex for 5-10s. Additional CSD induction techniques (pinprick or injection or high concentration KCL) were also performed.

Results:
In response to an optogenetically-induced CSD a biphasic response in pupil diameter was determined. An initial dilation time-locked to the length of the electrographic depolarisation; indicative of an increase in arousal state. This was followed by a constriction that persisted for several minutes, and until recovery of higher frequency activity suppression. To determine that this response was not specific to the induction method or cortical induction region, similar observations were made when CSD was induced in other cortical sites and by other methods (pinprick and KCL). IP injection of MK801 (an NMDA receptor antagonist), prevented the induction of CSD and pupil responses.

Conclusion:
This study demonstrates that CSD results in changes to subcortical structures that influence arousal state in awake brain. Further studies using functional ultrasound imaging are being conducted to identify which subcortical arousal areas are modulated by CSD.

Keywords: Graphene, Spreading Depolarisation, pupillometry, optogenetics

Declarations:
All experiments were performed in accordance with the United Kingdom Animals (Scientific Procedures) Act 1986 and have university ethical approvals.

Funding:
This work has received funding from the European Union's Horizon 2020 research and innovation programme under Grant Agreement No. 881603 (GrapheneCore3). R.C.W. is funded by a Senior Research Fellowship awarded by the Worshipful Company of Pewterers. K.A is awarded a post-doctorate grant by the Scientific and Technological Research Council of Turkey (TUBITAK)

OP-25 (ID:28)

SPONTANEOUS SPREADING DEPOLARIZATIONS IN ATP1A2 AND ATP1A3 MUTANT MICE

ELSE TOLNER , GEORGII KRIVOSHEIN , CHELSEY LINNENBANK , NICO JANSEN , MAARTEN SCHENKE , ROB VOSKUYL , SANDRA VAN HEININGEN , ARN VAN DEN MAAGDENBERG

LEİDEN UNİVERSİTY MEDİCAL CENTER

Background:

Defects in Na^+/K^+-ATPase pumps are associated with a variety of neurological disorders. *ATP1A2* encodes the α2 subunit of Na^+/K^+-ATPase pumps that, in adults, are expressed in astrocytes. *ATP1A2* loss-of-function mutations cause familial hemiplegic migraine type 2 (FHM2), a rare subtype of migraine with severe auras. *ATP1A3* encodes the α3 subunit of Na^+/K^+-ATPases that are predominantly expressed in neurons throughout life, for which loss-of-function mutations cause alternating hemiplegia of childhood (AHC). AHC is a severe neurodevelopmental disorder featuring hemi- and quadriplegic episodes, dystonia, gait ataxia, and epileptic attacks. Based on previous research on ATP1A2 and ATP1A3 mutant pumps, it can be hypothesized that both defective astrocytic and neuronal Na^+/K^+-ATPase function result in network hyperexcitability and susceptibility to seizures and/or spreading depolarization (SD). Lack of insight in spontaneous brain activity features hampers mechanistic insight underlying the clinical phenotypes.

Objective:

Functional characterization of spontaneous brain activity (including SDs, if occuring) and evoked SD features in freely behaving mice of (1) a novel mouse model expressing FHM2 T345A missense-mutated α_2NKA subunit-containing Na^+/K^+-ATPase pumps and (2) mouse models expressing AHC E815K missense- and D801N missense-mutated α3NKA subunit-containing Na^+/K^+-ATPase pumps.

Methods:

Heterozygous and homozygous *Atp1a2*^{T345A} knock-in (KI) mice were generated to study *in vivo* effects of the T345A mutation on brain function, for which the human FHM2 T345A missense mutation was introduced in the mouse *Atp1a2* gene by gene targeting. *Atp1a3*^{E815K} and *Atp1a3*^{D801N} KI mice were obtained from the Jackson Laboratory and bred in-house. Long-term recordings of cortical and hippocampal direct-current and local field potentials were performed in freely behaving mice to assess brain activity features. Cortical SD thresholds were assessed by electrical stimulation in awake freely behaving mice.

Results:

Homozygous *Atp1a2*^{T345A} mutant mice were viable and showed decreased survival with spontaneous death related likely due to sudden fatal apnea. The homozygous mutants showed spontaneous SDs that exhibited a diurnal rhythm with events originating from hippocampus and spreading to visual and motor cortex. Despite hippocampal hyperexcitability, spontaneous SDs were rarely associated with epileptic behavior; moreover, seizure expression during kindling was decreased. Heterozygous *Atp1a3*^{E815K} and *Atp1a3*^{D801N} mutant mice developed gait ataxia becoming evident from about 2-2.5 months of age. Both strains displayed epileptiform activity with interictal and giant spikes. Spontaneous SDs were observed, with an apparent hippocampal origin and occasional spreading to visual and motor cortex. Typical SD-related behaviors were head waving and body circling around the axis with (for AHC mutants) one-sided leg dragging. Cases of recorded death in *Atp1a3*^{E815K} mutant mice were preceded by clustered epileptiform bursts directly followed by SD.

Conclusions:

Occurrence of regular spontaneous SDs in homozygous *Atp1a2*^{T345A} mutant mice, and occasional SDs in the AHC mutant mice models provides a basis for a mechanistic understanding of the related phenotypes and may guide the development of therapies targeting SD and its consequences. Our findings may benefit not only people suffering from hemiplegic migraine and alternating hemiplegia but likely also people with other neurological disorders involving SD, such those at risk for sudden death and certain types of epilepsy syndromes.

OP-26 (ID:)

ACUTE LEVCROMAKALIM INJECTION INDUCES MIGRAINE-LIKE PHENOTYPE WITHOUT CORTICAL SPREADING DEPOLARIZATION IN MALE WISTAR RATS

BERKAY ALPAY[1] BARİSCAN CİMEN [1] ELİF AKAYDİN[1] HAYRUNNİSA BOLAY [2] YİLDİRİM SARA [1]

1-HACETTEPE UNİVERSİTY, FACULTY OF MEDİCİNE, DEPARTMENT OF MEDİCAL PHARMACOLOGY, ANKARA, TURKEY
2-GAZİ UNİVERSİTY, FACULTY OF MEDİCİNE, DEPARTMENT OF NEUROLOGY, ANKARA, TURKEY

Objective:
Migraine is a type of primary headache, disabling millions of people worldwide by affecting their quality of life significantly [1]. Almost one third of these patients experience migraine auras, that is transient, fully reversible neurological impairments mainly manifested in the visual sensory area [2]. Migraine auras are speculated to arise from spreading depolarization waves, called cortical spreading depolarization (CSD). Another electrophysiological finding encountered in migraineurs is sensory gating dysfunction, which is thought to underlie the sensory augmentation observed in these patients [3, 4]. There are several pharmacological agents known to provoke migraine headache in patients with migraine and migraine-like phenotype in experimental animals. So far, among the migraine-provoking drugs levcromakalim (LVC) is a well-established inducer of both aura and headache in migraineurs with aura [5]. Rest of the migraine-provoking agents, including nitroglycerine (NTG), were shown to induce aura with a very low rate. The objective of this work is to observe effects of single LVC and NTG administration on acute pain-related behaviours, CSD, sensory processing and overall cortical network activity.

Methods:
Migraine-like phenotype is provoked by NTG (10 mg/kg i.p.) and LVC (1 mg/kg i.p.) in male Wistar rats and compared to control (vehicle) groups. In all experiments, appropriate control groups are used in comparison with treatment groups. Periorbital and hind paw mechanical allodynia thresholds were tested with von Frey filaments. Anxiety-like behaviours, photophobia, and locomotion were evaluated with elevated plus maze (EPM), dark-light box (DLB) and open field arena (OFA). Effects of LVC and NTG on CSD, somatosensory evoked potential (SSEP) and cortical activity were investigated in rats under urethane anaesthesia (1,2 g/kg i.p.) via in vivo electrophysiology methods (KCl-induced CSD, SSEP, dural EEG). Quantification of SSEP was based on their amplitudes and latency-to-peaks. Possible CSD-induced c-fos expression was studied in parietal cortex with Western blotting. Power spectra of EEG recordings were analysed for the delta (δ), theta (θ), alpha (α), beta (β) and gamma (γ) range activity.

Results:
LVC significantly decreased mechanical allodynia thresholds in a shorter time with respect to NTG. Migraine-like phenotype induced by LVC recovered in two hours, whereas recovery period of NTG took longer (four hours). In addition, peak reduction in mechanical allodynia thresholds was observed sixty minutes earlier in LVC group (1st hour) compared to NTG group (2nd hour). LVC- and NTG-injected rats spent a shorter time in the open arms of EPM than the control group. LVC and NTG significantly reduced the time spent in the bright compartment of DLB. Decrease in time spent in the centre zone and number of entries to the centre zone were detected in LVC- and NTG-injected animals. NTG administration reduced the CSD threshold, while LVC increased the propagation failure rate. In both LVC and NTG groups, SSEP latencies were prolonged similarly before and after CSD. However no change in SSEP peak amplitudes was detected pre-and post-CSD. Cortical c-fos expression was not increased after LVC administration compared to appropriate control groups. In EEG experiments, no difference was found between pre-CSD recordings of all groups. However, LVC-treated group displayed weaker activity within the delta, theta, alpha, beta and gamma range following CSD.

Conclusion:
LVC reduced mechanical allodynia thresholds and induced pain-related behaviours within a shorter timeframe but otherwise effects were similar to that of NTG. However, as opposed to NTG, LVC did not alter CSD parameters (amplitude, duration, threshold, frequency, velocity) except for propagation failure. Moreover, weaker cortical activity is detected in EEG recordings of LVC-administered rats implicating impaired recovery following CSD. These findings suggest that migraine-like phenotype induction with LVC is an alternative method for studying acute migraine phenotype independent of CSD.

References:

1. Headache Classification Committee of the International Headache Society (IHS) The International Classification of Headache Disorders, 3rd edition. Cephalalgia, 2018. 38(1): p. 1-211.
2. Ferrari, M.D., et al., Migraine. Nature Reviews Disease Primers, 2022. 8(1): p. 2.
3. Coppola, G., et al., Effects of repetitive transcranial magnetic stimulation on somatosensory evoked potentials and high frequency oscillations in migraine. Cephalalgia, 2012. 32(9): p. 700-709.
4. de Tommaso, M., et al., Altered processing of sensory stimuli in patients with migraine. Nature Reviews Neurology, 2014. 10(3): p. 144-155.
5. Al-Karagholi, M.A.-M., et al., Opening of ATP sensitive potassium channels causes migraine attacks with aura. Brain, 2021. 144(8): p. 2322-2332.

OP-27 (ID:)

PALYTOXIN EVOKES REVERSIBLE SPREADING DEPOLARIZATION IN THE LOCUST CNS

YUYANG WANG[1], RACHEL VAN DUSEN[1], CATHERINE MCGUİRE[1], R. DAVID ANDREW[1],R. MELDRUM ROBERTSON[1]

1- QUEEN`S UNİVERSİTY AT KİNGSTON

Spreading depolarization (SD) describes the near-complete depolarization of CNS neural cells as a consequence of chemical, electrical, or metabolic perturbations. It is well-established as the central mechanism underlying insect coma and various mammalian neurological dysfunctions. Despite significant progress in our understanding, the question remains: which cation channel, if any, generates SD in the CNS?

Previously, we speculated that the sodium-potassium ATPase (NKA) might function as a cationic channel to initiate SD in insects, potentially mediated by a palytoxin (PLTX)-like endogenous activator. In the current study, we evaluate the effectiveness and properties of PLTX as an SD initiator in L. migratoria. Whereas bath-applied PLTX failed to ignite SD, direct injection into the neuropil triggered SD in 57% of the preparations. Notably, PLTX-induced SD onset was significantly more rapid compared to ouabain injection and azide controls, though their electrophysiological features remained similar. Furthermore, PLTX-induced SD was recoverable and resulted in a greater frequency of repetitive SD events compared to ouabain.

Surprisingly, prior PLTX treatment disrupted the onset and recovery of subsequent SD evoked by other means. PLTX injection could attenuate the amplitude and even completely inhibit the onset of azide-induced SD at higher doses.

These results show that PLTX can trigger repetitive and reversible SD-like events in locusts and simultaneously interfere with anoxic SD occurrence. We suggest that the well-documented NKA pump conversion into an open non-selective cationic channel is a plausible mechanism of SD activation in the locust CNS, warranting additional investigations.

OP-28 (ID:60)

THE SLOPE OF THE SPREADING DEPOLARIZATION RELATED BLOOD FLOW TRANSIENTS IS A POTENTIAL BIOMARKER FOR RISK STRATIFICATION IN EXPERIMENTAL ISCHEMIC STROKE

LUCKL JANOS [1], SALEHZADEH AMIRHOSSEIN [2], SZUCS MONIKA [2], RAROSI FERENC [2], DREIER JENS [3],

[1] CENTRE FOR STROKE RESEARCH BERLIN, CHARITÉ – UNIVERSITÄTSMEDIZIN BERLIN, CORPORATE MEMBER OF FREIE UNIVERSITÄT BERLIN, HUMBOLDT-UNIVERSITÄT ZU BERLIN, AND BERLIN INSTITUTE OF HEALTH, BERLIN, GERMANY

[2] DEPARTMENT OF MEDICAL PHYSICS AND INFORMATICS, UNIVERSITY OF SZEGED, SZEGED, HUNGARY

[3] DEPARTMENT OF NEUROLOGY, CHARITÉ – UNIVERSITÄTSMEDIZIN BERLIN, CORPORATE MEMBER OF FREIE UNIVERSITÄT BERLIN, HUMBOLDT-UNIVERSITÄT ZU BERLIN, AND BERLIN INSTITUTE OF HEALTH, BERLIN, GERMANY

Project Objectives:

Ischemic stroke is a heterogeneous condition regarding outcomes both in humans and in experimental stroke. Risk stratification in animal studies could be beneficial in several ways (improving statistics, allowing a more precise outcome analysis, and minimizing the pain and suffering of the research animals).

Materials and Methods:

We retrospectively analyzed 28 filament-occluded animals of a prospective study to test if risk stratification based on the predicted infarct size would be possible with biomarkers at 30, 60, and 90 minutes after occlusion. After 90 minutes of ischemia, the animals survived 72 hours and the infarct size was determined by hematoxylin staining. As potential biomarkers, we analyzed the parameters (amplitude, slope) of spreading depolarization-related flow transients collected by laser Doppler flowmetry and the relative changes of the ECoG-Power and DC-Integral recorded by silver-chloride electrodes epidurally. Multiclass ROC analysis was performed to select the best parameters. Spearman's rank correlation was also performed to find relationships between the electrophysiological and cerebral blood flow-related biomarkers.

Results:

The statistical analysis revealed that the slope of the flow transients is the best biomarker at any time point. The best electrophysiological marker proves to be the DC-Integral of the cranially placed electrode. Interestingly, Spearman's analysis shows a fair, inverse correlation between these two parameters at any time point (r_{90min} = - 0,72; r_{60min} = - 0,77; r_{30min} = - 0,71).

Conclusions:

The concept of risk stratification is feasible. In our experimental material, the slope of flow transients appears to be the best biomarker. The present work likely also has translational value.

Keywords: risk stratification, filament occlusion, spreading depolarization, the slope of flow transients

OP-29 (ID:64)

PROPHYLACTIC TREATMENT OF MIGRAINE WITH (100%) AURA: EVALUATING THE EFFICACY OF LAMOTRIGINE IN PRECLINICAL AND CLINICAL SETTINGS

SENA UZUN [1], BUKET DÖNMEZ DEMİR [3], GÜRDAL SAHİN [2], HÜLYA KARATAS KURSUN [4]

[1] *INTEGRATİVE NEUROPHYSİOLOGY AND NEUROTECHNOLOGY, DEPARTMENT OF EXPERİMENTAL MEDİCAL SCİENCES, LUND UNİVERSİTY, LUND, SWEDEN*

[2] *SKåNEURO NEUROLOGY CLİNİC, LUND, SWEDEN*

[3] *HACETTEPE UNİVERSİTY, INSTİTUTE OF NEUROLOGİCAL SCİENCES AND PSYCHİATRY, ANKARA, TURKEY*

[4] *NEUROSCİENCE AND NEUROTECHNOLOGY CENTER OF EXCELLENCE (NÖROM), ANKARA, TURKEY*

Background:

Prophylactic treatment options for migraine with aura are limited, with current practices involving antidepressants, calcium antagonists, antihypertensives, beta-blockers, and antiepileptics, all showing modest efficacy. Lamotrigine (LMT) has demonstrated effectiveness in small case series, and anecdotal reports suggest acetylsalicylic acid (ASA) might also be beneficial. However, further studies are needed to explore the preclinical effects of these treatments, alone and in combination, to potentially reduce side effects. Cortical spreading depolarization (CSD), an electrophysiological correlate of migraine aura, is used to investigate the effects of anti-migraine drugs. This study aims to evaluate the impact of chronic administration of LMT and ASA, individually or combined, on the generation, propagation, and electrophysiologic characteristics of CSD.

Methods:

Adult Swiss albino female mice were divided into five groups of six animals each, receiving 28 days of intraperitoneal injections: LMT (150 µL, 10 mg/kg in saline), ASA (150 µL, 30 mg/kg in saline), a combination of LMT (75 µL, 10 mg/kg) and ASA (75 µL, 30 mg/kg), sodium valproate (VPA) (150 µL, 200 mg/kg in saline), and saline. Saline served as a sham control, and VPA was a positive control. CSDs were induced by topical potassium chloride (KCl) application over the dura, recorded electrophysiologically with two Ag-AgCl2-coated pellet electrodes placed over the thinned parietal cranium. The CSD threshold was assessed by applying cotton balls soaked in increasing KCl concentrations (0.05 to 0.175 M) over the dura through a frontal burr hole at 5-minute intervals. Moreover, a retrospective analysis was conducted on patients with "migraine with 100% aura," treated with LMT based on clinical experience. The primary outcome was a minimum 50% reduction in monthly aura frequency post-LMT prophylaxis, with non-responders experiencing less than 25% reduction and super-responders experiencing more than 75% reduction. The study also recorded LMT's average dose and safety profile.

Results:

The CSD threshold significantly increased in the VPA, LMT, and ASA groups compared to the saline group ($p=0.0043$; Kruskal-Wallis test). No significant differences were found between the CSD thresholds of the drug-injected groups ($p>0.05$). The combination of lower doses of LMT and ASA did not alter the CSD threshold compared to saline, indicating no synergistic effect. Electrophysiologic characteristics and CSD propagation remained unchanged among the groups. In the clinical study, 79 patients were analyzed, with 78 experiencing visual disturbances, 13 motor weaknesses, 45 sensory symptoms, and 27 language difficulties during migraine attacks. Eight reported extreme photosensitivity. The average LMT dose was 148.8 ± 8.4 mg, with a mean treatment duration of 58.6 ± 4.9 months. Efficacy analysis in 75 patients (51 female, 24 male) showed 88% responders and 81.3% super-responders. The mean aura days per month decreased from 6.93 ± 0.89 to 1.19 ± 0.39. Continued treatment was necessary for almost all, with only one patient able to discontinue. Twenty-eight patients reported adverse events, with seven discontinuing due to these events. Common adverse events included skin changes, dizziness, tiredness, arthralgia, psychological, and metabolic disturbances.

Conclusion:

LMT and ASA show potential as prophylactic treatments for migraine with aura, but chronic administration of low-dose LMT and ASA does not alter the CSD threshold in mice, suggesting limited effectiveness for this combination at low doses. Clinically, LMT demonstrates high efficacy and a manageable side-effect profile for preventing migraine with aura, warranting consideration in migraine with (100%) aura treatment.

OP-30 (ID:87)

IMPACT OF NIMODIPINE ON HEMODYNAMIC FLUCTUATIONS AND CONNECTIVITY DYNAMICS FOLLOWING CORTICAL SPREADING DEPOLARIZATIONS IN A GYRENCEPHALIC SWINE MODEL

DIEGO ALBERTO SANDOVAL-LOPEZ [1], JUAN M. LOPEZ-NAVARRO [1], LYDIA HAWLEY [2], EDGAR SANTOS [3], RENáN SANCHEZ-PORRAS [1], JOHANNES WOITZIK [1], DAVID Y. CHUNG [2],

[1] DEPARTMENT OF NEUROSURGERY, CARL VON OSSİETZKY UNİVERSİTY OF OLDENBURG, OLDENBURG, GERMANY.
[2] MASSACHUSETTS GENERAL HOSPİTAL, CHARLESTOWN, MA, USA
[3] SPİNE CENTER STUTTGART, PAULİNENHİLFE, DİAKONİE-KLİNİKUM STUTTGART, STUTTGART, GERMANY

Introduction:
Cortical spreading depolarizations (CSDs) are associated with neurological conditions like subarachnoid hemorrhage, traumatic brain injury, stroke, and migraine. These events disrupt resting-state functional connectivity (RSFC) by causing ionic imbalances, metabolic stress, altered cerebral blood flow, inflammation, and synaptic dysfunction, leading to impaired neural network dynamics [1].
While lissencephalic models (e.g., rodents) are widely used [1-3], they differ significantly from the more complex gyrencephalic brains of humans and higher mammals. This distinction is critical, as it may affect CSD propagation, impact, and the brain's response to interventions. Research suggests that gyrencephalic models respond differently to CSDs and associated hemodynamic changes compared to lissencephalic models [4]. Moreover, the effects of interventions like nimodipine—a calcium channel blocker that stabilizes cerebral blood flow—remain underexplored in this context.
This study aims to bridge this gap by applying RSFC indices, typically used in lissencephalic models [5], to data from swine, a gyrencephalic model. We evaluate CSD effects on global and bihemispheric connectivity using intrinsic optical signal imaging and assess nimodipines modulatory effects. Additionally, we performed a power analysis to better understand the hemodynamic fluctuations in volume, specifically focusing on the differences in pre- and post-stimulation phases between nimodipine and placebo groups. This is the first study to evaluate RSFC in the context of CSDs in a gyrencephalic model, enhancing our understanding of RSFC dynamics and exploring nimodipines potential as a modulator of brain connectivity following acute and chronic brain injuries.

Methods:
A randomized, double-blind study was conducted on 10 female German Landrace swine (3-4 months old, 28-32 kg). The swine were randomly assigned to control or nimodipine-treated groups (n=5 each) using a computer-generated sequence, with both administrators and outcome assessors blinded. Ethical approval was obtained from the Institutional Animal Care and Use Committee in Karlsruhe, Germany.
Anesthesia was induced with Azaperone, Midazolam, and Ketamine, and maintained with Isoflurane and Midazolam. Vital parameters were continuously monitored, and a central venous catheter was placed for fluid and drug administration. Bilateral craniectomy and durotomy were performed, followed by a 60-minute preconditioning phase. Cortical activity was monitored using subdural electroencephalographic (ECoG) recordings, and intrinsic optical signal imaging with a 570 nm filter assessed hemodynamic changes.
Cortical spreading depolarization (CSD) was induced using local KCl (3 mmol) in each hemisphere. Baseline recordings lasted 10 minutes, followed by 90-minute post-stimulation recordings, with contralateral stimulation at 100 minutes, resulting in four single-hemisphere stimulations per pig. The control group received saline, while the treatment group received nimodipine (1 mg/h) during preconditioning and the experiment.
Functional connectivity was analyzed using custom MATLAB scripts. Optical density images were resized to 128x128 pixels, and connectivity maps were created from correlation coefficients. Global and bihemispheric connectivity indices were calculated, excluding CSD clusters and spontaneous CSDs in the contralateral hemisphere. A power analysis was conducted to evaluate nimodipines effect on hemodynamic fluctuations, comparing regressed and unregressed volume changes pre- and post-stimulation.
Statistical analyses were performed using SPSS. Normal distribution was assessed by the Shapiro-Wilk test, with the Wilcoxon signed-rank test comparing phases within groups and the Mann-Whitney U test comparing between groups. Significance was set at $p<0.05$.

Results:
After applying exclusion criteria, data from 7 animals were analyzed, with 4 in the control group (11 measurements) and 3 in the nimodipine group (10 measurements). Physiological variables were consistently within normal ranges throughout the study. Post-stimulation, the nimodipine group showed significantly lower global connectivity and bihemispheric connectivity compared to the placebo group ($p < 0.05$ for both). In the

power analysis, both Regressed and Unregressed Map Power were significantly lower in the nimodipine group post-stimulation compared to the placebo group ($p = 0.006$ and $p = 0.010$, respectively). Within-group comparisons revealed that the placebo group had a significant increase in Regressed and Unregressed Map Power from pre- to post-stimulation ($p = 0.016$ and $p = 0.021$), while the nimodipine group showed no significant changes. Other observed differences were not statistically significant.

Discussion:
This study provides insights into the effects of cortical spreading depolarizations (CSDs) on resting-state functional connectivity (RSFC) and hemodynamic fluctuations in a swine model. Notably, post-stimulation comparisons revealed that both Regressed and Unregressed Map Power were significantly lower in the nimodipine group compared to the placebo group, indicating a reduced hemodynamic response to CSD. Additionally, nimodipine significantly reduced both global and bihemispheric connectivity post-stimulation.
In terms of baseline comparisons, there were no significant differences between the nimodipine and placebo groups, suggesting similar hemodynamic conditions before stimulation. Post-stimulation, the placebo group showed a significant increase in Regressed and Unregressed Map Power, aligning with the known impact of CSD on cerebral autoregulation and hemodynamic fluctuations [4]. In contrast, the nimodipine group showed no significant changes, which may be attributed to nimodipines stabilizing effect on cerebral blood flow (CBF), limiting hemodynamic fluctuations and highlighting its neuroprotective potential [6, 7].
The reduction in connectivity and hemodynamic response associated with nimodipine may be linked to its broader neuroprotective actions, such as inhibition of calcium influx, reduction of excitotoxic damage, and modulation of inflammation [7]. Other differences observed in the study were not statistically significant.
Future studies should explore these findings further with global signal regression and evaluate other calcium channel blockers and neuroprotective agents in similar models. Increasing the sample size will be crucial to fully understand nimodipine's long-term effects on RSFC and its potential role in recovery from chronic brain injuries.

References

1. Chung, D. Y., …, Ayata, C. (2020). Subarachnoid hemorrhage leads to early and persistent functional connectivity and behavioral changes in mice. In Journal of Cerebral Blood Flow & Metabolism (Vol. 41, Issue 5, pp. 975–985)
2. Hougaard, A., et al. (2017). Increased intrinsic brain connectivity between pons and somatosensory cortex during attacks of migraine with aura. In Human Brain Mapping (Vol. 38, Issue 5, pp. 2635–2642).
3. Xie, H., …, Ayata, C. (2019). Differential effects of anesthetics on resting state functional connectivity in the mouse. In Journal of Cerebral Blood Flow & Metabolism (Vol. 40, Issue 4, pp. 875–884).
4. Santos, E., et al. (2017). Heterogeneous propagation of spreading depolarizations in the lissencephalic and gyrencephalic brain. In Journal of Cerebral Blood Flow & Metabolism (Vol. 37, Issue 7, pp. 2639–2643)
5. Kura, S., et al. (2018). Intrinsic optical signal imaging of the blood volume changes is sufficient for mapping the resting state functional connectivity in the rodent cortex. In Journal of Neural Engineering (Vol. 15, Issue 3, p. 035003)
6. Kirov SA, Fomitcheva IV, Sword J. Rapid neuronal ultrastructure disruption and recovery during spreading depolarization-induced cytotoxic edema. *Cereb Cortex*. 2020;30:5517-5531.
7. Frank, R., …, & Farkas, E. (2024). Nimodipine inhibits spreading depolarization, ischemic injury, and neuroinflammation in mouse live brain slice preparations. European Journal of Pharmacology (Vol. 977, p. 176718).

Table 1. Global and bihemispheric connectivity indices

Group	Global Z-value med (IQR)	Std. Global Z-value med (IQR)	Bi-hemi med (IQR)	Std. Bi-hemi Z-value med (IQR)
Control (n=11)				
Pre-stimulation	0.20 (0.05)	0.06 (0.01)	0.10 (0.08)	0.10 (0.02)
Post-stimulation	0.17 (0.06)	0.06 (0.03)	0.09 (0.09)	0.10 (0.03)
p-value	0.09		0.120	
Nimodipine (n=10)				
Pre-stimulation	0.20 (0.07)	0.05 (0.03)	0.08 (0.07)	0.09 (0.02)
Post-stimulation	0.15 (0.07)	0.05 (0.02)	0.05 (0.05)	0.09 (0.01)
p-value	**0.008**		0.172	

Abbreviations: med, median; IQR, interquartile range; Bi-hemi, bihemispheric.

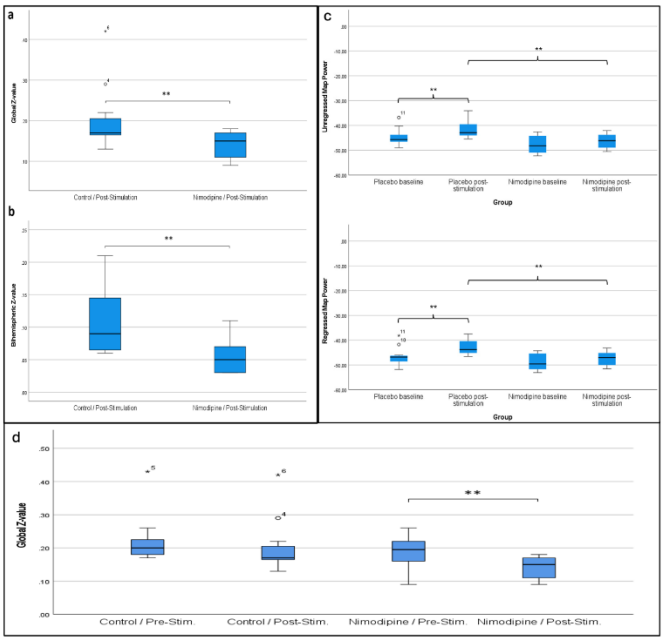

Fig. 1. a-b) Box plots showing the changes in the Global Z-value (a) and Bihemispheric Z-value (b) in the post-stimulation phase between the control and Nimodipine groups. (Mann-Whitney U test). c) This figure shows Unregressed (top) and Regressed (bottom) Map Power for placebo and nimodipine groups at baseline and post-stimulation. Baseline differences between groups were not significant for Unregressed (p = 0.099) or Regressed Map Power (p = 0.223). Post-stimulation, Map Power was significantly lower in the nimodipine group for both Unregressed (p = 0.010) and Regressed (p = 0.006) data. The placebo group exhibited a significant increase from baseline to post-stimulation in both measures (p = 0.021 and p = 0.016, respectively), while the nimodipine group showed no significant changes (p = 0.074 for both). **p-value < 0.05

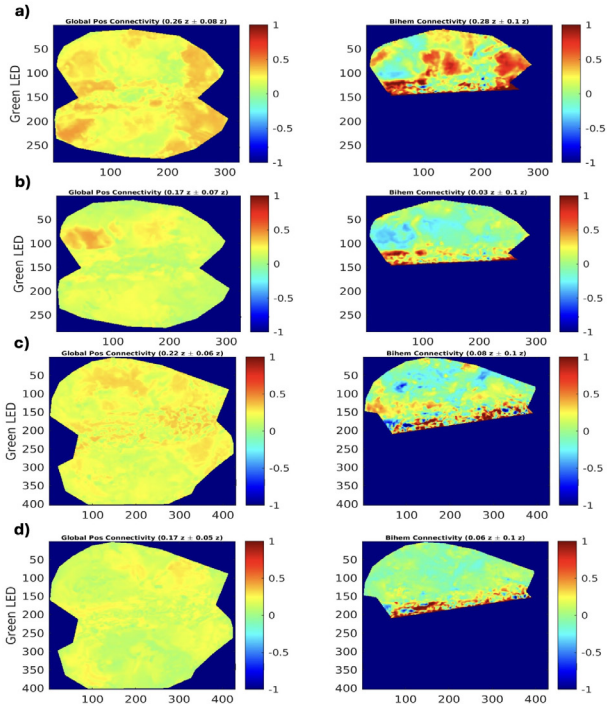

Fig. 2. Global and bihemispheric connectivity maps pre- and post-stimulation on the left hemisphere for control and nimodipine groups. (a) Nimodipine-treated group pre-stimulation. (b) Nimodipine-treated group post-stimulation. (c) Control group pre-stimulation. (d) Control group post-stimulation. In the maps, the right side corresponds to the frontal region, the left side to the occipital region, the upper part to the right hemisphere, and the lower part to the left hemisphere.

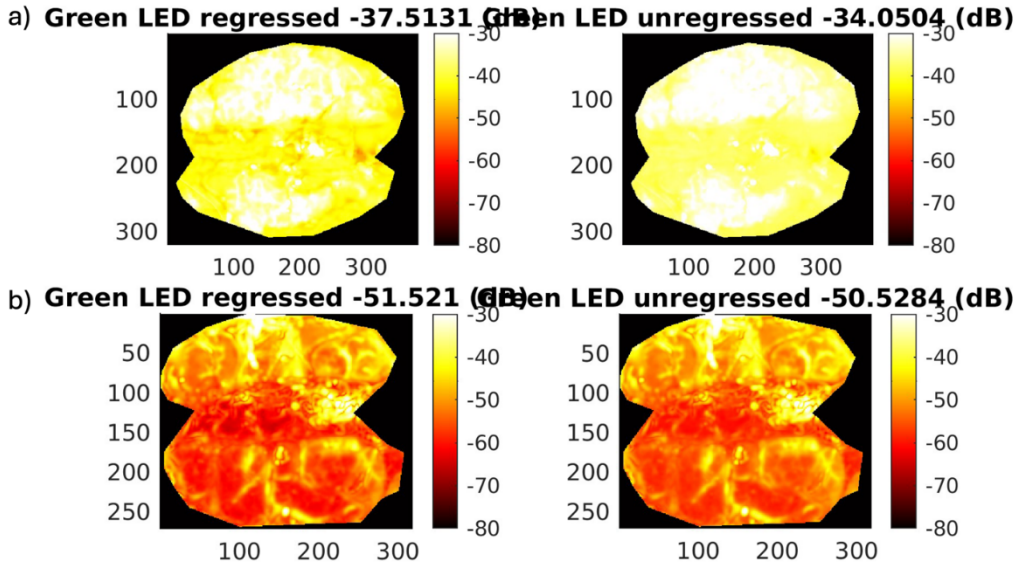

Fig. 3. a) Regressed and unregressed power maps in the placebo group post-stimulation on the right hemisphere (upper hemisphere). b) Regressed and unregressed power maps in the nimodipine group post-stimulation on the right hemisphere (upper hemisphere).

OP-31 (ID:42)

INHIBITION OF NITRIC OXIDE SYNTHASE TRANSFORMS CAROTID OCCLUSION-MEDIATED BENIGN OLIGEMIA INTO LARGE CEREBRAL INFARCTION

HA KİM [1], JINYONG CHUNG [1], ENG LO [2], JAMES FABER [3], CENK AYATA [4], DONG-EOG KİM [1]

[1] *DEPARTMENT OF NEUROLOGY, DONGGUK UNİVERSİTY ILSAN HOSPİTAL, SOUTH KOREA*
[2] *NEUROPROTECTİON RESEARCH LABORATORY, MGH, HARVARD, USA*
[3] *DEPARTMENT OF CELL BİOLOGY AND PHYSİOLOGY, UNİVERSİTY OF NORTH CAROLİNA, USA*
[4] *NEUROVASCULAR RESEARCH UNİT, MGH, HARVARD, USA*

Background and Objective:
It remains unclear why unilateral proximal carotid artery occlusion (UCAO) causes benign oligemia, without progressing to cerebral infarction, in mice, yet leads to a wide variety of outcomes (ranging from asymptomatic to death) in humans. We hypothesized that inhibition of nitric oxide synthase (NOS) both transforms UCAO-mediated oligemia into full infarction and expands pre-existing infarction.

Methods:
Using 900 mice, we i) investigated stroke-related effects of a single intraperitoneal dose of the NOS inhibitor N_{ω}-nitro-L-arginine methyl ester (L-NAME, 400 mg/kg) plus UCAO, with or without laser speckle imaging for 6 hours; ii) examined the rescue effect of the NO donor, molsidomine (200 mg/kg, intraperitoneally at 30 minutes); iii) performed intravital two-photon microscopy to observe vasoconstriction and thrombosis; iv) tested the impact of antiplatelet medications; v) queried if UCAO without L-NAME administration could induce infarction when mice had streptozotocin-mediated hyperglycemia and high fat diet-mediated hyperlipidemia; and vi) measured blood levels of endogenous NOS inhibitors (asymmetric and symmetric dimethylarginines; ADMA and SDMA) with or without inducing hyperglycemia and hyperlipidemia. Furthermore, we conducted i) a multi-center study (n=438 UCAO stroke patients) to identify predictors of infarct volume and ii) Mendelian randomization analysis to estimate the causal effect of the endogenous NOS inhibitors on human ischemic stroke.

Results:
UCAO alone induced infarction rarely (~2%) or occasionally (~14%) in C57BL/6 and BALB/c mice, respectively. However, L-NAME+UCAO induced large arterial infarction in ~75% of C57BL/6 and BALB/c mice. Laser speckle imaging for 6 hours detected spreading ischemia in ~40% of C57BL/6 and BALB/c mice with infarction (vs. none without), as assessed at 24 hours. In agreement with vasoconstriction and microthrombus formation shown by intravital microscopy, molsidomine and the endothelial NOS-activating antiplatelet cilostazol attenuated or prevented progression to infarction. Moreover, UCAO without L-NAME caused infarction in ~22% C57BL/6 and ~31% ApoE knock-out mice with hyperglycemia and hyperlipidemia, which, in turn, associated with ~60% greater SDMA levels. Further, increased levels of glucose and cholesterol associated with significantly larger infarct volumes in UCAO stroke patients. Lastly, Mendelian randomization identified a causative role of NOS inhibition, particularly in elevated SDMA concentration, in ischemic stroke risk (odds ratio=1.24; 95% CI, 1.11–1.38; P=7.69×10^{-5}).

Conclusions:
NOS activity is a key factor determining the fate of hypoperfused brain following acute carotid occlusion or clamping, where SDMA could be a potential risk predictor. Combining carotid occlusion with NOS inhibition allows stroke occurrence investigations that are not achievable with present experimental approaches.

OP-32 (ID:56)

HYPEROSMOTIC TREATMENT FOR NEUROPROTECTION: IN VITRO EFFECTS OF MANNITOL

RITA FRANK [1], PéTER ARCHIBALD SZARVAS [2], ÁKOS MENYHáRT [1], ESZTER FARKAS [1],

[1] HUNGARİAN CENTRE OF EXCELLENCE FOR MOLECULAR MEDİCİNE – CEREBRAL BLOOD FLOW AND METABOLİSM RESEARCH GROUP; DEPARTMENT OF CELL BİOLOGY AND MOLECULAR MEDİCİNE, ALBERT SZENT-GYÖRGYİ MEDİCAL SCHOOL AND FACULTY OF SCİENCE AND INFORMATİCS, UNİVERSİTY OF SZEGED, HUNGARY

[2] DEPARTMENT OF CELL BİOLOGY AND MOLECULAR MEDİCİNE, ALBERT SZENT-GYÖRGYİ MEDİCAL SCHOOL AND FACULTY OF SCİENCE AND INFORMATİCS, UNİVERSİTY OF SZEGED, HUNGARY

Background:

The pathology of acute ischemic stroke (AIS) is complex, involving both immediate and delayed damage mechanisms such as brain edema and spreading depolarization (SD). Brain edema occurs subsequent to the onset of AIS and it increases intracranial pressure. The initial, cytotoxic edema is triggered by ATP depletion and is characterized by the swelling of astrocytes and neuronal dendrites. Our previous experiments have demonstrated that hypoosmotic stress promotes neuronal hyperexcitability and significantly lowers the electrical threshold of SD elicitation. Despite the detrimental impact of edema formation and SD on neuronal tissue survival, hyperosmotic therapy is only used for large, space-occupying edema. The aim of the present work is to investigate the neuroprotective effects of hyperosmotic mannitol administration in acute brain slices. Also, we set out to find the lowest effective concentration of mannitol to minimize side effects.

Materials and methods:

350 µm thick coronal brain slices were prepared from C57BL/6 mice (n=22). AIS-related edema and SD were induced by hypo-osmotic solution (HM; 130mM to 60mM NaCl; 200 mosm/l) combined with transient hypoxia (2.5 min). Spatio-temporal characteristics of SD was detected by intrinsic optical signal (IOS) recordings. To counteract edema formation hyperosmotic mannitol solutions were administered at varying concentrations: 25 mM (364 mosm/l) and 50 mM (389 mosm/l). To determine the effect of edema and SD on astrocyte reactivity and neuronal survival GFAP and NeuN immunohistochemistry were carried out.

Results:

Hyperosmotic mannitol treatment at both concentrations reduced the occurrence of hypoxia-induced SD (60% vs. 24% vs. 74%; 25 mM mannitol vs. 50 mM mannitol vs. HM). Mannitol treatments decreased the propagation velocity of SD (3.3±2 vs. 3.5±0.7 vs. 5±1.7 mm/min; 25 mM mannitol vs. 50 mM mannitol vs. HM) and the cortical area affected by SD (45.4±21.5 vs. 31.9±17.4 vs. 67.6±17.2%; 25 mM mannitol vs. 50 mM mannitol vs. HM). Furthermore, mannitol treatments reduced the number of GFAP positive reactive astrocytes (10±4 vs. 16±2 vs. 23±0.01 cell/100 µm^2; 25 mM mannitol vs. 50 mM mannitol vs. HM) and elevated the cortical area covered by NeuN positive neurons (11±1 vs. 9±1 vs. 6±0.6%; 25 mM mannitol vs. 50 mM mannitol vs. HM).

Conclusions:

Our results suggest that hyperosmotic mannitol therapy inhibits SD and reduces neuronal injury. The lower concentration proved most effective, suggesting the potential for limiting side effects in vivo. Accordingly, we further plan to apply mannitol therapy in an *in vivo* focal AIS model, to increase the translational potential of our results. Based on our observations, we propose the acute use of hyperosmotic therapy for neuroimaging confirmed cytotoxic edema in the treatment of AIS.

Funding: H2020 No. 739593, NKFIH K134377, NAP3.0, TKP2021-EGA-28, SZAOK Research Fund, ÚNKP-23-4 -SZTE-636

OP-33 (ID:32)

EFFECT OF SIN-1 ON THE SD-INITIATED NUP AND THE NO-REFLOW PHENOMENON DURING FOREBRAIN ISCHEMIA AND REPERFUSION IN RATS

COLINE L. LEMALE [1], BAPTISTE BALANÇA [2], SARA SIMULA [3], SEBASTIAN MAJOR [1], JENS P. DREIER [1]

[1] *CENTER FOR STROKE RESEARCH BERLİN, DEPARTMENT OF EXPERİMENTAL NEUROLOGY AND NEUROLOGY, CHARİTé – UNİVERSİTäTSMEDİZİN, BERLİN, GERMANY*

[2] *HOSPİCES CİVİLS DE LYON, DEPARTMENT OF NEURO-ANESTHESİOLOGY AND NEURO-İNTENSİVE CARE, LYON NEUROSCİENCE RESEARCH CENTER, TEAM TIGER, LYON, FRANCE*

[3] *AİX MARSEİLLE UNİV, INSERM, INS, INT NEUROSCİ SYST, MARSEİLLE, FRANCE*

A systematic review on nitric oxide donors, including sydnonimines, has shown that they reduce the total volume of cerebral infarction in both permanent and transient ischemia models when administered within the so-called golden hour, i.e. the first hour after the onset of ischemia (1). However, they significantly increased regional cerebral blood flow (rCBF) during ischemia only in permanent, but not in transient models of experimental stroke. It was concluded that their beneficial effect in permanent models could be at least partly due to their vasodilatory effect on the cerebral circulation during ischemia. NO donors also lead to systemic hypotension which could potentially also lead to a reduction in rCBF. Net, this could be the reason why the NO donors failed to significantly increase rCBF during ischemia in transient models. In the context of transient ischemia models, however, in addition to the level of rCBF during ischemia, it also plays a role for the subsequent infarct size whether there is a complete reopening of the microcirculation after recanalization of the proximal vessel occlusion or whether this is partially absent, which is usually referred to as the no-reflow phenomenon. Whether NO donors have a favorable influence on the no-reflow phenomenon has, to our knowledge, not yet been sufficiently investigated.

In the present study, we investigated 48 stroke-prone spontaneously hypertensive rats (SHRsp) as an animal model for a human population with vascular risk factors and 48 Wistar-Kyoto control rats (WKY), i.e. the normotensive parental strain, as an animal model for a healthy human population without vascular risk factors (2). The protocol was divided into five steps: (i) baseline recording period, (ii) occlusion of the left common carotid artery (CCA), (iii) additional occlusion of the contralateral CCA (= bilateral (B)CCAO), (iv) reperfusion of the brain, and (v) death of the animal. Each of the first four steps lasted 60 minutes. From ten minutes after the start of BCCAO until the end of the experiment, the sydnonimine SIN-1 was administered intravenously at a rate of 1.8 mg/kg/h in one group each of SHRsp and WKY, resulting in four groups of 24 rats each. Treatment administration was randomized. Analysis of raw data was blinded and semi-automatized. Most variables were analyzed using two-way ANOVA with the two factors 'strain' and 'treatment'. $p<0.05$ was considered significant. SIN-1 significantly reduced systemic mean arterial pressure (BCCAO: $p<0.001$; reperfusion: $p<0.001$) and at the same time increased Enhanced Perfusion and O2 Saturation (EPOS)-recorded rCBF in absolute units at the right hemisphere during BCCAO ($p<0.05$) and reperfusion ($p<0.001$). At the left hemipshere, SIN-1 significantly increased laser speckle contrast analysis (LASCA)-recorded rCBF in % from baseline ($p<0.001$) and reduced microelectrode-measured extracellular K^+ concentration ($[K^+]_o$) ($p<0.01$) in the last 5 minutes of ischemia. The cumulative duration of the negative direct current (DC) shift indicating SD and SD-initiated negative ultraslow potential (NUP) (3) as well as the area under the curve (AUC) of $[K^+]_o$ were lower in SIN-1 treated rats (negative DC-shift duration: $p<0.05$; AUC $[K^+]_o$: $p<0.01$). SIN-1 also significantly reduced the cumulative duration of the depression of spontaneous brain activity during BCCAO ($p<0.05$). LASCA imaging at the end of reperfusion was significant for a smaller proportion of areas presenting lower rCBF than during baseline in SIN-1-treated animals ($p<0.001$), suggesting that SIN-1 reduced the no-reflow phenomenon. This was associated with an increased normalized-to-baseline amplitude of the spontaneous brain activity ($p<0.001$) as well as higher microelectrode-measured tissue partial pressure of O_2 ($p<0.05$) and EPOS-measured O_2 saturation ($p<0.001$) and oxyhemoglobin ($p<0.001$) at the end of reperfusion in SIN-1 treated groups.

In summary, SIN-1 attenuated the drop in rCBF due to proximal vessel occlusion, reduced the no-reflow phenomenon, and improved electrocorticographic parameters and $[K^+]_o$ during ischemia and reperfusion in both WKY and SHRsp. Together, these changes could lead to a delay in the commitment point and consecutively to smaller infarcts as demonstrated after transient ischemia in the previous systematic review (1). In principle, our data support the idea that intravenous administration of SIN-1 could be an interesting adjunctive therapy to recanalizing treatments after stroke such as intravenous thrombolysis and mechanical recanalization.

1. Willmot M, Gray L, Gibson C, Murphy S, Bath PM. A systematic review of nitric oxide donors and L-arginine in experimental stroke; effects on infarct size and cerebral blood flow. Nitric Oxide. 2005;12(3):141-9.
2. Kang EJ, Prager O, Lublinsky S, Oliveira-Ferreira AI, Reiffurth C, Major S, et al. Stroke-prone salt-sensitive spontaneously hypertensive rats show higher susceptibility to spreading depolarization (SD) and altered hemodynamic responses to SD. J Cereb Blood Flow Metab. 2023;43(2):210-230.
3. Luckl J, Lemale CL, Kola V, Horst V, Khojasteh U, Oliveira-Ferreira AI, et al. The negative ultraslow potential, electrophysiological correlate of infarction in the human cortex. Brain. 2018;141(6):1734-52.

OP-34 (ID:55)

INVESTIGATING THE EFFECTS OF NANOENCAPSULATED KETAMINE ON CEREBRAL BLOOD FLOW RESPONSES POST FOCAL CORTICAL ISCHEMIA USING FUNCTIONAL ULTRASOUND IMAGING

LORENA FIGUEIREDO FERNANDES [1], SAMUEL FLAHERTY [1], ALEJANDRO LABASTIDA RAMIREZ [1], KOSTAS KOSTARELOS [2], STUART ALLAN [1], ROB WYKES [3]

[1] DİVİSİON OF NEUROSCİENCE, BRAİN INFLAMMATİON GROUP, UNİVERSİTY OF MANCHESTER, UNİTED KİNGDOM
[2] CENTRE FOR NANOTECHNOLOGY İN MEDİCİNE, UNİVERSİTY OF MANCHESTER, UNİTED KİNGDOM
[3] DEPARTMENT OF CLİNİCAL & EXPERİMENTAL EPİLEPSY, UCL QUEEN SQUARE INSTİTUTE OF NEUROLOGY, UNİTED KİNGDOM

Abstract:
Stroke is one of the leading causes of death and disability worldwide and ischemic stroke accounts for more than 80% of all strokes. Spreading depolarization (SD), spontaneous waves of depolarisation, emerge from the metabolically compromised ischemic area within minutes after ischemia. SDs can induce a range of haemodynamic responses, from vasodilation in relatively uncompromised tissue, to vasoconstriction in tissue with substantial underlying perfusion deficit. Prevention of SD-induced vasoconstriction is a therapeutic target to improve stroke outcome. Ketamine, an NMDA receptor antagonist, has the ability to modulate SD waveform and previous work from the lab indicates that this prevents SD-induced vasoconstriction. However following a single dose, free ketamine is quickly metabolized in rodents (~45 min), preventing a long-lasting effect. Nanoparticles, including liposomes, can protect drugs against physiological degrading events and increase their circulation time. Liposomes have also shown the ability to accumulate in the brain at the infarct region after ischemic stroke. They are biodegradable and biocompatible, making them one of the most common nanosystems used in in vivo studies. We are therefore evaluating nanoencapsulated ketamine as a potential strategy for stroke therapy. This study aims to monitor the cerebral blood flow changes following focal cortical ischaemia, including SD-induced haemodynamic responses using functional ultrasound imaging. We will determine whether nanoencapsulated ketamine provides a longer lasting suppression of SD-induced vasoconstriction compared to free ketamine. In parallel, we will determine neurobehavioural scores and infarct size 24 hours post-induction of ischaemia from animals receiving control (empty liposomes or saline), versus free ketamine or liposome encapsulated ketamine.

OP-35 (ID : 25)

BLOOD-BRAIN BARRIER DYSFUNCTION IN ABNORMAL BRAIN PREDICTS EPILEPSY AFTER SUBARACHNOID HEMORRHAGE

DREIER JENS [1], LUBLINSKY SVETLANA [1], MAJOR SEBASTIAN [1], LEMALE COLINE [1], HECHT NILS [1], HARTINGS JED [1], WOITZIK JOHANNES [1], MARTUS PETER [2], FRIEDMAN ALON [3],

[1] *CHARİTé UNİVERSİTY MEDİCİNE BERLİN*
[2] *UNİVERSİY OF TÜBİNGEN*
[3] *DALHOUSİE UNİVERSİTY*

Subarachnoid hemorrhage (SAH) is a devastating form of stroke that accounts for more than a quarter of all potential years of life lost to stroke before age 65. Survivors often face long-term consequences such as motor, cognitive and emotional disabilities and epilepsy. To reduce this burden, there is a need to improve post-injury treatment by discovering early mechanistic biomarkers that can predict long-term complications such as late epilepsy and guide early targeted interventions.
Accordingly, the aim of this observational, multicenter study was to define early predictors of post-hemorrhagic epilepsy. We selected patients from a prospectively collected database based on predefined criteria. The primary analysis of the present study was performed on 118 patients who met the following criteria: They (1) did not suffer from epilepsy before SAH, (2) received an early contrast-enhanced (CE)-MRI on Day 2 (interquartile range (IQR): 1-3) (n=101) and/or a CE-MRI on Day 15 (IQR: 13-16) (n=111), and (3) did not die before the fourth week after the initial hemorrhage. The first of the patients who met these criteria was recruited in January 2007 and the last in March 2018 (11.3 years). Ninety-two of 118 patients (78.0%) underwent a survey on the development of epilepsy 3.7 (IQR: 0.9-5.2) years after the initial hemorrhage. Twenty-six of the 118 patients (22.0%) could not be interviewed for the following reasons: (1) Patients/carers were unable to provide information or refused (n=4), (2) the patient died and carers were unable to provide more information (n=10), (3) patients/carers were not reachable (n=12).
MRI scans (including T1w, FLAIR and DWI sequences) were semi-automatically segmented into lateral ventricles, subarachnoid space, apparently normal brain tissue (NBT) in the combined gray and white matter, or abnormal brain tissue (ABT) comprising apparently abnormal signal, reflecting cytotoxic or vasogenic edema, gliosis or hemorrhage as previously described [1, 2]. NBT as a percentage of total intracranial volume (NBT%) was divided into the two categories NBT associated with blood-brain barrier dysfunction (BBBDNBT%) and NBT with intact BBB (iBBBNBT%). Likewise, ABT in percent of total intracranial volume (ABT%) was subdivided into ABT associated with BBBD (BBBDABT%) and ABT with intact BBB (iBBBABT%). Recording, analysis and interpretation of spreading depolarizations (SD) and electrographic seizures followed the published recommendations of the Co-Operative Studies on Brain Injury Depolarizations (COSBID) group [3]. Evaluators were blinded to other measures.
The following 15 variables were a priori defined as potential predictors: World Federation of Neurosurgical Societies Score (WFNS) and Rosen-Macdonald Score (RMS) on admission, four variables of the early MRI (iBBBABT%Day2, iBBBNBT%Day2, BBBDABT%Day2 and BBBDNBT%Day2), peak seizure duration of a recording day, peak number of seizures of a recording day, peak total SD-induced depression duration of a recording day (PTDDD), peak number of SDs of a recording day, four variables of the post-monitoring MRI (iBBBABT%Day15, iBBBNBT%Day15, BBBDABT%Day15 and BBBDNBT%Day15) and the Modified Rankin Scale (MRS) on Day 14.
In the primary analysis in 118 patients with the outcome death later than 21 days after the initial hemorrhage or development of epilepsy, the following variables revealed uncorrected p-values of less than 0.05: WFNS 0.04, RMS 0.049, BBBDABT%Day2 (p=0.04), iBBBABT%Day15 (p=0.05), iBBBNBT%Day15 (p=0.04), BBBDABT%Day15 (p=0.001), and MRS (0.02). Thus, after Bonferroni correction only BBBDABT%Day15 remained significant. This was also the only variable that showed a p-value below 0.05 in multivariate analysis (0.010). The area under the curve (AUC) was 0.793 and 0.767 after leaving one out.
In the first sensitivity analysis with 92 patients with available outcome (development of late-onset epilepsy versus no such development) but imputation of predictors, the area under the curve was 0.758 after leaving one out correction. In complete case analysis without imputation, the area was 0.763 after leaving one out. In both analyses, BBBDABT%Day15 was the only significant variable.
In summary, our study suggests that semi-automatically segmented BBBDABT%Day15 is a promising mechanistic biomarker for epileptogenesis after SAH. This is interesting for three reasons: (1) Experimental models of cerebral injury suggest that BBBD plays a key role in epileptogenesis and neurodegeneration via

transforming growth factor-β receptor-activated signaling in astrocytes [4, 5], (2) BBBDABT% can in principle be determined at the push of a button after the patient has received an MRI, and (3) preliminary studies suggest that BBBD is an interesting novel target for the prophylactic treatment of epileptogenesis and neurodegeneration.

1. Dreier JP, Winkler MKL, Major S, Horst V, Lublinsky S, Kola V et al. Spreading depolarizations in ischaemia after subarachnoid haemorrhage, a diagnostic phase III study. Brain. 2022;145(4):1264-84. doi:10.1093/brain/awab457.
2. Lublinsky S, Major S, Kola V, Horst V, Santos E, Platz J et al. Early blood-brain barrier dysfunction predicts neurological outcome following aneurysmal subarachnoid hemorrhage. EBioMedicine. 2019;43:460-72. doi:10.1016/j.ebiom.2019.04.054.
3. Dreier JP, Fabricius M, Ayata C, Sakowitz OW, William Shuttleworth C, Dohmen C et al. Recording, analysis, and interpretation of spreading depolarizations in neurointensive care: Review and recommendations of the COSBID research group. J Cereb Blood Flow Metab. 2017;37(5):1595-625. doi:10.1177/0271678X16654496.
4. Seiffert E, Dreier JP, Ivens S, Bechmann I, Tomkins O, Heinemann U, Friedman A. Lasting blood-brain barrier disruption induces epileptic focus in the rat somatosensory cortex. J Neurosci. 2004;24(36):7829-36. doi:10.1523/JNEUROSCI.1751-04.2004.
5. Ivens S, Kaufer D, Flores LP, Bechmann I, Zumsteg D, Tomkins O et al. TGF-beta receptor-mediated albumin uptake into astrocytes is involved in neocortical epileptogenesis. Brain. 2007;130(Pt 2):535-47. doi:10.1093/brain/awl317.

OP-36 (ID:72)

THE ROLE OF AN INNATE IMMUNE SYSTEM PATHWAY IN CORTICAL SPREADING DEPOLARIZATION AND NOCICEPTION

KADIR OGUZHAN SOYLU [1], DILAN BOZANOGLU [1], HULYA KARATAS [2], MUGE YEMİSCİ [3]

[1] HACETTEPE UNİVERSİTY, INSTİTUTE OF NEUROLOGİCAL SCİENCES AND PSYCHİATRY, ANKARA, TÜRKİYE
[2] HACETTEPE UNİVERSİTY, INSTİTUTE OF NEUROLOGİCAL SCİENCES AND PSYCHİATRY, ANKARA, TÜRKİYE / NEUROSCİENCE AND NEUROTECHNOLOGY CENTER OF EXCELLENCE (NÖROM), ANKARA, TÜRKİYE
[3] HACETTEPE UNİVERSİTY, INSTİTUTE OF NEUROLOGİCAL SCİENCES AND PSYCHİATRY, ANKARA, TÜRKİYE / NEUROSCİENCE AND NEUROTECHNOLOGY CENTER OF EXCELLENCE (NÖROM), ANKARA, TÜRKİYE / HACETTEPE UNİVERSİTY, FACULTY OF MEDİCİNE, DEPARTMENT OF NEUROLOGY, ANKARA, TÜRKİYE

Objective:

Cortical Spreading Depolarization (CSD) is an intense neuronal and glial depolarization wave that causes profound disruption in ionic and energy homeostasis in the brain (1). CSD is strongly linked to a sterile inflammation in brain parenchyma and meninges through activation of both innate and adaptive immune system components (2). The cyclic-GMP-AMP-synthase (cGAS)-Stimulator of interferon genes (STING) pathway is an innate immune system cascade that triggers type 1 interferon (interferon alfa and beta) signaling in response to pathogen infection and cellular stress. cGAS-STING pathway is demonstrated to play important roles in neuroinflammatory conditions such as ischemic stroke, traumatic brain injury, and neurodegenerative diseases, significantly influencing disease outcomes (3). Additionally, the cGAS-STING pathway has been implicated in the regulation of nociception (4). In our previous work, we have shown that CSD enhances the expression of cGAS-STING pathway proteins and type 1 interferon in neurons but not microglia, in mouse cerebral cortex. Moreover, our findings suggested that cGAS-STING pathway might play a regulatory role on CSD susceptibility, as inhibition of STING altered CSD thresholds (5). It is unclear whether increased cGAS-STING pathway activity following CSD is limited to neurons or involves other cell types in the cerebral cortex. Furthermore, the extent to which cGAS-STING pathway regulates CSD susceptibility and nociception has not been fully explored. In this study, we aimed to investigate the expression of cGAS-STING pathway proteins and type 1 interferon in astrocytes following non-invasive induction of CSD and to assess the impact of STING inhibition and activation on CSD susceptibility and nociception.

Methods:

For CSD induction, optogenetic approach was used using Thy1-ChR2-YFP genotype mice. Optogenetic stimulation was performed by 460 nm laser light over the intact frontal bone, and CSD(s) were detected by electrophysiological recording over the intact parietal bone. One or six CSD waves were induced in the groups, and sham surgery was performed as control (n=6/group). Mice were sacrificed 5 or 24 h after CSD induction and transcardially perfused with 4% paraformaldehyde. Brains were harvested and 20 micrometer thick sections were obtained using a cryostat. Immunohistochemical staining was performed on brain sections for cGAS-STING pathway proteins (cGAS, STING, phospho-Interferon Regulatory Factor 3, and Interferon beta), along with an astrocyte marker S100 beta. Cerebral cortex regions of the sections were imaged with confocal microscope and three nonoverlapping images were captured from each section. Positively stained cells were counted, and positive cell/total cell ratios were used for comparison. To investigate the role of cGAS-STING pathway in the regulation of CSD susceptibility and nociception, the STING antagonist C-176 and STING agonist 2’3’ cGAMP were used. C-176 (or its vehicle) was administered intraperitoneally (20 mg/kg), and 2’3’ cGAMP (or its vehicle) was administered intranasally (1 mg/kg) to wild type C57BL/6J mice (n=6/group). Four hours after drug administration, periorbital mechanical sensitivity and CSD susceptibility were assessed. Periorbital sensitivity was also assessed before drug administration to establish baseline. The evaluators were blinded to the treatment status. CSD thresholds were determined using topical potassium chloride (KCl) application on the dura. A burr hole with a 2 mm diameter was opened on the frontal bone while keeping the dura intact, and gradually increasing KCl concentrations were applied on the dura until the first CSD was detected as a typical DC potential shift in electrophysiological recording. Periorbital mechanical sensitivity was assessed using the manual Von Frey test. Briefly, animals were placed in a custom-made chamber to restrict their movements in a way that exposes their head and front paws. Mice were acclimatized to restriction chamber for 1 hour before each assessment. Von Frey filaments with increasing force were applied perpendicularly with slight bending on periorbital area of mice for 3 seconds or until a positive withdrawal response was observed. Brisk head withdrawal, head shaking and rubbing the face with front paws on the stimulated side were accepted as positive responses. Mechanical withdrawal thresholds were determined as the force that elicits a positive response at least 3 out of 5 times of applications. For statistical analyses Kruskal-Wallis H, Mann-Whitney U and Wilcoxon tests were used.

Results:
Neither single nor multiple CSDs significantly changed the expression of cGAS-STING pathway proteins in astrocytes compared to sham controls at 5 and 24 h time points (p=0.420 and p=0.095, respectively). After CSD induction, interferon beta expression in astrocytes was low compared to neurons and it was not significantly different from sham controls (p=0.150). STING inhibition with C-176 led to decreased CSD thresholds compared to vehicle treatment (p=0.007). In contrast STING activation with 2'3' cGAMP resulted in increased CSD thresholds (p=0.015). In line with the change in CSD thresholds, STING activation significantly increased periorbital mechanical withdrawal thresholds compared to baseline (p=0.015), while STING inhibition decreased the thresholds. Vehicle treatments did not cause a change in mechanical withdrawal thresholds (p=0.999).

Discussion:
Our findings indicate that CSD, whether it is single or multiple, does not lead to an increase in the expression of cGAS-STING pathway proteins in astrocytes. In our previous work, we observed that both neurons and microglia expressed cGAS-STING pathway proteins; however, an increase in the expression of cGAS-STING pathway proteins following single and multiple CSDs was detected only in neurons (5). These findings suggest that CSD leads to cGAS-STING pathway activation primarily in neurons within the cerebral cortex, emphasizing the central role of neurons in neuroinflammation induced by CSD. Importantly, in this study we also observed that pharmacological manipulation of cGAS-STING pathway affected CSD thresholds and periorbital mechanical sensitivity, highlighting that this pathway may play a role in the regulation of CSD susceptibility and craniofacial nociception. cGAS-STING pathway was demonstrated to have both pro- and anti-nociceptive effects in pain models by regulating neuronal excitability through type 1 interferon signaling (4). Therefore, elevated cGAS-STING pathway activity in neurons after CSD might explain its role as a regulator of CSD susceptibility and nociception.

Conclusion:
The cGAS-STING pathway shows great potential as a key player in CSD-associated neuroinflammation and as a promising new therapeutic target for neurological disorders associated with CSD. Further investigation of the role of cGAS-STING pathway in headache and other pain disorders could provide valuable insights and uncover new disease mechanisms.
This study is supported by Hacettepe University No: TSA-2022-19749

References
1. Ayata, C., & Lauritzen, M. (2015). Spreading Depression, Spreading Depolarizations, and the Cerebral Vasculature. *Physiological reviews*, *95*(3), 953–993.
2. Takizawa T, Qin T, Lopes de Morais A, et al. Non-invasively triggered spreading depolarizations induce a rapid pro-inflammatory response in cerebral cortex. Journal of Cerebral Blood Flow & Metabolism. 2020;40(5):1117-1131.
3. Fritsch, L. E., Kelly, C., & Pickrell, A. M. (2023). The role of STING signaling in central nervous system infection and neuroinflammatory disease. *WIREs mechanisms of disease*, *15*(3), e1597.
4. Donnelly, C. R., Jiang, C., Andriessen, A. S., Wang, K., Wang, Z., Ding, H., Zhao, J., Luo, X., Lee, M. S., Lei, Y. L., Maixner, W., Ko, M. C., & Ji, R. R. (2021). STING controls nociception via type I interferon signalling in sensory neurons. *Nature*, *591*(7849), 275–280.
5. Soylu KO, Gurlek OC, Karatas H, Yemisci M. cGAS-STING pathway as a novel target in the context of spreading depolarization. Cephalalgia 2023;43:185-186.

OP-37(ID:17)

DOES SPREADING DEPRESSION REWIRE CORTICAL PAIN NETWORKS?

BENGISU SOLGUN , BUKET DONMEZ-DEMIR , HULYA KARATAS-KURSUN , SEFIK EVREN ERDENER ,

HACETTEPE UNIVERSITY INSTITUTE OF NEUROLOGICAL SCIENCES AND PSYCHIATRY

Abstract:

Resting-state functional imaging is increasingly used to understand how distinct brain networks modulate and respond to pain. As migraine, a common headache disorder, can be experimentally modeled by triggering cortical spreading depolarizations (CSD) in rodents, it is crucial to understand its impact on network connectivity to find imaging markers for experimental evaluation of headache and trigeminovascular activation. We used widefield intrinsic optical-signal imaging (IOSI) to investigate the impact of CSDs on bihemispheric resting-state functional connectivity. C57BL6-ChR2 mice underwent head plate installation and skull optical clearing with EDTA. After habituation to the imaging setup, we performed IOSI for 8 minutes under 530nm light to observe changes in total hemoglobin (HbT) concentration in awake mice. Next, CSD was triggered optogenetically using 450nm light and confirmed by laser speckle contrast imaging. A subset of mice received i.p. naproxen after CSD to modulate headache. IOSI was performed at 30 minutes, 60 minutes, 4 hours and 24 hours after CSD. Mouse grimace scale was scored at each time point for behavioral headache documentation. Time traces of HbT were bandpass filtered and regressed. Seeds were placed in primary somatosensory, primary motor, secondary motor and retrosplenial cortices. We observed time-dependent changes in contralateral somatosensory cortex connectivity after CSD, specifically involving the contralateral barrel cortex. The left barrel cortex and the left retrosplenial cortex became more anticorrelated, while the left barrel cortex and the right barrel cortex became more positively correlated with each other compared to the baseline. We also saw an increase in the left barrel cortex's intra-regional functional connectivity values. These findings may reflect the activation of pain processing networks and can serve as a proxy for the headache experience. Our work will help identify imaging markers for migraine headache assessment in rodents and will be beneficial for the elucidation of migraine pathophysiology.

OP-38 (ID:86)

CORTICAL SPREADING DEPOLARIZATION-INDUCED NLRP3 INFLAMMASOME ACTIVATION VIA P2X7 RECEPTOR ACTIVITY İN TRIGEMINAL GANGLIA

BEYZA TURKEN [1], BUKET DONMEZ [1], CANAN CAKIR AKTAS [1], MUGE YEMISCI OZKAN [3], HULYA KARATAS KURSUN [2],

[1] *INSTITUTE OF NEUROLOGICAL SCIENCES AND PSYCHIATRY, HACETTEPE UNIVERSITY*
[2] *INSTITUTE OF NEUROLOGICAL SCIENCES AND PSYCHIATRY, HACETTEPE UNIVERSITY, 2- NEUROSCIENCE AND NEUROTECHNOLOGY CENTER OF EXCELLENCE*
[3] *INSTİTUTE OF NEUROLOGİCAL SCİENCES AND PSYCHİATRY, HACETTEPE UNİVERSİTY 2- DEPARTMENT OF NEUROLOGY, HACETTEPE UNİVERSİTY FACULTY OF MEDİCİNE, 3- NEUROSCİENCE AND NEUROTECHNOLOGY CENTER OF EXCELLENCE*

Objective:

Cortical spreading depolarization (CSD) is an electrophysiological phenomenon characterized by a wave of neuronal and glial depolarization, followed by a period of decreased electrical activity in the brain (1). CSD propagates through the cortex, disrupting ion homeostasis and hemodynamics, and is implicated in several neurological disorders, including ischemic stroke, traumatic brain injury, and subarachnoid hemorrhage (2). Besides, CSD is thought to be the electrophysiological correlate of migraine aura. Recent studies showed that CSD-induced cortical neuroinflammation contributes to trigeminovascular activation, hence headache (3). This parenchymal neuroinflammatory cascade includes neuronal pannexin-1 (Panx1) channel opening and NLRP3 inflammasome activation which lead significant cytokine release in the cortex. Pannexin-1 megachannels are known to be closely associated with purinergic P2X7 receptors (P2X7R) that are activated by extracellular ATP and that can further activate the inflammatory cascade, rendering them a worthy target in investigating the spread of the CSD and its consequent neuroinflammation (4). A study showed that genetic depletion of P2X7R as part of the P2X7/Panx1 pore suppresses spreading depolarization, its inflammatory effects and the trigeminovascular activation in wild-type rats and mice (5). Upon activation, the P2X7 receptor facilitates cationic ion flow across the membrane, potentially exacerbating depolarization waves. Recently, P2X7 receptor antagonism has been shown to reduce inflammatory cytokine release in the cortex following spreading depolarization (6). This study aims to characterize CSD-induced P2X7 receptor expression and its effects on NLRP3 inflammasome activation in trigeminal ganglion cells, with an emphasis on time-dependent changes and the impact of P2X7 receptor antagonism.

Methods:

Male adult Balb/cJ mice (8-12 weeks old, n=2/group) were used for *in vivo* CSD induction experiments. This strain was selected since C57BL/6 mice are known for defective P2X7 receptors due to a natural P451L mutation (7). Mice were divided into 4 groups receiving either the P2X7 receptor antagonist, JNJ47965567, or its vehicle (B cyclodextrin sulfobutyl ether-Na^+ salt), and sham controls. The antagonist was chosen for its ability to rapidly penetrate the central nervous system and its specific affinity for the P2X7 receptor (8). Mice were administered intraperitoneally either the P2X7 receptor antagonist or its vehicle (10 µl/g) 15 minutes prior to the administration of isoflurane anesthesia. The animals were then placed in a stereotaxic frame, and the right parietal bone was thinned for electrophysiological recordings. A circular area with a diameter of 2 mm was thinned on the right frontal bone to serve as the CSD induction site, leaving only the internal compact bone layer intact. A cotton ball soaked in 1 M KCl (or 1 M NaCl for sham groups) was placed on the thinned area. A single CSD wave was recorded electrophysiologically using an Ag-$AgCl_2$-coated pellet electrode placed over the right parietal cranium. Mice were perfused with heparinized saline and 4% paraformaldehyde (PFA) at 30 minutes or 24 hours following CSD induction. Bilateral trigeminal ganglia (TG) were extracted and cryopreserved with 4% PFA for 24h and 30% sucrose solutions for 48h. TG were cryosectioned at 20 µm thickness (n=3 sections/ganglion). Immunofluorescent staining was performed with P2X7 receptor, NLRP3, the neuronal marker NeuN, and the nuclear marker Hoechst 33258. Images were acquired using confocal microscopy (Leica TCS SP8) and analyzed with ImageJ software. Statistical analyses were conducted using one-way ANOVA and unpaired t-tests to compare the immediate (30 minutes) and acute (24 hours) phases after CSD, antagonist effects on P2X7 receptor and NLRP3 expression, and differences between the right and left trigeminal ganglia.

Results:

According to our results, P2X7 receptor and NLRP3 inflammasome expression significantly increased in both right and left trigeminal ganglia 30 minutes and 24 hours after CSD induction compared to sham groups ($p<0.001$). There was obvious colocalization of P2X7 receptor and NLRP3 inflammasome expression in NeuN-positive trigeminal ganglion cells following CSD. No significant difference in P2X7 receptor or NLRP3 inflammasome expression was observed between the right and left trigeminal ganglia in any experimental group.

Therefore, data from the right and left ganglia were combined for subsequent analysis. P2X7 receptor expression was significantly reduced in the P2X7 antagonist-treated group 30 minutes after CSD compared to vehicle-treated groups (p=0.0044). A similar tendency was observed at 24 hours, though not statistically significant. NLRP3 inflammasome expression was also reduced in the P2X7 antagonist-treated group 30 minutes after CSD compared to vehicle-treated groups (p=0.0011). Moreover the reduction at 24 hours was not statistically significant. Our results are summarized in Table 1 and 2.

Table 1. P2X7R/NeuN positive and NLRP3/NeuN positive cell ratio 30-min after CSD

	Sham 30-min vehicle	CSD 30-min vehicle	Sham 30-min antagonist	CSD 30-min antagonist
P2X7R/NeuN ratio (mean + SEM)	0.8 ±0.5	91.1 ±1.5	1.37 ± 0.7	81.1 ± 2.2
NLRP3/NeuN ratio (mean + SEM)	1.9 ± 1.1	90.3 ± 0.8	0.5 ± 0.3	79.5 ± 2.2

Table 2. P2X7R/NeuN positive and NLRP3/NeuN positive cell ratio 24-h after CSD

	Sham 24-h vehicle	CSD 24-h vehicle	Sham 24-h antagonist	CSD 24-h antagonist
P2X7R/NeuN ratio (Mean + SEM)	2.6 ± 1.1	88.6 ± 1.4	1.4 ± 0.9	86.0 ±1.9
NLRP3/NeuN ratio (Mean +SEM)	0.6 ± 0.4	87.5 ± 1.5	0.2 ± 0.2	84.3 ± 2.2

Conclusion:

Cortical spreading depolarization exacerbates initial neuropathological effects and contributes to electrophysiological imbalances and inflammatory cytokine release in various neurological conditions. CSD is believed to correlate with the migraine aura phase, and subsequent migraine headaches may be attributed to both homeostatic disturbances and inflammatory processes triggered by CSD. Activation of the P2X7 receptor following CSD induces membrane electrical imbalance and participates in the signaling cascade of CSD-induced neuroinflammation. This study demonstrates that P2X7 receptor antagonism reduces NLRP3 inflammasome expression in trigeminal ganglion cells during the early phase of CSD-induced inflammation. According to our knowledge this is the first study demonstrating the expression of NLRP3 inflammasome and P2X7 receptor in trigeminal ganglion neurons shortly after CSD induction. Our findings highlight the role of the purinergic system in CSD-induced trigeminovascular activation through NLRP3 inflammasome activation. Previous studies have shown that P2X7 receptor inhibition reduces neuroinflammatory cytokine release in the cortex following CSD. This research elucidates the relationship between NLRP3 inflammasome and P2X7 receptor activity after CSD in TG, offering potential new targets for interventions aimed at modulating the trigeminovascular inflammatory cascade induced by CSD.

References

1. Leão AAP, Morison RS. Propagation Of Spreading Cortical Depression. J Nerv Ment Dis [Internet]. 1945;102(5).
2. Dreier JP. The role of spreading depression, spreading depolarization and spreading ischemia in neurological disease. *Nat Med* 2011; **17**: 439–447.
3. Karatas H, Erdener SE, Gursoy-Ozdemir Y et al (2013) Spreading depression triggers headache by activating neuronal Panx1 channels. Science 339(6123):1092–1095
4. Lister MF, Sharkey J, Sawatzky DA et al (2007) The role of the purinergic P2X7 receptor in inflammation. J Inflamm (Lond) 4:5
5. Chen S-P, Qin T, Seidel J et al Inhibition of the P2X7-PANX1 complex suppresses spreading depolarization and neuroinflammation. Brain 2017;140
6. Uzay B, Donmez-Demir B, Ozcan SY, Kocak EE, Yemisci M, Ozdemir YG, Dalkara T, Karatas H. The effect of P2X7 antagonism on subcortical spread of optogenetically-triggered cortical spreading depression and neuroinflammation. J Headache Pain. 2024 Jul 24;25(1):120. doi: 10.1186/s10194-024-01807-1
7. Er-Lukowiak M, Duan Y, Rassendren F et al (2020) A P2rx7 passenger mutation affects the vitality and function of T cells in congenic mice. iScience 23(12):101870
8. Jimenez-Pacheco A, Diaz-Hernandez M, Arribas-Blázquez M, Sanz-Rodriguez A, Olivos-Oré LA, Artalejo AR, et al. Transient P2X7 receptor antagonism produces lasting reductions in spontaneous seizures and gliosis in experimental temporal lobe epilepsy. J Neurosci. 2016;36(22):5920–32

OP-39 (ID:40)

HOW SPREADING DEPOLARIZATIONS SHAPE EPILEPTIC ACTIVITY

ROUSTEM KHAZIPOV [1], DARIA VINOKUROVA [2], AZAT NASRETDINOV [2], GULSHAT ZAKIROVA [2], MARAT MINLEBAEV [1], ANDREI ZAKHAROV [2]

[1] INMED, AİX-MARSEİLLE UNİV
[2] KAZAN FEDERAL UNİVERSİTY

Objectives:

Spreading Depolarization (SD, as a wave of spreading depression) was first described by Leão following an epileptic discharge induced by tetanic electrical stimulation. Since then, the co-occurrence of seizures and SDs has since been demonstrated both in patients and in various experimental models, with SDs typically terminating epileptic discharges or producing transient suppression of ongoing epileptic activity. However, SDs exhibit remarkable three-dimensional dynamics with a variety of vertical propagation patterns across cortical layers, including full SDs propagating through the entire cortical depth and partial SDs involving only some cortical layers. Here, we investigated how seizure-associated SD is initiated and propagates across cortical depth and how SD affects epileptic activity across cortical layers.

Methods:

We used silicon probe recordings of the local field potential and multiple unit activity across cortical layers in combination with ECoG and intrinsic optical signal recordings in rat somatosensory barrel cortex in a flurothyl model of generalized seizures and during partial seizures induced by focal injection of 4-aminopyridine/gabazine. In a subset of animals with partial seizures, we also examined the effects of remote high-potassium-induced SDs on ongoing epileptic activity.

Results:

In models of both generalized and partial seizures, epileptic activity was associated with SD in almost half of the cases. SDs were most commonly initiated in the superficial layers and propagated downward, either through all cortical layers or stopping at the L4/L5 border. Downstream SD propagation strongly affected epileptic activity within a column with complete suppression of activity in the layers recruited by the SD, and segregation of seizures in the layers located below the SD-involved cortex. Importantly, during partial superficial SDs, recordings from electrodes at the cortical surface showed persistent epileptic popspike activity during SD DC transients. In some cases, there was even an increase in the frequency of epileptic popspikes during partial SDs. Depth-recordings showed that these epileptiform events at the cortical surface reflected passive sources of epileptic popspikes generated in deep cortical layers to which the SD failed to propagate. A similar transient state of deep layer-supported epileptic activity with silenced surface layers was also observed during the initial phase of full SDs, when SD had invaded the superficial but not yet deep layers.

Conclusions:

Thus, vertical propagation of SD across the cortical column during seizures creates dynamic network states in which epileptic activity is confined to layers not recruited by SD, while epileptic activity is suppressed in layers invaded by SD. The results of the present study point to the importance of vertical SD spread in the SD-induced suppression of epileptic activity across cortical layers.

OP-40 (ID:57)

NATURAL HISTORY OF SEIZURES, SPREADING DEPOLARIZATIONS AND SEIZURE-ASSOCIATED SPREADING DEPOLARIZATION IN MOUSE MODELS OF EPILEPSY.

ROB WYKES [1], NEELA CODADU [2], KEVAN HASHEMİ [3]

[1] *DİVİSİON OF NEUROSCİENCE, THE UNİVERSİTY OF MANCHESTER, UK*
[2] *UCL QUEEN SQUARE INSTİTUTE OF NEUROLOGY, UK*
[3] *OPENSOURCEİNSTRUMENTS*

Introduction:
In recent years it has become apparent that spreading depolarizations (SDs) can occur in epileptic brain; either independently or concurrently with seizures. To understand the natural history of spontaneous seizure-associated SDs we have implemented an opensourceinstruments 4 channel DC-coupled wireless video telemetry system. This allows continuous monitoring of epileptiform activity (both seizures and SDs) in rodent models of epilepsy.

Methods:
We used viral vectors (Cre-recombinase) to focally knockout (KO) Kir4.1 in astrocytes within the hippocampus of adult Kir4.1-floxed mice (Kir4.1 cKO). This models unilateral temporal lobe epilepsy with sclerosis. A depth electrode was implanted in the ipsilateral hippocampus, two electrodes implanted in the ipsilateral somatosensory and motor cortex, and a fourth electrode implanted into the contralateral somatosensory cortex, (reference contralateral cerebellum). Continuous video-telemetry was performed for 3 weeks.

Results:
Spontaneous epileptiform events arise ~7 days post injection of virus. From 6 mice, 3 event types were characterised; seizures alone, SD alone, or seizure plus SD. 53/111 events were seizure alone, 12/111 events were SD alone, and 46/111 were seizures temporally associated with an SD. Interestingly, for seizure associated SD, the SD was always initiated in the cortex (occasionally contralateral cortex) to the presumed hippocampal seizure onset zone. Delayed SD invasion of the hippocampus was sometimes detected. 1/6 animals succumbed to Sudden Unexpected Death in Epilepsy (SUDEP). The fatal seizure was associated with an SD recorded in both the cortex and hippocampus. Data from additional models of temporal lobe epilepsy and a mouse model of glioblastoma-related epilepsy are currently ongoing and will be presented.

Conclusion:
Long-term wireless DC-coupled recordings allow the natural history of seizure associated SD to be characterized and will be a useful tool to study the impact of SD in epileptic brain.

OP-41 (ID:93)

SEIZURE PROPAGATION TRIGGERS A PROTECTIVE CONTRALESIONAL SPREADING DEPOLARIZATION DURING FOCAL HIPPOCAMPAL STROKE IN FREELY BEHAVING FEMALE MICE

ANDREW BOYCE , ROGER THOMPSON ,

UNİVERSİTY OF CALGARY

Abstract:

During an ischemic stroke, obstructed cerebral blood flow triggers focal metabolic crisis and, without reperfusion, the eventual death of tissue fed by the occluded vessel. Middle cerebral artery (MCA) occlusions make up about half of all large vessel strokes in humans and thus several murine MCA models have been established to tackle this issue; yet strokes also occur deeper in the brain. Here, stroke is less understood and, at present, is understudied in murine models thanks to limited optical and surgical access to induce/record stroke, particularly in awake conditions. Although relatively rare, hippocampal strokes trigger unique and devastating symptoms, including transient or permanent amnesia, disorientation, alexia without agraphia, and can lead to major neurocognitive disorders. Stroke symptoms can be focal, linked to deficits in the infarcted tissue, or non-focal, linked to perturbations in remote tissue.

Ischemic tissue is permissive to additional sequelae that can radiate outward from the core, including seizure and spreading depolarization (SD), whose propagation may regulate the balance of focal and non-focal symptom presentation as well as stroke recovery. In penumbra, SD triggers ionic dysregulation amidst metabolic failure, providing an intense challenge to already hypoperfused tissue. While deleterious in penumbra, emerging evidence suggests SD propagation through healthy tissue may not be detrimental. To understand the impact of SD on peri-stroke symptomology and recovery, we improved upon the photothrombotic stroke model to allow all-optical induction of focal unilateral stroke and monitoring of SD in freely behaving Thy1-GCaMP6f mice by delivering and collecting light through chronic bilateral fibreoptic implants dorsal to each hippocampus. The ipsilesional fibre was used for both stroke induction and monitoring neuronal Ca^{2+} influx in the ischemic core. Shortly after photothrombosis, a terminal spreading depolarization was recorded that was similar between sexes. Somewhat surprisingly, after ipsilesional terminal depolarization, SDs appeared in the contralesional hippocampus, which were larger and more frequent in females. The onset of SD in the contralesional hippocampus was coincident with increased environmental exploration. Hippocampal stroke generated retrograde amnesia, but when contralesional SD occurred, mice later showed improved functional recovery and reduced anterograde amnesia. During unilateral hippocampal stroke, SDs propagating out from the ischemic core were restricted to the ipsilesional hemisphere. Using paired LFP recordings, we identified that secondary seizures in the contralesional hippocampus triggered these contralesional SDs. Disrupting contralesional SD via NMDAR antagonism led to persistent and generalized seizure, worsening anterograde amnesia post-stroke. Here, we established a model for evaluating ischemia-evoked SD in behaving mice and identified how SD might act as a double-edged sword in a region-specific manner during the early phase of stroke.

OP-42 (ID:51)

CHARACTERIZATION OF SPREADING DEPOLARIZATION AND EPILEPTIFORM ACTIVITY FOLLOWING INDUCTION OF FOCAL CEREBRAL ISCHEMIA IN AWAKE MICE.

SAMUEL FLAHERTY [1], LORENA FIGUEIREDO FERNANDES [1], EDUARD MASVIDAL-CODINA [3], XAVIER ILLA [4], ELISABET PRATS-ALFONSO [4], KOSTAS KOSTAERLOS [2], STUART ALLAN [1], JOSE ANTONIO GARRIDO [3], ANTON GUIMERà-BRUNET [4], ROBERT C WYKES [1],

[1] THE DİVİSİON OF NEUROSCİENCE AND THE BRAİN INFLAMMATİON GROUP, UNİVERSİTY OF MANCHESTER, UNİTED KİNGDOM.
[2] THE CENTRE FOR NANOTECHNOLOGY İN MEDİCİNE, UNİVERSİTY OF MANCHESTER, UNİTED KİNGDOM
[3] CATALAN INSTİTUTE OF NANOSCİENCE AND NANOTECHNOLOGY ICN2, CSIC AND THE BARCELONA INSTİTUTE OF SCİENCE AND TECHNOLOGY BIST, CAMPUS UAB, BELLATERRA, BARCELONA, SPAİN.
[4] CENTRO DE INVESTİGACIóN BİOMéDİCA EN RED EN BİOİNGENİERíA, BİOMATERİALES Y NANOMEDİCİNA CIBER-BBN, MADRİD, SPAİN.

Introduction:
Most pre-clinical stroke research is performed in rodents under anaesthesia. However, anaesthetics modulate cerebral blood flow, spreading depolarisation (SD) and neurovascular coupling, all essential in the pathophysiology of stroke. Additionally, anaesthetics inhibit seizure and epileptiform activity, a known manifestation present post focal cerebral ischaemia. Refinements in stroke research now enables the induction of focal cerebral ischaemia in awake mice with concurrent DC-coupled electrophysiology. Graphene micro-transistor (gSGFET) arrays can record wide bandwidth signals allowing high resolution spatial mapping of SD's and focal epileptiform activity. Due to their transparency, gSGFETs can simultaneously operate with laser speckle contrast imaging (LSCI) allowing direct correlation with underlying regional cerebral blood flow (rCBF).

Methods:
Induction of focal cerebral ischaemia was conducted using the photothrombotic model in awake head-fixed mice. A 30 channel epicortical DC-coupled gSGFET was positioned over the somatosensory cortex. An area of ischaemia was formed 0.5 mm from the gSGFET permitting the recording from neural tissue within a gradient of perfusion deficits. LSCI was employed providing direct monitoring of rCBF directly below up to 30 recording transistors. Behavioural changes in response to ischaemic induction, SDs and epileptic activity, were monitored.

Results:
DC-coupled recordings and rCBF measurements in awake head-fixed mice were compared to data acquired from anaesthetised mice that received an identical experimental paradigm. Preliminary analysis indicates that, compared to data acquired from mice under anaesthesia, SD frequency is increased, and focal epileptiform activity occurs which often precedes SD initiation resulting in hyperactivity. Animal behavioural arrest appears with SD initiation, followed by increased movement during SD repolarisation. Detailed characterization of SD waveform, clustering, and haemodynamic responses to SD is ongoing and will be presented.

Conclusions:
Removing the confounding effects of anaesthetics from pre-clinical stroke research may advance our understanding of the cerebral impact of SD and potentially improve the clinical translation of therapeutics.

POSTER PRESENTATIONS

POSTER-1 (ID:80)

DETECTION OF SPREADING DEPOLARIZATION-ASSOCIATED BLOOD-BRAIN BARRIER DISRUPTION USING DYNAMIC CONTRAST-ENHANCED MRI

MAGNUS P.B. KREIBERG [1], NINA S. V. SØRENSEN [1], JAKOB MØLLER [2], KAREN L. GANDRUP [2], ULRICH LINDBERG [3], HENRIK B.W. LARSSON [3], ANDERS HOUGAARD [1]

[1] DEPARTMENT OF NEUROLOGY, COPENHAGEN UNİVERSİTY HOSPİTAL – HERLEV AND GENTOFTE, COPENHAGEN, DENMARK
[2] DEPARTMENT OF RADİOLOGY, COPENHAGEN UNİVERSİTY HOSPİTAL – HERLEV AND GENTOFTE, COPENHAGEN, DENMARK
[3] FUNCTİONAL IMAGİNG UNİT, DEPARTMENT OF CLİNİCAL PHYSİOLOGY AND NUCLEAR MEDİCİNE, COPENHAGEN UNİVERSİTY

Background:

In patients, spreading depolarization (SD) events can give rise to characteristic signs and symptoms in the form of transient episodes of gradually spreading visual, sensory, motor, and/or speech symptoms. Such clinical episodes are a hallmark of migraine with aura but are also well-documented in patients as a direct consequence of cortical injury or irritation, including ischemic stroke and transient ischemic attacks, CNS neoplasms, arteriovenous malformations, and traumatic brain injury. Diagnosis of clinical SD episodes is currently limited by the lack of a clinically useful non-invasive biomarker of SD. Clinical SD episodes are unpredictable and usually short-lasting (less than 1 h). For this reason, it is virtually impossible in a clinical setting to carry out diagnostic investigations, such as brain scans, while symptoms are still present.
Animal studies have consistently shown that SD leads to a transient increase of blood-brain barrier permeability, likely peaking approximately 24 hours after an SD episode. Dynamic-contrast enhanced magnetic resonance imaging (DCE-MRI) is a sophisticated method for detection of subtle changes in BBB permeability in patients.
In the present study, we will apply an optimized DCE-MRI protocol to investigate patients presenting with clinical symptoms suggestive of SD and patients with transient ischemic attacks (TIAs). We hypothesize that increased BBB permeability detected using DCE-MRI at 12-48 hours following symptoms can serve as a clinically applicable neuroimaging marker of SD. We further hypothesize, that similar BBB disruption is not seen following TIA without symptoms suggestive of SD.

Methods:

We will screen patients presenting to the emergency department due to transient neurological symptoms. Patients with symptoms fulfilling ad-hoc criteria for clinical SD (Table 1), patients with a history of migraine with aura according to the criteria of the International Classification of Headache Disorders (Table 2) presenting with attacks of migraine with aura, and patients with symptoms fulfilling the Modified Explicit Diagnostic Criteria for Transient Ischemic Attacks (Table 3) are potentially eligible for participation. Patients will receive an initial acute brain MRI as part of the standard clinical workup at the department. Patients without neuroimaging evidence of acute brain pathology will be offered to undergo DCE-MRI at 3 Tesla to quantitatively estimate regional BBB permeability between 12 hours and 48 hours following onset of a clinical SD or TIA episode. The scan will be repeated when patients have been free of symptoms for minimum 7 days.
Scans will be analyzed using in-house software to calculate the influx constant K_i, using the Patlak model, as a measure of BBB permeability. Maps of changes in K_i between the first and second DCE-MRI scan will be evaluated for each individual patient.

Potential outcome

The study has the potential to establish delayed BBB permeability increase detected using DCE-MRI as a non-invasive biomarker of transient SD episodes in patients.
If possible, preliminary data from the study will be presented at the iCSD 2024 Congress.

Table 1.
Ad-hoc criteria for clinical episodes suggestive of spreading depolarization

Diagnostic criteria:

A. At least one attacks fulfilling criteria B-D

B. One or more of the following fully reversible symptoms/signs:

1. visual
2. somatosensory
3. speech and/or language
4. motor weakness

C. At least one of the following two characteristics:

1. at least one symptom/sign spreads gradually over ≥5 minutes
2. two or more symptoms/signs occur in succession

A. At least two of the following three characteristics:

Table 2.
International Classification of Headache Disorders criteria for Migraine with aura

Diagnostic criteria:
A. At least two attacks fulfilling criteria B and C
B. One or more of the following fully reversible aura symptoms:

1. visual
2. sensory
3. speech and/or language
4. motor
5. brainstem
6. retinal

C. At least three of the following six characteristics:

1. at least one aura symptom spreads gradually over ≥5 minutes
2. two or more aura symptoms occur in succession
3. each individual aura symptom lasts 5-60 minutes[1]
4. at least one aura symptom is unilateral[2]
5. at least one aura symptom is positive[3]
6. the aura is accompanied, or followed within 60 minutes, by headache

D. Not better accounted for by another ICHD-3 diagnosis.

1. Aphasia is always regarded as a unilateral symptom; dysarthria may or may not be.

Table 3.
Modified Explicit Diagnostic Criteria for Transient Ischemic Attacks

Diagnostic criteria:

A. Sudden onset of fully reversible neurological or retinal symptoms (typically hemiparesis, hemihypesthesia, aphasia, neglect, amaurosis fugax, or hemataxia).
B. Duration < 24 h
C. At least 2 of the following:
   1. All symptoms are maximal in <1 min (no gradual spread)
   2. All symptoms occur simultaneously
   3. All symptoms are deficits (no irritative symptoms such as photopsias, pins, and needles, etc)
   4. No headache accompanies or follows the neurological symptoms within 1 h
D. None of the following isolated symptoms (can occur together with more typical symptoms); shaking spells, diplopia, dizziness, vertigo, syncope, decreased level of consciousness, confusion, hyperventilation-associated paresthesia, unexplained falls, and amnesia.
E. No evidence of acute infarction in the relevant area on neuroimaging

POSTER-2 (ID:34)

IMPAIRMENT OF NA+-K+-ATPASE IN THE HUMAN CORTEX UNDER HALOGENATED ETHER ANESTHETICS IS ASSOCİATED WTH DISRUPTED IN HOMEOSTASIS

MATHILDE MAECHLER , COLINE LEMALE , JORG GEIGER , AGUSTIN LIOTTA , NIKOLAUS BERNDT ,

CHARİTé UNİVERSTäTSMEDİZİN BERLİN

The sodium-potassium ATPase (NKA) establishes the essential electrochemical gradient responsible for maintaining the resting membrane potential of cells. In the brain, impairment of the NKA can lead to increased neuronal excitability and contribute to pathological phenomena such as epileptic seizures and the occurrence of spreading depolarization. In the mammalian brain, there are three isoforms of the NKA catalytic subunit: α1, α2, and α3. While the α1 is ubiquitously present, the α2 (found in astrocytes and glial cells) and α3 (found in neurons) are highly expressed in the brain. In 2023 we described for the first time the specific impairment of the α2/3 isoforms of the NKA activity in the rat brain during deep isoflurane anesthesia inducing burst-suppression brain activity. This suggests that the observed impairment may be a side effect of isoflurane, primarily affecting the central nervous system. Since burst-suppression anesthesia is deliberately induced in clinical practice for severe brain diseases, such as status epilepticus, traumatic brain injuries, or elevated intracranial pressure, confirming this finding and its impact on the ion homeostasis in the human brain is essential.

Here, we examine the impact of deep isoflurane and sevoflurane anesthesia in vitro in paired experiments on human cortical brain slices. The human cortical tissue was obtained from anterior temporal lobe epilepsy surgery in patients diagnosed with pharmacoresistant epilepsy. For this study, 13 patients (11 males, 2 females) aged 4 to 62 years (median age 22) were included. We performed electrophysiological recordings of extracellular ion concentrations (K^+, Na^+, and $Ca^{2+)}$ in an interface chamber, with and without neuronal activity and two-pore-domain potassium channels inhibition. The NKA activity was assessed using a coupled enzyme assay.

Our findings demonstrate a dose-dependent elevation in extracellular potassium concentration, along with decreased levels of extracellular sodium and calcium under both anesthetics ($p<0.05$). These effects are independent of synaptic activity and two-pore-domain potassium channels and are significantly stronger under isoflurane compared to sevoflurane anesthesia ($p<0.05$). Additionally, the clearance times for sodium and potassium after stimuli are prolonged ($p<0.05$). A decline in total NKA activity is detected in the enzyme assay under isoflurane and sevoflurane anesthesia ($p<0.05$).

Here we show that not only deep isoflurane anesthesia but also deep sevoflurane anesthesia impairs NKA in human cortical brain tissue, thereby disrupting ion homeostasis. Thus, these results provide evidence for human NKA impairment at electrophysiological and biochemical levels under halogenated ether anesthesia. Regarding pathophysiology, specific deficiencies in the α2 and α3 isoforms are associated with neurological disorders, and inhibition of NKA activity is known to produce a state of cortical hyperexcitability. This could be one of the mechanisms explaining the occurrence of bursting activity during deep anesthesia and could help understand the neurocognitive adverse outcomes associated with burst-suppression anesthesia.

POSTER-3 (ID:48)

ELECTROPHYSIOLOGICAL CHARACTERIZATION OF THE PERICYTE-ENDOTHELIAL CELL SYNCYTIUM IN HUMAN BRAIN SLICES FROM PATIENTS WITH PHARMACORESISTANT MESIAL TEMPORAL LOBE EPILEPSY

MIRJA GROTE LAMBERS [1], MAJED KIKHIA [2], AGUSTIN LIOTTA [1], HENRIKE PLANERT [1], THILO KALBHENN [5], RAN XU [3], JULIA ONKEN [3], THOMAS SAUVIGNY [6], ULRICH W. THOMALE [7], ANGELA KAINDL [8], MARTIN HOLTKAMP [2], PAWEL FIDZINSKI [4], MATTHIAS SIMON [5], HENRIK ALLE [1], CHRISTIAN MADRY [1], JÖRG R. P. GEIGER [1], RICHARD KOVÁCS [1],

[1] *INSTITUTE OF NEUROPHYSIOLOGY, CHARITÉ - UNIVERSITÄTSMEDIZIN BERLIN, GERMANY*
[2] *DEPARTMENT OF NEUROLOGY AND EXPERIMENTAL NEUROLOGY, CHARITÉ - UNIVERSITÄTSMEDIZIN BERLIN, GERMANY*
[3] *DEPARTMENT OF NEUROSURGERY, CHARITÉ - UNIVERSITÄTSMEDIZIN BERLIN, GERMANY*
[4] *NEUROSCIENCE CLINICAL RESEARCH CENTER, CHARITÉ - UNIVERSITÄTSMEDIZIN BERLIN, GERMANY*
[5] *DEPARTMENT OF NEUROSURGERY, BETHEL HOSPITAL - UNIVERSITY OF BIELEFELD MEDICAL CENTER OWL, GERMANY*
[6] *DEPARTMENT OF NEUROSURGERY, UNIVERSITY MEDICAL CENTER HAMBURG-EPPENDORF, GERMANY*
[7] *DEPARTMENT OF PEDIATRIC NEUROSURGERY, CHARITÉ - UNIVERSITÄTSMEDIZIN BERLIN, GERMANY*
[8] *DEPARTMENT OF PEDIATRIC NEUROLOGY, CHARITÉ - UNIVERSITÄTSMEDIZIN BERLIN, GERMANY*

Mesial temporal lobe epilepsy (mTLE) is one of the main indications for epilepsy surgery as patients are frequently refractory to antiepileptic treatment. In search for potential drug targets to prevent epileptogenesis, the involvement of the neurovascular unit (NVU), and in particular of pericytes, which regulate capillary diameter, has come to the forefront of interest. While individual seizures are followed by periods of postictal neurovascular uncoupling, seizure focus is characterized by a general interictal hypoperfusion (1, 2). Post-mortem analysis reveals alterations in the vasculature and epilepsy patients with different etiologies show pericytes with altered morphology (3, 4).

Using organotypic hippocampal slice cultures from rats, we have previously shown that pericytes build a functional syncytium with capillary endothelial cells, which transmits electrical signals associated with epileptiform activity. Seizure onset was preceded by adenosine and Kir 2.x channel-mediated hyperpolarization, whereas seizures themselves were characterized by massive depolarization due to potassium accumulation at the vasculature. However, these effects were obtained in healthy tissue, while almost nothing is known about the alterations in functioning of the pericyte-endothelial syncytium in chronic epileptic tissue.

In our current study, we examined temporal lobe tissue specimens from patients undergoing surgery for refractory mTLE, while resection material from tumor cases served as controls. We performed whole-cell patch-clamp recordings on capillary pericyte-pericyte, pericyte-endothelial cell pairs and analyzed the patched cells morphologically via dye injection. Calculation of intercapillary distance and evidence on vascular abnormalities were obtained by immunofluorescence reconstruction of the vasculature.

Morphological and electrophysiological classes of human capillary pericytes corresponded to those described for the rat, i.e. mesh-, thin strand-, and junctional pericytes. Despite the absence of blood flow and transmural pressure, the resting Em of the syncytium was more positive (-38.2 mV) than in culture (-78.5 mV). Nevertheless, onset of epileptiform activity, elevation of potassium to 5 mM or activation of K_{ATP} channels by pinacidil resulted in a hyperpolarization while seizure-associated potassium rises were presented as synchronous depolarization of the syncytium.

Dye coupling from endothelial cells to pericytes was significantly faster and stronger than vice versa. Unlike the pericyte-pericyte pairs, the electrical coupling between endothelial cells and pericytes showed less rectification in culture compared to human. Reconstruction of the vasculature revealed the presence of nonfunctional string vessels (without a lumen) even in the temporal cortex, albeit at a lower density than in sclerotic hippocampus.

The present study is the first to give an electrophysiological characterization of human pericytes in situ. In conclusion, endothelial cells and pericytes retain electrical coupling and reactivity to the signals mediating hyperpolarization at seizure onset, despite the generally more positive resting Em, likely due to the slicing procedure.

1. Farrell JS, Gaxiola-Valdez I, Wolff MD, David LS, Dika HI, Geeraert BL, Rachel Wang X, Singh S, Spanswick SC, Dunn JF, Antle MC, Federico P, Teskey GC. Postictal behavioural impairments are due to a severe prolonged

hypoperfusion/hypoxia event that is COX-2 dependent. Elife. 2016 Nov 22;5:e19352. doi: 10.7554/eLife.19352. PMID: 27874832; PMCID: PMC5154758.

2. Prager O, Kamintsky L, Hasam-Henderson LA, Schoknecht K, Wuntke V, Papageorgiou I, Swolinsky J, Muoio V, Bar-Klein G, Vazana U, Heinemann U, Friedman A, Kovács R. Seizure-induced microvascular injury is associated with impaired neurovascular coupling and blood-brain barrier dysfunction. Epilepsia. 2019 Feb;60(2):322-336. doi: 10.1111/epi.14631. Epub 2019 Jan 4. PMID: 30609012.
3. van Lanen RH, Melchers S, Hoogland G, Schijns OE, Zandvoort MAV, Haeren RH, Rijkers K. Microvascular changes associated with epilepsy: A narrative review. J Cereb Blood Flow Metab. 2021 Oct;41(10):2492-2509. doi: 10.1177/0271678X211010388. Epub 2021 Apr 17. PMID: 33866850; PMCID: PMC8504411.
4. Yamanaka G, Takata F, Kataoka Y, Kanou K, Morichi S, Dohgu S, Kawashima H. The Neuroinflammatory Role of Pericytes in Epilepsy. Biomedicines. 2021 Jun 30;9(7):759. doi: 10.3390/biomedicines9070759. PMID: 34209145; PMCID: PMC8301485.

POSTER- 4 (ID:81)

CASE REPORT: A PATIENT WITH HEMIPLEGIC MIGRAINE AND UNILATERAL TRANSIENT CEREBRAL HYPERPERFUSION

ARDA DUMAN , FAHRETTİN SERTAÇ YAPAR , YASEMİN GÜRSOY-ÖZDEMİR

KOÇ UNIVERSITY SCHOOL OF MEDICINE- DEPARTMENT OF NEUROLOGY

Background:

Transient cerebral hyperperfusion is defined as the temporary increase to arteries of the brain following hypoperfusion and could result with symptoms on the corresponding side. Patients may present to the clinic with hemiplegia, aphasia, neglect and/or epileptic seizures. Although carotid artery stenting and carotid artery endarterectomy are known to be the most common causes of transient cerebral hyperperfusion[1], other rare conditions such as hemiplegic migraine[2], intravascular lymphoma[3], radiation therapy[4] could be of etiology. In this case report, a 52-years old male patient presenting to our Neurology clinic with the symptoms of aphasia, headache, confusion, right-sided hemiplegia will be discussed.

Case Presentation:

A 52-year-old male patient with the history of hypertension, diabetes mellitus, obsessive compulsive disorder, cornea transplant, migraine with aura and cognitive features presented to the clinic for the evaluation of aphasia and confusion. Family history was not significant for migraine and other neurodegenerative disorders. His first symptom was forgetting the password of his computer. In the following hours, he developed confusion and aphasia. He was evaluated on the first day of the symptoms and hospitalized with the preliminary diagnoses of transient ischemic attack and migraine with aura episode. The following day, he developed right-sided hemiplegia and concomitant left-sided headache. Headache lasted for a couple hours, and hemiplegia lasted almost 3 days and disappeared at the end of the third day. Upon further evaluation, two prior episodes were spotted in the patient's medical history. At the age of 42, he was hospitalized and followed up due to a similar episode of aphasia, confusion and concomitant headache after rhinoplasty surgery. His symptoms had improved in three days without any specific treatment, and he was diagnosed with migraine with aura and cognitive features at the time. At the age 43, he had another similar episode of confusion and concomitant headache similarly lasting almost 3 days without any treatment. In the electroencephalography (EEG) on the second day of the symptoms, low amplitude trace was found on the left hemisphere. Brain Magnetic Resonance Imaging (MRI) was done on the fourth day of symptoms. Left-sided cerebral hyperperfusion and meningeal and cortical contrast enhancement on the left hemisphere was observed. Contrast enhancement was found to be more prominent on the left insular cortex. Patient was followed up with the treatment of acetylsalicylic acid for transient ischemic attack. On the eighth day of his symptoms, patient had five consecutive epileptic seizures lasting 5 to 10 seconds in which he had tonic and clonic movements in the upper extremities and gaze deviation. He was started on oral levetiracetam 2000 mg/day. Lumbar puncture was performed. Cerebrospinal fluid (CSF) protein and glucose levels were found to be normal, and less than five leukocytes were detected in the CSF. No bacterial growth was detected in the CSF culture. No paraneoplastic antibody marker and autoimmune encephalitis marker was detected in the serum and in the CSF. CSF IgG index was found to be within normal limits. Patient was also evaluated for myelin oligodendrocyte glycoprotein (MOG) related disorders. MOG live cell-based assay was found to be clear negative. Patient was started on high-dose intravenous methylprednisolone (IVMP) treatment for seven days with the preliminary diagnosis of hemiplegic migraine. On the second day of IVMP, a significant improvement in confusion and aphasia was observed. After the end of 7-day high dose IV steroid treatment, he was tapered with oral steroid starting from the dose of 1 mg/kg. On the 1-week follow-up, confusion had disappeared, and aphasia was only observed at the very end of long sentences. He was referred to the Genetics Department for the evaluation of familial hemiplegic migraine syndromes.

Discussion:

Hemiplegic migraine has been suggested as a possible cause for unilateral transient cerebral hyperperfusion[5]. Hemiplegic migraine is a relatively rare type of migraine which can imitate other neurologic conditions including ischemic stroke, transient ischemic attack, or seizure. Hemiplegic migraine could be familial or may occur sporadically. The most common symptoms of hemiplegic migraine are recurrent headache and concomitant hemiplegia episodes. Sensory loss, visual disturbances and aphasia/dysphasia could also be observed during migraine episodes. Migraine episodes have been known to last hours to days and neurological deficits may outlast the headache[6]. Imaging methods such as MRI could be helpful in the further evaluation of the differential

diagnosis. Genetic tests could be used in hemiplegic migraine patients especially for CACNA1A mutation which is known to be detected in familial hemiplegic migraine patients.

1. Reigel MM, Hollier LH, Sundt TM Jr, Piepgras DG, Sharbrough FW, Cherry KJ. Cerebral hyperperfusion syndrome: a cause of neurologic dysfunction after carotid endarterectomy. J Vasc Surg. 1987 Apr;5(4):628-34. PMID: 3560356.
2. Masuzaki M, Utsunomiya H, Yasumoto S, Mitsudome A. A case of hemiplegic migraine in childhood: transient unilateral hyperperfusion revealed by perfusion MR imaging and MR angiography. AJNR Am J Neuroradiol. 2001 Oct;22(9):1795-7. PMID: 11673182; PMCID: PMC7974427.
3. Imamura D, Fujiwara S, Amagase H, Kawamoto M. Unilateral Hemispheric Hyperperfusion in Intravascular Large B-cell Lymphoma. Cureus. 2024 Jun 28;16(6):e63417. doi: 10.7759/cureus.63417. PMID: 39077292; PMCID: PMC11285681.
4. Irizato N, Hashimoto H, Chiba Y. Unexpected Cerebral Hyperperfusion after Transient Hypoperfusion Associated with Stroke-like Migraine Attacks after Radiation Therapy Syndrome. NMC Case Rep J. 2024 May 17;11:135-140. doi: 10.2176/jns-nmc.2024-0037. PMID: 38863579; PMCID: PMC11165263.
5. Oberndorfer S, Wöber C, Nasel C, Asenbaum S, Lahrmann H, Fueger B, Grisold W. Familial hemiplegic migraine: follow-up findings of diffusion-weighted magnetic resonance imaging (MRI), perfusion-MRI and [99mTc] HMPAO-SPECT in a patient with prolonged hemiplegic aura. Cephalalgia. 2004 Jul;24(7):533-9. doi: 10.1111/j.1468-2982.2003.00706.x. PMID: 15196295.
6. Jen JC. Familial Hemiplegic Migraine. 2001 Jul 17 [updated 2024 Jul 4]. In: Adam MP, Feldman J, Mirzaa GM, Pagon RA, Wallace SE, Bean LJH, Gripp KW, Amemiya A, editors. GeneReviews® [Internet]. Seattle (WA): University of Washington, Seattle; 1993–2024. PMID: 20301562.

POSTER-5 (ID:89)

PROTOCOL OVERVIEW: INHIBITING THE NMDAR/TRPM4 INTERACTION AS A NEUROPROTECTIVE STRATEGY IN A GYRENCEPHALIC BRAIN MODEL OF ISCHEMIC STROKE THROUGH MODULATION OF SPREADING DEPOLARIZATION

JUAN M. LOPEZ-NAVARRO [1], DIEGO A. SANDOVAL-LOPEZ [1], KAREN VELAZQUEZ1 [1], MARCOS A. SUAREZ-GUTIERREZ [1], FERNANDO A. NUñEZ [1], RENAN SANCHEZ-PORRAS [1], JOHANNES WOITZIK [1], EDGAR SANTOS [2],

[1] DEPARTMENT OF NEUROSURGERY, CARL VON OSSİETZKY UNİVERSİTY OF OLDENBURG, OLDENBURG, GERMANY.
[2] SPİNE CENTER STUTTGART, PAULİNENHİLFE, DİAKONİE-KLİNİKUM STUTTGART, STUTTGART, GERMANY.

Background:

Ischemic stroke, accounting for 87% of all stroke cases, remains a leading cause of death and disability globally, posing significant challenges for patients and healthcare systems.[1] Timely intervention and advanced imaging techniques are vital for improving outcomes.[2] For example, mechanical thrombectomy within 16 hours of symptom onset can significantly reduce long-term disability.[3] However, this procedure is unsuitable for patients with extensive infarctions, prompting interest in neuroprotective therapies to mitigate post-stroke neuronal damage.[4]

Spreading depolarizations (SDs), linked to ischemic stroke, are associated with increased infarct size and worse clinical outcomes.[5] These depolarization waves can extend neuronal damage in adjacent brain tissue, making them a potential prognostic marker and therapeutic target.[6] Despite extensive research, effective neuroprotective treatments have been elusive. Ketamine, however, shows promise in reducing neuronal damage, highlighting the need for further studies.[7]

N-methyl-D-aspartate receptors (NMDARs) are crucial for neuronal plasticity but can also cause cell death when activated, contributing to the spread of SDs. This dual role has limited the success of NMDAR antagonists in clinical trials, although s-ketamine has shown effectiveness in reducing SDs in brain injury models.[8] Recently, a small-molecule inhibitor, Compound 8, was developed to protect against excitotoxic cell death by inhibiting NMDAR/TRPM4 interaction.[9] However, concerns about long-term toxicity have led to the development of FP802, a variant that selectively reduces toxic effects of extrasynaptic NMDARs while preserving synaptic functions.[10] This approach may enhance neuroprotection after ischemic stroke.

In this study, we aim to use a translational gyrencephalic model of middle cerebral artery occlusion (MCAo) to assess short-term (18 hours) and long-term (3 weeks) outcomes. Our primary goal is to evaluate infarct size reduction following treatment with S-ketamine or FP802, along with a detailed analysis of functional outcomes through clinical and neurological assessments. We will also investigate SDs and their hemodynamic responses using advanced techniques like multispectral and photoacoustic imaging (PAI). Additionally, we will assess brain connectivity during the acute and chronic phases of the infarct to gain a comprehensive understanding of treatment effects.

Methods:

The study, beginning in August 2024, will use female German Landrace pigs (30-35 kg, 3-4 months old) due to their anatomical suitability for urethral catheterization. The project is divided into two experimental models: short-term (18 hours post-infarction) and long-term (3 weeks post-infarction). Each model includes three groups: a control group (saline), an S-Ketamine group (5 mg/kg/hour), and an FP802 group (40 mg/kg/day). Treatments will be administered randomly and double-blind. Ethical approval was obtained from the Institutional Animal Care and Use Committee in Karlsruhe, Germany.

Throughout the experiments, physiological variables like oxygen saturation, end-tidal CO2, heart rate, mean arterial pressure, capillary glucose, rectal temperature, and hourly urine output will guide fluid management. Sample sizes (22 animals per group) were calculated based on a prior pilot study, anticipating a 30% infarct size reduction, with 5% alpha error and 80% power.

Perioperative management includes habituation, anesthesia induction with Azaperone (8 mg/kg), Midazolam (1 mg/kg), and Propofol (1-2 mg/kg), followed by intubation, and catheter placements. Continuous sedation is maintained with Isoflurane (1-1.5%) and Midazolam (0.1-0.5 mg/kg/hour), with Buprenorphine boluses (0.05 mg/kg) every 6 hours for analgesia.

The short-term model involves a bilateral craniectomy for imaging access. The middle cerebral arteries (MCAs) will be clipped using a transorbital approach. Electrocorticography (ECoG) will be recorded for 10 minutes before and 18 hours after clipping, using 4-contact platinum electrodes. Imaging will involve a 5 MP grayscale camera with a 570-nanometer filter and a 16-sensor multispectral camera to assess hemodynamic responses and brain connectivity. For half of the animals in each group, recordings will be made with PAI to evaluate changes in

oxygen saturation and total hemoglobin in the thickness of the entire cerebral cortex and underlying white matter, while the other half will be assessed using the cameras. One hour after infarction, treatment begins and continues for 17 hours. After 18 hours, the brain will be extracted, frozen, sectioned, stained, and analyzed for infarct size using ImageJ software. Molecular assays will measure markers of excitotoxicity, apoptosis, neurogenesis, and gliogenesis.
The long-term model uses a retro-orbital approach for MCA clipping and 24-contact electrode insertion for wireless ECoG monitoring over 3 weeks, though signal quality may be affected by movement. After infarction, treatment continues for 17 hours under deep sedation. After 18 hours, the pig will be awakened, extubated, and monitored for 3 weeks with clinical and neurological assessments, including an object recognition test for memory evaluation. After the monitoring period, a bilateral craniectomy will be performed for 6 hours of imaging, followed by brain staining and molecular testing as in the short-term model. For half of the animals in each group, recordings will be made with the cameras, while the other half will be assessed using the PAI.

Conclusion:
This study aims to explore the neuroprotective potential of inhibiting the NMDAR/TRPM4 interaction in a gyrencephalic model of ischemic stroke. By employing S-ketamine and FP802, we anticipate a significant reduction in infarct size and improved functional outcomes, while also assessing the role of spreading depolarizations in neuronal damage. Through advanced imaging techniques and rigorous monitoring of physiological parameters, this research seeks to contribute valuable insights into potential therapeutic strategies for mitigating the devastating effects of ischemic stroke and enhancing patient recovery. If favorable results are obtained, these findings may pave the way for subsequent clinical trials in humans to evaluate the efficacy and safety of these interventions.

References
1. Benjamin EJ, Muntner P, Alonso A, Bittencourt MS, Callaway CW, Carson AP, et al. Heart disease and stroke statistics—2019 update: A report from the American heart association. Circulation. 2019;139(10).
2. Powers WJ, Rabinstein AA, Ackerson T, Adeoye OM, Bambakidis NC, Becker K, et al. 2018 guidelines for the early management of patients with acute ischemic stroke: A guideline for healthcare professionals from the American heart association/American stroke association. Stroke [Internet]. 2018;49(3).
3. Albers GW, Marks MP, Kemp S, Christensen S, Tsai JP, Ortega-Gutierrez S, et al. Thrombectomy for stroke at 6 to 16 hours with selection by perfusion imaging. N Engl J Med. 2018;378(8):708–18.
4. Chamorro Á, Dirnagl U, Urra X, Planas AM. Neuroprotection in acute stroke: targeting excitotoxicity, oxidative and nitrosative stress, and inflammation. Lancet Neurol. 2016;15(8):869–81.
5. Hartings JA, Shuttleworth CW, Kirov SA, Ayata C, Hinzman JM, Foreman B, et al. The continuum of spreading depolarizations in acute cortical lesion development: Examining Leão's legacy. J Cereb Blood Flow Metab. 2017;37(5):1571–94.
6. Binder NF, Glück C, Middleham W, Alasoadura M, Pranculeviciute N, Wyss MT, et al. Vascular response to spreading depolarization predicts stroke outcome. Stroke. 2022;53(4):1386–95.
7. Bell JD. In vogue: Ketamine for neuroprotection in acute neurologic injury. Anesth Analg. 2017;124(4):1237–43.
8. Sánchez-Porras R, Kentar M, Zerelles R, Geyer M, Trenado C, Hartings JA, et al. Eighteen-hour inhibitory effect of s-ketamine on potassium- and ischemia-induced spreading depolarizations in the gyrencephalic swine brain. Neuropharmacology. 2022;216(109176):109176.
9. Yan J, Bengtson CP, Buchthal B, Hagenston AM, Bading H. Coupling of NMDA receptors and TRPM4 guides discovery of unconventional neuroprotectants. Science. 2020;370(6513).
10. Yan J, Wang YM, Hellwig A, Bading H. TwinF interface inhibitor FP802 stops loss of motor neurons and mitigates disease progression in a mouse model of ALS. Cell Rep Med. 2024;5(2):101413.

POSTER-6 (ID:90)

A MEMS-BASED THIN FILM MICROELECTRODE ARRAY FOR MONITORING OF TRAUMATIC BRAIN INJURY

ALİ CAN ATİK [1], ÖZLEM TOPÇU [1], AKIN MERT YILMAZ [2], LEMAN DİCLE BALCI [1], ŞAHİN HANALİOĞLU [3], HASAN ULUŞAN [1], MAHMUT KAMİL ASLAN [4], HALUK KÜLAH [1],

[1] *DEPARTMENT OF ELECTRICAL AND ELECTRONICS ENGINEERING, MIDDLE EAST TECHNICAL UNIVERSITY (METU), ANKARA, TURKEY*
[2] *METU MEMS RESEARCH AND APPLICATIONS CENTER, ANKARA, TURKEY*
[3] *DEPARTMENT OF NEUROSURGERY, FACULTY OF MEDICINE, HACETTEPE UNIVERSITY, ANKARA, TURKEY*
[4] *INSTITUTE FOR CHEMICAL AND BIOENGINEERING, DEPARTMENT OF CHEMISTRY AND APPLIED BIOSCIENCES, ETH ZURICH, SWITZERLAND*

According to the World Health Organization (WHO), head trauma is one of the top 10 causes of death worldwide, accounting for the deaths of 1.3 million people and causing disabilities in over 100 million individuals each year [1]. In recent years, in cases of traumatic brain injury (TBI) and brain strokes, it has been recognized that cortical spreading depolarization (CSD) waves, also known as "brain tsunamis," cause significant ionic changes, suppress normal brain activity, and reduce blood flow, which could lead to secondary brain injury, an increased risk of late post-traumatic seizures, and epilepsy in conditions such as TBI, stroke, and brain hemorrhage [2,3]. Therefore, the prediction of CSD as an electrographic biomarker is of great importance in scientific knowledge and clinical practice for the early diagnosis and treatment of secondary brain injury and post-traumatic seizures. The presence of a CSD wave can be confirmed physiologically by tracking this negative change in the DC potential (<0.5 Hz) and subsequently confirmed by spontaneous activity changes in frequency bands between 0.5–45 Hz (AC-ECoG) [4,5]. However, CSD waves can exhibit varying irregular patterns and propagation speeds due to structural barriers such as blood vessels, brain sulci, and the presence of multiple simultaneous CSD wave sources. At this point, the use of conventional macro-electrode arrays in strip configurations results in insufficient spatio-temporal resolution, hindering detailed modeling of depolarization propagation [6,7]. To overcome this limitation, we propose a micro-electromechanical system (MEMS)-based high-density microelectrode array to investigate the spatial and temporal dynamics of CSD waves and their correlation with patient physiology in TBI. In this context, parylene-C has emerged as a flexible substrate for electrocorticography (ECoG) devices due to its exceptional biocompatibility, electrical insulation properties, chemical and moisture-resistant characteristics, mechanical flexibility, and transparency for optical imaging [8,9]. Therefore, a porous parylene-C substrate is designed to allow tissue perfusion during measurements, improve adhesion properties, and reduce the effective modulus of elasticity, thereby enhancing the ability of the thin electrode array base to wrap around the brain. The prototype microelectrode array, designed for placement on a mouse brain, consists of Euclidean circular micro-sized electrodes spaced at a sufficient resolution to distinguish the functional units of similar types of neurons. With the long-term continuous monitoring of CSD events using the microelectrode array, characteristic parameters such as the duration and magnitude of DC shifts, depression patterns, and propagation models will be obtained, allowing for a detailed understanding of their interactions in the brain. Moreover, MEMS technology enables the integration of microchannels or microsensors into the system, facilitating localized delivery of pharmacological agents or real-time monitoring of various physical and chemical parameters. Since CSD events can be predicted in real-time, pharmacological targeting of the cortical region can be precisely timed to minimize secondary injury and monitor the effectiveness of the applied treatment**.** Consequently, the MEMS-based flexible thin-film parylene microelectrode array is proposed to advance brain-machine interface technology by improving the understanding of CSD dynamics after TBI, with the potential for future enhancement into hybrid interfaces to guide patient-specific therapeutic interventions.

Acknowledgement:
This work was funded by The Scientific and Technological Research Council of Turkey (TUBITAK) within the scope of 1004 - Center of Excellence Support Program with the grant number of 22AG008.

References

[1] "The Top 10 Causes of Death," World Health Organization, [Online]. Available: https://www.who.int/news-room/fact-sheets/detail/the-top-10-causes-of-death. [Accessed: Aug. 10, 2023].
[2] D. R. Kramer, T. Fujii, I. Ohiorhenuan, and C. Y. Liu, "Interplay between cortical spreading depolarization and seizures," *Stereotactic and Functional Neurosurgery*, vol. 95, no. 1, pp. 1-5, 2017, doi: 10.1159/000452841.

[3] J. P. Dreier *et al.*, "Recording, analysis, and interpretation of spreading depolarizations in neurointensive care: Review and recommendations of the COSBID Research Group," *Journal of Cerebral Blood Flow & Metabolism*, vol. 37, no. 5, pp. 1595–1625, Jul. 2016. doi:10.1177/0271678x16654496.
[4] A. Nasretdinov *et al.*, "Diversity of cortical activity changes beyond depression during spreading depolarizations," *Nature Communications*, vol. 14, article 7729, 2023, doi: 10.1038/s41467-023-43509-3.
[5] J. A. Hartings *et al.*, "Full band electrocorticography of spreading depolarizations in patients with aneurysmal subarachnoid hemorrhage," *Cerebral Vasospasm: Neurovascular Events after Subarachnoid Hemorrhage*, pp. 131-141, 2013, doi: 10.1007/978-3-7091-1192-5_27.
[6] S. W. Cramer, I. P. Pino, A. Naik, D. Carlson, M. C. Park, and D. P. Darrow, "Mapping spreading depolarizations after traumatic brain injury: a pilot clinical study protocol," *BMJ Open*, vol. 12, no. 7, p. e061663, Jul. 2022, doi: 10.1136/bmjopen-2022-061663.
[7] E. Masvidal-Codina *et al.*, "Characterization of optogenetically-induced cortical spreading depression in awake mice using graphene micro-transistor arrays," *J. Neural Eng.*, vol. 18, no. 5, p. 055002, Apr. 2021, doi: 10.1088/1741-2552/abecf3.
[8] X. Wang *et al.*, "A parylene neural probe array for multi-region deep brain recordings," *J. Microelectromech. Syst.*, vol. 29, no. 4, pp. 499-513, 2020, doi:10.1109/jmems.2020.3000235.
[9] N. Torres-Martinez *et al.*, "Reliability of parylene-based multi-electrode arrays chronically implanted in adult rat brains, and evidence of electrical stimulation on contact impedance," *Journal of Neural Engineering*, vol. 16, no. 6, p. 066047, 2019, doi: 10.1088/1741-2552/ab3836.

POSTER-7 (ID: 67)

ALZHEIMER-STROKE CONTINUUM: THE ROLE OF SPREADING DEPOLARIZATION

ANNA TORTELI [1], MELINDA E. TÓTH [2], RITA FRANK [1], NOÉMI KOVÁCS [3], ILDIKÓ HORVÁTH [4], DOMOKOS MÁTHÉ [5], ZSOLT TOROK [2], ESZTER FARKAS [1], ÁKOS MENYHÁRT [1],

[1] DEPARTMENT OF CELL BIOLOGY AND MOLECULAR MEDICINE, ALBERT SZENT-GYÖRGYI MEDICAL SCHOOL AND FACULTY OF SCIENCE AND INFORMATICS, UNIVERSITY OF SZEGED; HUNGARIAN CENTRE OF EXCELLENCE FOR MOLECULAR MEDICINE – UNIVERSITY OF SZEGED CEREBRAL BLOOD FLOW AND METABOLISM RESEARCH GROUP, SZEGED, HUNGARY

[2] HUN-REN BIOLOGICAL RESEARCH CENTRE, CENTRE OF EXCELLENCE OF THE EUROPEAN UNION, INSTITUTE OF BIOCHEMISTRY, LABORATORY OF MOLECULAR STRESS BIOLOGY, SZEGED, HUNGARY

[3] HUNGARIAN CENTRE OF EXCELLENCE FOR MOLECULAR MEDICINE -SU, IN VIVO IMAGING ADVANCED CORE FACILITY, BUDAPEST, HUNGARY

[4] DEPARTMENT OF BIOPHYSICS AND RADIATION BIOLOGY, SEMMELWEIS UNIVERSITY, FACULTY OF MEDICINE, BUDAPEST, HUNGARY

[5] HUNGARIAN CENTRE OF EXCELLENCE FOR MOLECULAR MEDICINE -SU, IN VIVO IMAGING ADVANCED CORE FACILITY; DEPARTMENT OF BIOPHYSICS AND RADIATION BIOLOGY, SEMMELWEIS UNIVERSITY, FACULTY OF MEDICINE, BUDAPEST, HUNGARY

Introduction:

Over the last two decades, both experimental and clinical evidence suggested that protein aggregation in Alzheimer's disease (AD) is associated with chronic cortical and hippocampal hyperexcitability. Indeed, a considerable number of patients diagnosed with late-onset Alzheimers disease (AD) also present with epilepsy or bursting electroencephalogram (EEG) activity, which is indicative of altered neuronal excitability. Furthermore, the onset of epilepsy has been demonstrated to correlate with a more rapid progression of AD in patients. Although hyperexcitability is thought to enhance neurodegeneration, there is no data to confirm that epilepsy causes significant neuronal death. In this study, we report the novel and frequent occurrence of spreading depolarizations (SD) in the mouse model of Alzheimers disease (AD) following an experimental acute ischemic stroke (AIS). The objective of this study is to confirm that SD evolution, which has never been observed in AD, significantly contributes to neurodegeneration.

Methods:

Aged (19-23 months) female and male APP/PS1 (AD, n=7) and control (WT, n=8) mice were used in this study. AIS was induced under isoflurane anesthesia (0.8-1%) by the transient (60 min) microfilament guided occlusion of the middle cerebral artery (MCAO). At the end of AIS, complete reperfusion was induced by removal of the microfilament. To evaluate the sensorimotor deficit during the 72 hours of survival after AIS, mice were tested daily using the Composite Garcia Neuroscore Scale (GNS, intact animal: 21 points) scoring system. After three days, T2 and DWI MRI sequences were recorded to assess infarction, and functional ultrasound imaging was used to characterize neurovascular coupling (NVC) during mechanical whisker stimulation (2-5 Hz).

Results:

We have observed no significant difference in the AIS-related neurological deficit of mice (GNS: 13±2 vs. 12±4 points; AD vs. WT). AD mice developed diffuse and expanded AIS morphology and frequent SD evolution in response to whisker stimulation (SD number: 13 vs. 3; AD vs. WT). The appearance of SDs reflects the progression infarct growth in AIS and confirms enhanced hyperexcitability to somatosensory activation in AD mice. In addition, the amplitude of the whisker stimulation triggered functional hyperemia of NVC was also reduced in the AD group (NVC: 9.3±5 vs. 15.5±3.1%; AD vs. WT) suggesting the impaired neurovascular function in AD mice.

Conclusions:

Our results demonstrate that SDs resulting from hyperexcitability can intensify the progression of AIS in a mouse model of AD. However, the complete exclusion of the key role of epilepsy in the neurodegenerative processes fostered by hyperexcitability is futile, as seizures can trigger SDs in experimental models. While epilepsy may have less damaging potential, it is thought to be the antechamber of SD. The findings of our study indicate that SD may occur spontaneously in AD. The objective of our future experiments is to investigate the potential contribution of SD to neurodegeneration and to determine whether SD represents a novel approach to AD pathophysiology.

Acknowledgements: EU H2020-HCEMM (No. 739593), NKFIH (No. K134377, FK142218, TKP2021-EGA-28), The Hungarian Brain Research Program 3.0

POSTER-8 (ID:95)

COGNITIVE IMPAIRMENT AND PLATELET DYNAMICS IN MILD TRAUMATIC BRAIN INJURY: INSIGHTS FROM A NORTH INDIAN COHORT

ARULSELVI SUBRAMANIAM , VENENCIA ALBERT , DEEPAK AGARWAL , RAJESH SAGAR , ASHIMA NEHRA

ALL INDİA INSTİTUTE OF MEDİCAL SCİENCES, NEW DELHİ

Background:
Mild traumatic brain injuries (mTBIs) constitute the majority of head injuries, with approximately 80% of patients experiencing post-concussion syndrome symptoms within a month of injury. Untreated mTBIs can lead to long-term changes in brain pathology and increased risk of cognitive function impairment. Platelets, sharing biochemical similarities with neurons, are implicated as a peripheral model for neuronal disorders. We sought to investigate whether coated-platelets are associated with cognitive impairment post-mTBI.

Methodology:
A prospective observational cohort study was be conducted on mTBI patients (GCS ≥13). Detailed clinical and psychiatric assessments were performed after obtaining informed consent. Blood samples were collected for flow cytometry studies to measure coated platelet levels upon admission and at two weeks post-injury. Neuropsychological evaluations were conducted assess cognition at two weeks and three months post-injury. Fifty age and gender-matched healthy controls were also included in the study.

Results:
The study included 390 subjects (mean age: 31.8 ± 10.89 years; 72.2% males). Based on cognitive assessments, patients were classified into cognitive impairment (84.8%) and no cognitive impairment (15.2%) subgroups. Following mTBI the coated platelet levels were found to be slightly lower to healthy control (22.9±10.1 vs. 23.2±4.5; p0.9), but was not statistically significant. Platelet activation (Annexin V) was significantly lower in mTBI patients with cognitive decline compared to no cognitive decline (10.4(1.8-5.4) vs 26.5(16.4-34.7); p 0.03). At two weeks post injury the Coated platelet levels were elevated in mTBI patients with cognitive decline compared to no cognitive decline (33.5 vs 26.4; p 0.04). Conversely, at three months, coated platelet levels decreased in patients with cognitive decline. (25.9 vs 28.3; p 0.07)

Conclusion:
our study suggests a potential link between impaired coated-platelet function and declining cognitive abilities after mTBI. Platelets may serve as a peripheral indicator for molecular changes associated with neurocognitive functions in mTBI and could be a potential candidate for developing diagnostic and therapy-predictive tools for cognitive decline

POSTER-9 (ID:84)

THE EFFECT OF NONINVASIVE CORTICAL SPREADING DEPOLARIZATIONS ON A TEST OF EXECUTIVE FUNCTION

LYDIA HAWLEY , ELYSSA ALBER , ANGELYNA SIV , JOANNA YANG , JAMES LAI , MICHAEL DORA , ANDREIA MORAIS , KATHLEEN VINCENT , ANDREA HARRIOT , KEN SOLT , CENK AYATA , DAVID CHUNG ,

MASSACHUSETTS GENERAL HOSPİTAL

Cortical spreading depolarizations (CSD) often occur after acute brain injury and have been associated with worse cognitive outcomes. However, there are limited animal models that incorporate non-invasive induction of CSD with cognitive behavioral readouts. Therefore, we used a transgenic optogenetic mouse line to chronically and non-invasively induce CSDs with light. Adult Thy1-ChR2-YFP mice (n = 8 female and 7 male) were tested using a touch screen visual pairwise discrimination task. The mice underwent two stages of training, an initial training period, where they learn how to use the touch screen and discriminate between two images, and an experimental period during which CSDs were induced (Figure 1A). A chronic intact skull cover slip, covering the entire dorsal surface of the brain was implanted following the initial training period. We then stratified the mice into a CSD induction group (n = 9), and a sham group (n=6) based on their baseline visual discrimination performance. After three days of recovery, they began the experimental phase in which a new set of images were used. On the first three days of testing, light stimulation (460 nm blue light at 23.9 mW/mm^2) or sham stimulation was performed in awake, head fixed mice every 5 minutes for 4 rounds. The occurrence of a CSD was determined non-invasively with intrinsic signal imaging (Figure 1B). Light stimulation always produced a CSD and no CSDs were observed in sham mice. After the first 3 days of CSD or sham, the mice continued to train on the pairwise task without the induction of CSDs. We saw no differences between the CSD and sham groups using Kaplan-Meier survival curve analysis, with survival equating to passing the task, both pre- (p = 0.41) and post-CSD induction (p = 0.43) (Figure 2A). Additionally, we ran a mixed-effects analysis on the mean of percent correct pre-CSD induction (p = 0.71) and post-CSD induction (p = 0.83) (Figure 2B). Using our paradigm to induce bilateral optogenetic CSDs in awake mice, there were no deficits in cognitive function. Subsequent experiments, increasing the number of stimulations, or adding a form of acute brain injury, such as subarachnoid hemorrhage, are needed to determine the effects of chronic and noninvasive CSDs on executive function.

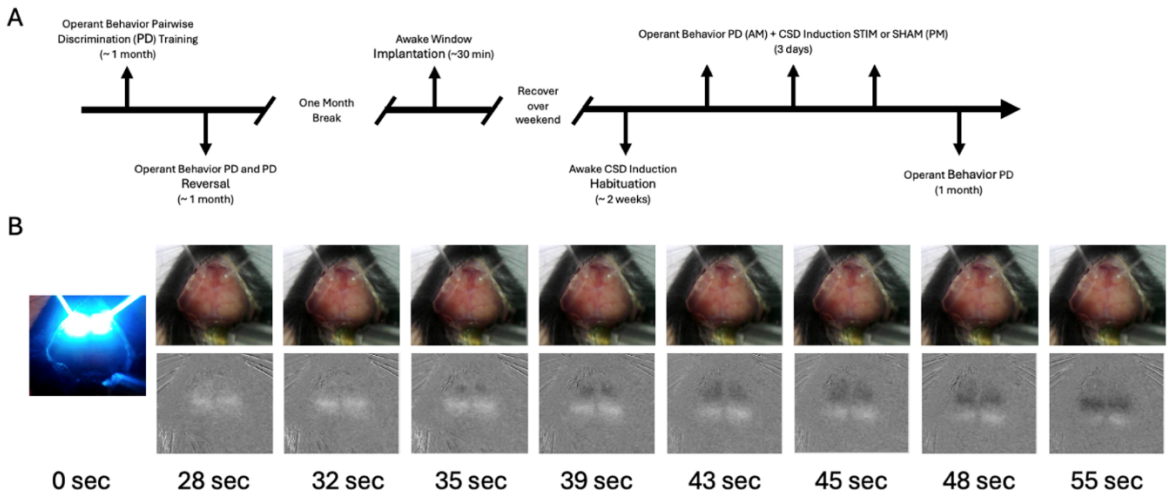

Figure 1. Experimental set up and detection of optogenetic cortical spreading depolarization (CSD). (A) Timeline of procedures. (B) Induction of bilateral CSD (colored images). Difference images of CSD propagation through the hemispheres (greyscale).

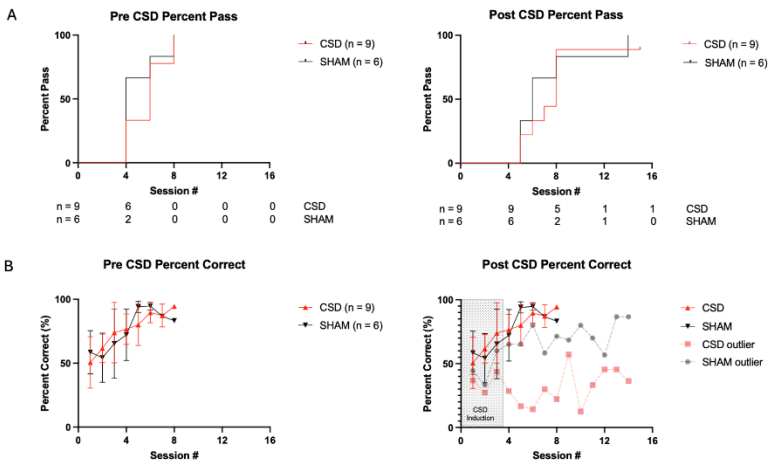

Figure 2. Optically induced CSDs do not affect executive function. (A) Pre- and post-CSD survival curves, with survival equating to passing the task. (B) Pre- and post-CSD mean ± SD of percent correct

POSTER-10 (ID:39)

NIMODIPINE REDUCES MICROGLIAL ACTIVATION BY SPREADING DEPOLARIZATION AND IN RESPONSE TO LIPOPOLYSACCHARIDE, AS EVIDENCED BY MORPHOLOGICAL PHENOTYPE AND RNA SEQUENCING

ISTVáN PESTI[1], RITA FRANK [1], VALENTIN VARGA [2], ERDA QORRI [2], DIANA KATA [3], FERENC BARI [4], ÁKOS MENYHáRT [1], ESZTER FARKAS [1],

[1] HUNGARİAN CENTRE OF EXCELLENCE FOR MOLECULAR MEDİCİNE – UNİVERSİTY OF SZEGED CEREBRAL BLOOD FLOW AND METABOLISM RESEARCH GROUP, SZEGED, HUNGARY; DEPARTMENT OF CELL BİOLOGY AND MOLECULAR MEDİCİNE, ALBERT SZENT-GYÖRGYİ MEDİCAL SCHOOL AND FACULTY OF SCİENCE AND INFORMATİCS, UNİVERSİTY OF SZEGED; SZEGED, HUNGARY

[2] DELTA BİO 2000 LTD., SZEGED, HUNGARY

[3] INSTİTUTE OF LABORATORY MEDİCİNE, UNİVERSİTY OF SZEGED, SZEGED, HUNGARY

[4] DEPARTMENT OF MEDİCAL PHYSİCS AND INFORMATİCS, ALBERT SZENT-GYÖRGYİ MEDİCAL SCHOOL, UNİVERSİTY OF SZEGED, SZEGED, HUNGARY

Background:

Microglia exhibit elevated intracellular Ca^{2+} concentrations that coincide in space and time with the wavefront of spreading depolarization (SD). In turn, intracellular Ca^{2+} transients have been postulated to regulate microglial activation that initiates neuroinflammation. Indeed, SD has been associated with microglial activation and pro-inflammatory cytokine production. Therefore, inhibition of microglial Ca^{2+} transients appears to be an attractive approach to attenuate SD-related microglial responses. Microglia are endowed with L-type voltage-gated Ca^{2+} channels (LVGCCs), which have been implicated in microglial Ca^{2+} accumulation. Here, we tested whether pharmacological inhibition of L-type voltage-gated Ca^{2+} channels with nimodipine suppresses the shift of microglia from a quiescent to an activated phenotype and how it modulates microglial gene expression.

Materials and methods:

First, microglial activation with SD was recapitulated and the effect of nimodipine on microglial morphological phenotype was evaluated in live brain slice preparations. Coronal, 350 µm thick brain slices prepared from C57BL/6 mice (body weight: 18-24 g; n=6) were bathed in artificial cerebrospinal fluid (aCSF). After 30 min nimodipine (10 µM) incubation, low glucose aCSF (5 mM) and transient anoxia (1 min) were applied to mimic ischemia and to induce SD. Intrinsic optical signal imaging was used to analyze SD characteristics. Microglial morphology was analyzed in paraffin-embedded sections processed for Iba1 immunocytochemistry.

Next, primary microglial cultures were prepared from the cortex of neonatal Sprague Dawley rats. On day 6, the plated cells were treated with lipopolysaccharide (LPS; 20 ng/ml) to activate microglia, and with nimodipine alone (5-10-20 µM) or in combination with LPS for 24 h. Microglial activation was evaluated by Iba1 immunolabeling. The degree of arborization was expressed by a transformation index (TI) calculated from the cell perimeter and surface area in both cell culture and brain slice preparations. Iba1 protein levels were quantified by Western blot analysis, and the phagocytic activity was visualized with fluorescent microbeads. TNFα cytokine levels in the cell culture medium were measured with ELISA. Total RNA was isolated from collected cells and processed for RNA sequencing (RNA-seq) to determine differentially expressed genes (DEGs).

Results:

In brain slices, microglia acquired an amoeboid, activated morphological phenotype after SD. Nimodipine reduced microglial activation as reflected by the more ramified morphology and higher TI values compared to the mOGD group (5.6±3.29 and 8.65±4.1, TI, mOGD vs. nimodipine).

When the LPS-challenged cell cultures were treated with nimodipine, significantly more ramified cells were seen on the 10 µM and 20 µM concentration (1.53±0.18 and 3.58±1.68, TI, LPS vs. 10 µM nimodipine in pure microglia culture). Increased Iba1 signal intensity in Western blot analysis confirmed microglial activation due to LPS treatment, which was decreased particularly by 10 and 20 µM nimodipine (108.3±20.1 and 77.2±8.49 vs 213.4±29.7 integrated optical density, nimodipine 10 and 20 µM vs LPS in pure microglia culture). Control microglia engulfed a few microbeads (4.54±0.87 bead/cell). In contrast, LPS challenge increased microglial phagocytic activity (10.87±1.49 bead/cell), which was significantly attenuated by nimodipine (4.39±1.03 bead/cell 10 µM nimodipine). Nimodipine produced a stepwise reduction in TNF-a levels along its increasing concentration (27.76±19.54, 23.25±12.27 and 13.61±10.26 pg/ml, 5, 10 and 20 µM), although without statistical significance.

The RNA-seq data here identified the expression of the Cacna1c and the Cacna1d genes in primary microglia cultures, which encode Cav1.2 and Cav1.3 subtypes of the α1 subunit of LVGCCs. As expected, LPS

treatment resulted in robust transcriptomic changes in rat microglia affecting 3554 genes including proteins of the TLR4 intracellular signaling cascade, chemokines and interleukins. Nimodipine treatment of LPS-activated microglia altered the expression of 110 genes compared to LPS treatment alone. Notably, nimodipine counteracted LPS effects on the complement cascade (C1qc, C2) and on the primary active transport of Ca^{2+} via the plasmalemma (Atp2b1) and to the endoplasmic reticulum (Atp2a2 and Atp2a3).

Conclusions:
Nimodipine is used to alleviate delayed ischemic deficit after aneurismal subarachnoid hemorrhage. Our data suggest that nimodipine may also be applicable to attenuate microglial activation with SD. Nimodipine appears to exert its anti-inflammatory effects by inhibiting the microglial complement cascade, and by modulating microglial Ca^{2+} homeostasis. In conclusion, the effect of nimodipine goes beyond cerebral vasorelaxation and its anti-inflammatory potential may be considered in cerebral ischemia, where progressive neuronal injury is thought to be associated with SD and neurotoxic microglial activation.

Funding:
H2020 No. 739593, NKFIH No. K146725 and K134334, NAP3.0, TKP2021-EGA-28, SZAOK Research Fund.

POSTER-11 (ID:46)

PRE-STROKE OR POST-STROKE SPREADING DEPOLARIZATION AND ISCHEMIA DO NOT AFFECT STROKE OUTCOMES IN A NEW MOUSE MODEL OF FOCAL ISCHEMIC STROKE, NAIM

KYUSUN HAN , HA KIM , DONG-EOG KIM

MOLECULAR IMAGİNG AND NEUROVASCULAR RESEARCH LABORATORY, DEPARTMENT OF NEUROLOGY, DONGGUK UNİVERSİTY ILSAN HOSPİTAL

We recently developed a new mouse model of ischemic stroke (BioRxiv 604214), where unilateral common carotid artery occlusion (UCAO)-mediated benign oligemia can transform into acute hemispheric infarction by a single-dose intraperitoneal injection of the nitric oxide synthase inhibitor Nω-nitro-L-arginine methyl ester (L-NAME, 400 mg/kg). This NOSi-mediated large Artery Ischemic stroke Model (NAIM) induced large arterial infarction in ~75% of C57BL/6 mice, allowing stroke occurrence investigations that are not achievable with traditional stroke models. Here, using the NAIM (with 100 mg/kg L-NAME) and laser speckle contrast imaging, we investigated whether recurrent bouts of either pre-stroke (n = 40) or post-stroke (n = 80) spreading depolarization and ischemia (SDI), which were evoked by repeated (12 times for 1 hour) applications of a membrane disc soaked with 300 mM KCl (vs. saline) to the brain surface through the burr hole, affect the mortality as well as the occurrence and the volume of cerebral infarction, as assessed by 2,3,5-triphenyltetrazolium chloride staining at 24 hours. Topical KCl application-mediated SDIs prior to NAIM induction (n = 20), compared to the saline group (n = 20), did not significantly affect stroke outcomes in C57BL/6 mice, in terms of the infarct incidence (45% and 40%, respectively; $p = 0.74$, Fishers exact test), the lesion volume (mean ± standard error [SE] 85 ± 25 mm^3 and 85 ± 28 mm^3, respectively; $p = 0.94$, Mann-Whitney *U* test), and the mortality (0% for both). Likewise, post-NAIM SDIs did not significantly affect stroke outcomes compared to the saline group (n = 40 / group): infarct incidence (63% and 60%, respectively; $p > 0.99$), lesion volume (71 ± 19 mm^3 and 51 ± 17 mm^3, respectively; $p = 0.42$), and mortality (10% and 7.5%, respectively; $p > 0.99$, Fishers exact test). Of note, KCl application-mediated SDI occurrences for 1 hour were significantly higher in the pre-treatment group (mean 9.2, 5 to 14) than in the post-treatment group (mean 5.5, 2 to 8). However, there were no significant inter-group differences in the infarct incidence (45% and 63%, respectively; $p = 0.58$), the lesion volume (85 mm^3 and 71 mm^3, respectively; $p = 0.86$, Mann-Whitney *U* test), and the mortality (0% and 10%, respectively; $p = 0.29$). In conclusion, neither pre-stroke SDIs nor post-stroke SDIs do not affect stroke outcomes in NAIM.

POSTER-12 (ID:7)

EFFECTS OF METABOLIC INHIBITION ON INTRACELLULAR CA2+ AND ATP IN HUMAN CORTICAL BRAIN ORGANOID SLICE CULTURES (CBOS)

LAURA PETERSILIE [1], KARL W. KAFITZ [1], SONJA HEIDUSCHKA [2], JOEL S. E. NELSON [1], LOUIS A. NEU [1], STEPHANIE LE [2], ALESSANDRO PRIGIONE [2], CHRISTINE R. ROSE [1],

[1] *INSTİTUTE OF NEUROBİOLOGY, FACULTY OF MATHEMATİCS AND NATURAL SCİENCES, HEİNRİCH HEİNE UNİVERSİTY DUESSELDORF, 40225 DUESSELDORF, GERMANY*

[2] *DEPARTMENT OF GENERAL PEDİATRİCS, NEONATOLOGY AND PEDİATRİC CARDİOLOGY, UNİVERSİTY CHİLDRENS HOSPİTAL AND HEİNRİCH HEİNE UNİVERSİTY DUESSELDORF, 40225 DUESSELDORF, GERMANY*

Rodents are a widely employed model system in neurosciences. However, the translation of results generated in these models to humans is limited due to species-specific differences. Alternative approaches are therefore needed to overcome the resulting setbacks in clinical trials. Three-dimensional (3D) brain organoids derived from human induced pluripotent stem cells (hiPSCs) are a promising translational model system to study developmental processes of the human CNS (Le et al., doi: 10.3791/62756.). However, 3D brain organoids often develop a necrotic core, and to overcome this limitation, air-liquid interface cultures of organoids have recently been introduced (Giandomenico et al., doi: 10.1038/s41593-019-0350-2.). Here, we describe the generation of cortical brain organoid slices (cBOS); which can be maintained as long-term interface cultures (Petersilie et al, doi: 10.1016/j.isci.2024.109415).

(I) Immunofluorescence labelling revealed the presence of astrocytes and neurons with putative dendritic spines in cBOS. (II) Subthreshold synaptic inputs and neurons firing action potentials were recorded by whole-cell patch-clamp. (III) Cells in cBOS showed spontaneous intracellular calcium signaling and evoked network activity upon disinhibition of NDMA receptors and blocking of $GABA_A$ receptors. (IV) Bath application of glutamate induced calcium signals in all recorded cells, indicating presence of ionotropic glutamate receptors. (V) A two-minute perfusion with metabolic inhibitors of glycolysis and oxidative phosphorylation ("chemical ischemia") resulted in a transient increase in intracellular calcium concentrations in cBOS. (VI) and finally, cBOS allow the expression of genetically encoded sensors to monitor intracellular ATP in neurons and astrocytes. A two-minute period of chemical ischemia induced a reversible decrease in neuronal and astrocytic ATP levels as measured by $ATeam1.03^{YEMK}$.

Overall, cBOS thus provide a powerful platform to study cellular function and/or dysfunction of human neural cells in intact minimal networks and to investigate the pathways leading to cellular damage in response to metabolic stress.

Supported by the DFG (RU 2795 "Synapses under stress", RO 2327/13-2).

POSTER-13(ID:27)

ACTIVATION OF TRPV4 CHANNELS PROMOS THE LOSS OF CELLULAR ATP IN MOUSE NEOCORTEX EXPOSED TO CHEMICAL ISCHEMIA

NILS PAPE , CHRISTINE R. ROSE

INSTITUTE OF NEUROBIOLOGY, HEİNRİCH HEİNE UNİVERSİTY DUSSELDORF

The vertebrate brain has an exceptionally high energy need. During ischemia, intracellular ATP concentrations decline rapidly, resulting in the breakdown of ion gradients and cellular damage. Here, we employed the nanosensor ATeam1.03^{YEMK} to analyze the pathways driving the loss of ATP upon transient metabolic inhibition in neurons and astrocytes of the mouse neocortex. We demonstrate that brief chemical ischemia, induced by combined inhibition of glycolysis and oxidative phosphorylation, results in a transient decrease in intracellular ATP. Neurons experienced a larger relative decline and showed less ability to recover from prolonged (>5 minutes) metabolic inhibition than astrocytes. Blocking voltage-gated Na^+ channels or NMDA receptors ameliorated the ATP decline in neurons and astrocytes, while blocking glutamate uptake aggravated the overall reduction in neuronal ATP, confirming the central role of excitatory neuronal activity in the cellular energy loss. Unexpectedly, pharmacological inhibition of transient receptor potential vanilloid 4 (TRPV4) channels significantly reduced the ischemia-induced decline in ATP in both cell types. Imaging with Na^+-sensitive indicator dye ING-2 furthermore showed that TRPV4 inhibition also reduced ischemia-induced increases in intracellular Na^+. Altogether, our results demonstrate that neurons exhibit a higher vulnerability to brief metabolic inhibition than astrocytes. Moreover, they reveal an unexpected strong contribution of TRPV4 channels to the loss of cellular ATP and suggest that the demonstrated TRPV4-related ATP consumption is most likely a direct consequence of Na^+ influx. Activation of TRPV4 channels thus provides a hitherto unacknowledged contribution to the cellular energy loss during energy failure, generating a significant metabolic cost in ischemic conditions.

POSTER-14 (ID:44)

COMBINED DASATINIB AND QUERCETIN TREATMENT AFTER CAROTID ARTERY STENOSS LIMITS SPREADING DEPOLARIZATION DURING SUBSEQUENT ACUTE ISCHEMIC STROKE IN AGING RATS

SZILVIA KECSKéS , ÁKOS MENYHáRT , ESZTER FARKAS

HCEMM-USZ CEREBRAL BLOOD FLOW AND METABOLİSM RESEARCH GROUP, HCEMM NONPROFİT LTD., SZEGED, HUNGARY; DEPARTMENT OF CELL BİOLOGY AND MOLECULAR MEDİCİNE, UNİVERSİTY OF SZEGED, SZEGED, HUNGARY

Background:
In addition to aging, carotid artery stenosis is a significant risk factor for acute ischemic stroke. Identification of risk factors offers the opportunity for preventive treatment of patients at high risk for acute ischemic stroke. Numerous studies have reported the beneficial effects of senolytic treatment with dasatinib (an anticancer drug) and quercetin (an antioxidant flavonoid) in various pathologies, but little is known about the efficacy of the drug combination (D&Q) in the prevention of acute ischemic stroke. The recurrent pattern of spreading depolarizations (SDs) has been recognized as an electrophysiological biomarker of cerebral injury severity or injury progression. Here, we tested the hypothesis that administration of D&Q after carotid artery stenosis mimicked in rats provides protection against subsequent acute ischemic stroke. SD characteristics and cellular senescence markers were examined to evaluate the treatment effect.

Materials and methods:
In young (6-7 weeks) and old (18-24 months) isoflurane anesthetized Wistar rats, carotid stenosis common in the elderly was mimicked by the unilateral ligation of the right common carotid artery. Over the next 2 weeks, D&Q (a cocktail of dasatinib - 5 mg/kg body weight and quercetin - 50 mg/kg body weight) or vehicle (0.1 % DMSO in saline) was administered intraperitoneally every other day. Then, focal cerebral ischemia was induced by the occlusion of the distal branch of the middle cerebral artery (dMCAO) ipsilateral to the carotid artery ligation. Spontaneous SDs in the parietal region were recorded for 1 hour using a glass capillary microelectrode, and cerebral blood flow (CBF) changes were assessed by laser speckle contrast imaging. The brains were harvested for further immunohistochemical analysis of cellular senescence and neuronal injury.

Results:
Treatment with D&Q had no significant effect on physiological parameters monitored during focal ischemia (blood pressure, baseline CBF). Induction of acute ischemic stroke resulted in a significant drop of CBF in all groups. The aged brain was more prone to spontaneous SDs during focal ischemia compared to the young brain. In the aged animals, the occurrence of spontaneous SDs was less frequent in the D&Q-treated group compared to the vehicle-treated control group. The slope of repolarization and the duration of SD, both of which indicate the ability of the tissue to recover from SD, were also reduced in the D&Q-treated group compared to the vehicle-treated group. Immunohistochemical analysis of the number of senescent arteriolar smooth muscle cells and senescent astrocytes showed a significant reduction in the D&Q-treated compared to untreated old animals in the cortex, striatum and hippocampus.

Conclusions:
The recurrence of SDs in the ischemic penumbra has been proposed to exacerbate neuronal injury. The treatment with D&Q after carotid artery stenosis but before the onset of acute ischemic stroke inhibited SD in the focal ischemic penumbra, which suggests a neuroprotective effect. The combined administration of D&Q guided by the diagnosis of carotid artery stenosis offers a personalized therapeutic opportunity as a preventive measure to limit the consequences of acute ischemic stroke.

Funding: H2020 No. 739593, NKFIH K134377, NAP3.0, TKP2021-EGA-28, SZAOK Research Fund.

POSTER-15 (ID:54)

PRO-EPILEPTIC EFFECTS OF SPREADING DEPOLARIZATIONS

DARIA VINOKUROVA [1], AZAT NASRETDINOV [1], KARINA TUKHVATULLINA [1], ROUSTEM KHAZIPNOV [2], ANDREY ZAKHAROV [3],

[1] *KAZAN (VOLGA REGİON) FEDERAL UNİVERSİTY*
[2] *KAZAN (VOLGA REGİON) FEDERAL UNİVERSİTY; INMED, INSERM, AİX-MARSEİLLE UNİVERSİTY, MARSEİLLE, FRANCE*
[3] *KAZAN (VOLGA REGİON) FEDERAL UNİVERSİTY; KAZAN STATE MEDİCAL UNİVERSİTY, KAZAN, RUSSİA*

Objective:

SDs are generally thought to be associated with a suppression of epileptic activity in the cortical region invaded by SD. However, how SD affects epi-activity in surrounding and remote cortical areas remains largely unknown. Here, we investigated remote effects of SD on the ongoing epileptic activity in a model of partial epilepsy.

Methods:

We used two silicon probes for recordings of the local field potentials and multiple unit activity across cortical layers in combination with 60-channel ECoG and intrinsic optical signal recordings in rat somatosensory cortex in a model of partial seizures evoked by intracortical injection of 4-aminopyridine/gabazine cocktail. SD clusters were induced by distant epipial potassium chloride application.

Results:

Intracortical injection of 4-aminopyridine/gabazine induced persistent epileptic activity which manifested as recurrent epileptic popspikes that were synchronized over the entire somatosensory cortex. To study the effect of SDs on ongoing epileptic activity, high K+ was applied to the visual cortex, inducing a series of SDs that propagated through the somatosensory cortex. SDs were often associated with ictal-like bursts of epileptic popspikes that were synchronized across the recording area. However, the relative timing of the ictal-like bursts and SDs varied between cortical sites. At the electrodes in proximity to high K+ application site, which exhibited the earliest SDs onset, ictal-like bursts were observed during SD. These bursts were associated with an increase in the frequency of popspikes in layers not yet invaded by SD during vertical top-down SD propagation, specifically during pre-SD excitation phase and in the "sub-SD excitation" zone. Along with horizontal SD propagation, the delay of SD from the ictal-like bursts increased, so that SDs occurred after the ictal-like bursts at the electrodes most distant from the high K+ application site. In all cases, the epileptiform activity (both ongoing regular popspikes and ictal-like bursts) was completely suppressed at the cortical area where SD invaded all cortical layers.

Conclusions:

Our results suggest that in addition to its well-known suppressive effect on epileptic activity, SDs may also exert pro-epileptic effects in the hyperexcitable cortex. These likely involve enhancement of neuronal activity during depolarization in the pre-SD excitation phase and in the sub-SD excitation zones, which are formed during horizontal and vertical SD propagation. The synchronization of SD-associated epileptic bursts across large cortical regions via horizontal connections, and the timing of SD and epileptic bursts is predominantly determined by delays in SD propagation.

Acknowledgments:

This research was funded by the Russian Science Foundation grant № 22-15-00236

POSTER-16 (ID:66)

IMPACT OF CORTICAL SPREADING DEPOLARIZATION ON NEURAL PRECURSOR DYNAMICS AND NEUROGENESIS IN THE ADULT DENTATE GYRUS

SAM JAROD QUAAS , NILS KROMMER , MIRIAM WEIßHAAR , OTTO W. WITTE , ANJA URBACH

DEPT. OF NEUROLOGY, UNİVERSİTY HOSPİTAL JENA

Cortical spreading depolarizations (CSD) are waves of massive neuroglial mass depolarization that are highly prevalent in almost all forms of acute brain injury. Previous studies suggest that, in addition to their harmful effects in injured or metabolically compromised brain areas, CSD can be neuroprotective and promote plasticity and regeneration in surrounding well-supplied tissue. For instance, we have shown that CSD lead to a robust increase in adult hippocampal neurogenesis (AHN), a unique form of plasticity that generates neurons from a pool of adult neural stem cells via differentiating intermediate progenitors throughout life. These new neurons integrate into local circuits of the dentate gyrus, contributing to hippocampal functions such as pattern separation, memory, cognitive flexibility, and mood regulation. Yet, several important questions remain, such as the stage of AHN at which CSD exert its pro-neurogenic effects and the long-term impact on AHN.

We will summarize our previous findings based on bromodeoxyuridine incorporation, showing that CSD is a potent stimulator of precursor cell proliferation in the ipsilateral subgranular zone, a region between the dentate granular cell layer and the hilus harboring adult neural stem and progenitor cells (Urbach et al., 2008 and 2017). These early events result in the generation of up to three times more new neurons at six weeks post CSD than in control animals, both, in rats and mice. This increase is associated with task- and delay-dependent changes in psychomotor behavior and spatial memory. While place memory in a location novelty recognition task was continuously improved at two up to six weeks post CSD, spatial reference memory in a Barnes maze was initially impaired at two weeks when new neurons start to integrate and compete with pre-existing neurons for synaptic connections, improved at four weeks when the newborn neurons are highly excitable and exceptionally plastic, and was unchanged at six weeks when most of the newborn cells are fully mature and indistinguishable from developmentally born neurons (Urbach et al., 2017).

We will also present preliminary data on the neurogenic response of individual precursor stages, with a particular focus on neural stem cells. Under physiologic conditions, these cells are actively maintained in quiescence, with only 2-5% dividing at a given time. This is crucial, as adult neural stem cells have limited self-renewal potential *in vivo* and can exhaust after several divisions, contibuting to the age-related decline in AHN. If overactivated, such as with epileptic seizures, the neural stem cell pool transiently expands before premature depletion, with detrimental effects for AHN in the long-term. To investigate the impact of CSD on individual stages of AHN, we induced repetitive CSD in stem- and progenitor-specific Nestin-eGFP reporter mice using topical application of 1.5 M potassium chloride (both genders, 10-12 weeks old; 1.5 M sodium chloride as control). Bromodeoxyuridine fate mapping, confocal immunofluorescence based on specific marker sets and cell morphology are used to characterize the proliferative response of individual precursor types and their numbers at different time points post CSD.

Collectively, these data will further our understanding of whether we have to categorize the neurogenic response to CSD as beneficial or detrimental to long-term hippocampal function and recovery post injury.

www.brain2025.org

BRAIN & BRAIN PET 2025

The 32nd International Symposium on Cerebral Blood and Metabolism and Function
& The 17th International Conference on Quantification of Brain Function with PET

June 1(Sun) – 4(Wed), 2025

COEX Convention Center and Exhibition Center
Seoul, Republic of Korea

Supported by SEOUL TOURISM ORGANIZATION

BRAIN & BRAIN PET 2025

In June 2025, we will host Brain & Brain PET 2025 in Seoul, the capital of Korea. This event will provide an opportunity to share outstanding research outcomes between Korea and our neighboring countries. It will also bring together researchers from various fields to expand the Brain & Brain PET society network and foster friendships. Under the leadership of ISCBFM, we hope to encourage more active participation from Brain & Brain PET society members worldwide.
If you've never visited Korea, this event offers a great opportunity to experience the beauty of Seoul. For those who have visited before, Seoul's ever-changing trends and culture ensure there are always new and exciting experiences to enjoy. We hope you can create memorable moments in this vibrant city.

Yong Jeong
KAIST
Brain & Brain PET 2025
LOC Co-chair

Yun Seon Song
Sookmyung Women's University
Brain & Brain PET 2025
LOC Co-chair

SEOUL

SEOUL is the nation's academic center. Metropolitan Seoul has more than 100 universities and colleges as well as many prestigious research institutes such as KIST (Korea Institute of Science Technology). Korea's technological development, with world-leading competencies in electronics, also stands out in the medical field. SEOUL is the hub of innovation with active clinical research projects now utilizing AI platforms, bio-startups working on the cutting-edge of technology, and a booming venture capital scene. SEOUL is one of the cities where PET is very actively used for research and clinical purposes.
Also, Seoul bridges many neighboring countries in the Asia-Pacific region. Hosting Brain & Brain PET in Seoul will serve its functions as the main vehicle of promoting the science of brain regionally and internationally.

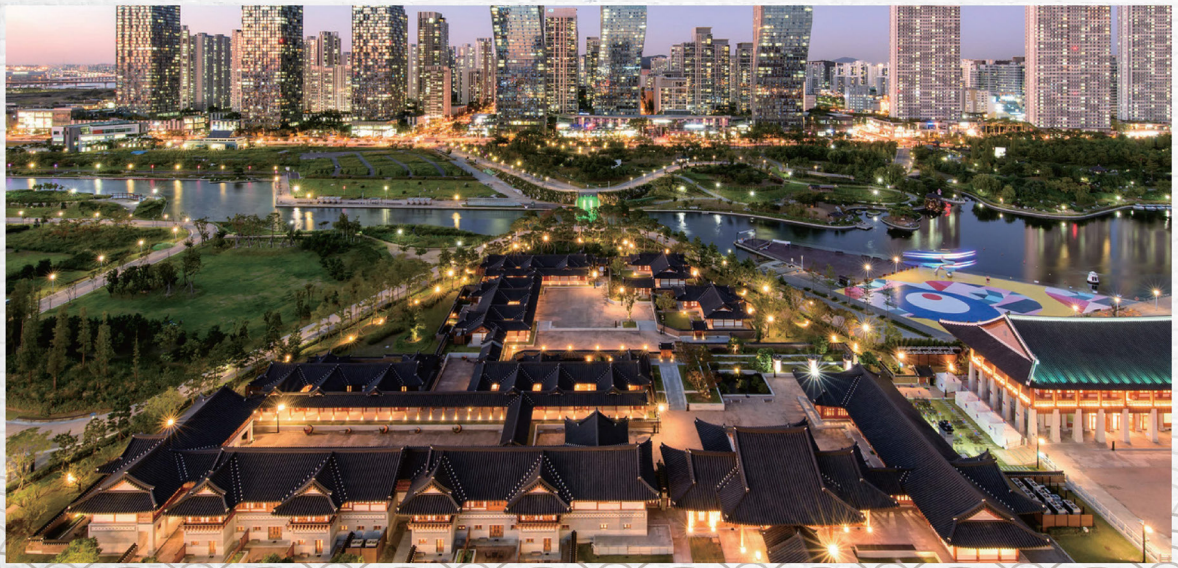

Supported by SEOUL TOURISM ORGANIZATION

SPONSORSHIPS

SPONSORSHIPS

Thank you for all supprts.

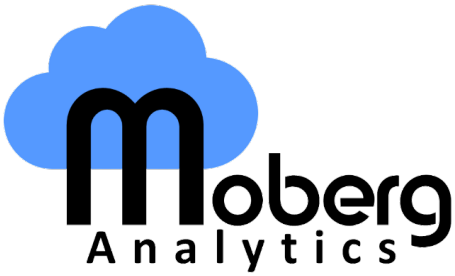

Open Source Instruments